STUDIES IN THE RESEARCH PROFILE BUILT ENVIRONMENT
DOCTORAL DISSERTATION NO. 4

Natural Ventilation and Air Infiltration in Large Single Zone Buildings

Measurements and Modelling with Reference to Historical Churches

Abolfazl Hayati

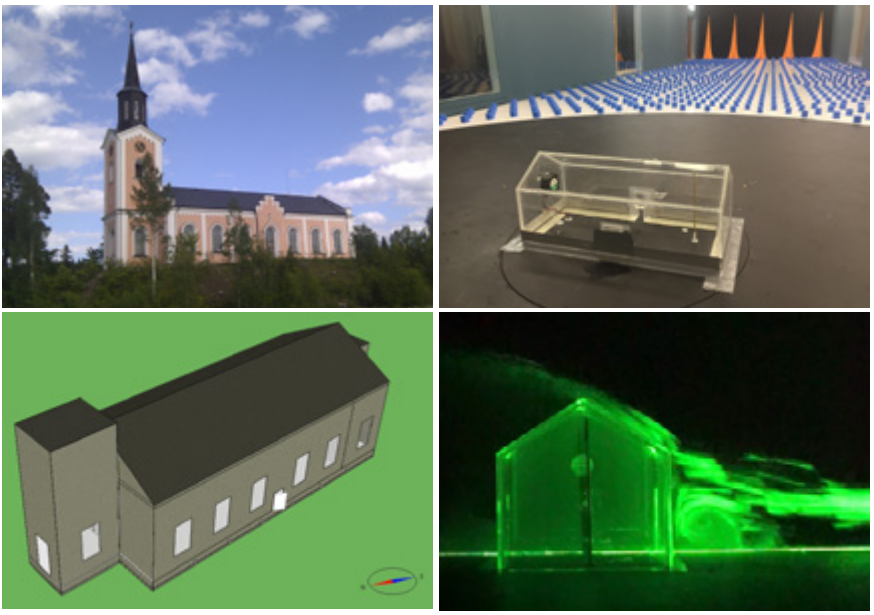

UNIVERSITY OF GÄVLE

FACULTY OF ENGINEERING AND SUSTAINABLE DEVELOPMENT
Department of Building, Energy and Environmental Engineering

STUDIES IN THE RESEARCH PROFILE BUILT ENVIRONMENT
DOCTORAL DISSERTATION NO. 4

Natural Ventilation and Air Infiltration in Large Single Zone Buildings

Measurements and Modelling with Reference to Historical Churches

Abolfazl Hayati

UNIVERSITY
OF GÄVLE

Gävle University Press
ISBN 978-91-88145-17-8
ISBN 978-91-88145-18-5 (PDF)
urn:nbn:se:hig:diva-24612

Distribution:
University of Gävle
Faculty of Engineering and Sustainable Development
SE-801 76 Gävle, Sweden
+46 26 64 85 00
www.hig.se

Print: Ineko AB, Kållered 2017
Cover page photos: Abolfazl Hayati & Magnus Mattsson

Abstract

Natural ventilation is the dominating ventilation process in ancient buildings like churches, and also in most domestic buildings in Sweden and in the rest of the world. These buildings are naturally ventilated via *air infiltration* and *airing*. *Air infiltration* is the airflow through adventitious leakages in the building envelope, while *airing* is the intentional air exchange through large openings like windows and doors. Airing can in turn be performed either as *single-sided* (one or several openings located on the same wall) or as *cross flow* ventilation (two or more openings located on different walls). The total air exchange affects heating energy and indoor air quality. In churches, deposition of airborne particles causes gradual soiling of indoor surfaces, including paintings and other pieces of art. Significant amounts of particles are emitted from visitors and from candles, incense, etc. Temporary airing is likely to reduce this problem, and it can also be used to adjust the indoor temperature. The present study investigates mechanisms and prediction models regarding air infiltration and open-door airing by means of field measurements, experiments in wind tunnel and computer modelling.

In natural ventilation, both air infiltration and airing share the same driving forces, i.e. wind and buoyancy (indoor-outdoor temperature differences). Both forces turn out to be difficult to predict, especially wind induced flows and the combination of buoyancy and wind. In the first part of the present study, two of the most established models for predicting air infiltration rate in buildings were evaluated against measurements in three historical stone churches in Sweden. A correction factor of 0.8 is introduced to adjust one of the studied models (which yielded better predictions) for fitting the large single zones like churches. Based on field investigation and IR-thermography inspections, a detailed numerical model was developed for prediction of air infiltration, where input data included assessed level of the neutral pressure level (NPL). The model functionality was validated against measurements in one of the case studies, indicating reasonable prediction capability. It is suggested that this model is further developed by including a more systematic calibration system for more building types and with different weather conditions.

Regarding *airing*, both single-sided and cross flow rates through the porches of various church buildings were measured with tracer gas method, as well as through direct measurements of the air velocity in a porch opening. Measurement results were compared with predictions attained from four previously developed models for single-sided ventilation. Models that include terms for wind turbulence were found to yield somewhat better predictions. According to the performed measurements, the magnitude of one hour single-sided open-door airing in a church typically yields around 50% air exchange, indicating that this is a workable ventilation method, also for such large building volumes. A practical kind of diagram to facilitate estimation of suitable airing period is presented.

The ability of the IDA Indoor Climate and Energy (IDA-ICE) computer program to predict airing rates was examined by comparing with field measurements in a church. The programs' predictions of single-sided airflows through an open door of the church were of the same magnitude as the measured ones; however, the effect of wind direction was not well captured by the program, indicating a development potential.

Finally, wind driven air flows through porch type openings of a church model were studied in a wind tunnel, where the airing rates were measured by tracer gas. At single-sided airing, a higher flow rate was observed at higher wind turbulence and when the opening was on the windward side of the building, in agreement with field measurements. Further, the airing rate was on the order of 15 times higher at cross flow than at single-sided airing. Realization of cross flow thus seems highly recommendable for enhanced airing. Calibration constants for a simple equation for wind driven flow through porches are presented. The measurements also indicate that advection through turbulence is a more important airing mechanism than pumping.

The present work adds knowledge particularly to the issues of *air infiltration* and *airing through doors*, in *large single zones*. The results can be applicable also to other kinds of large single-zone buildings, like industry halls, atriums and sports halls.

Keywords: Natural ventilation, Airing, Air infiltration, Single-sided ventilation, Cross flow, Large single zones, Historical Churches, Model evaluation/optimization, Field measurements, Wind tunnel, Indoor climate and energy simulation, IDA-ICE, Tracer gas technique, Pressurization test.

Sammanfattning

Naturlig ventilation är den dominerande ventilationsprocessen i äldre byggnader såsom kyrkor, och även i de flesta småhus i Sverige och övriga delar av världen. *Luftinfiltration* och *vädring* utgör viktiga komponenter i naturlig ventilation, där *luftinfiltration* är luftflöde genom oavsiktliga läckage i byggnadsskalet, medan *vädring* är avsiktligt luftutbyte genom stora öppningar såsom fönster och dörrar/portar. Vädring kan i sin tur ske *ensidigt* (genom en eller flera öppningar belägna på samma yttervägg) eller som *tvärdrag* (genom två eller flera öppningar belägna på olika ytterväggar). Det totala luftutbytet påverkar värmeförluster och inomhusluftens kvalité. I kyrkor orsakar avsättning av luftpartiklar en gradvis nedsmutsning av invändiga ytor, inklusive väggmålningar och andra konstföremål. Betydande mängder partiklar avges från besökare, tända ljus, rök-else, o.d. Tillfällig vädring kan minska detta problem, men även användas för att justera innetemperaturen. Föreliggande studie analyserar mekanismer och predikteringsmodeller gällande luftinfiltration och dörrvädring genom fältmätningar, vindtunnelförsök och datorsimuleringar.

Luftinfiltration och vädring har samma drivkrafter, d.v.s. vind och termik (inne ute temperaturskillnader). Båda dessa drivkrafter är svåra att predicera, särskilt vindinducerade flöden och kombinationen av termik och vind. Två av de mest etablerade modellerna för luftinfiltrationsprediktering i byggnader har utvärderats via mätningar i tre kulturhistoriska stenkyrkor i Sverige. En korrigeringsfaktor av 0,8 föreslås för bättre prediktion av den ena modellen (som gav bäst resultat) gällande höga en-zonsbyggnader såsom kyrkor. En detaljerad numerisk modell är utvecklad för luftinfiltrationsprediktering, där indata baseras på fältundersökningar, inkl. IR-termografering och uppmätt av neutrala tryckplanet (NPL). Modellens funktionalitet har validerats via mätningar i en av fallstudierna och pekar på tämligen god prediktionsprestanda. Vidare utveckling av modellen föreslås, inkl. ett mer systematiskt kalibreringssystem, för olika typer av byggnader och väderförhållanden.

Gällande *vädring* mättes både ensidigt flöde och tvärdrag genom portar i olika kyrkobyggnader med hjälp av spårgas samt direkta lufthastighetsmätningar i portöppning. Mätresultaten jämfördes med erhållna prediktioner från fyra tidigare utvecklade modeller för ensidig ventilation. De modeller som tog hänsyn till vindturbulens gav något bättre resultat. Enligt utförda mätningar medför en timmes ensidig portvädring i en kyrka cirka 50 % luftutbyte, vilket indikerar att detta är en tillämpbar ventilationsmetod, även för så pass stora byggnadsvolymer. Ett särskilt vädringsdiagram presenteras, som syftar till att underlätta uppskattning av erforderlig vädringsperiod.

Vidare studerades predikteringsprestanda hos IDA Indoor Climate and Energy (IDA-ICE) simuleringsprogram avseende vädring, där simuleringsdata jämfördes med fältmätningar i en kyrka. Programmets prediktion av ensidigt luftflöde genom en öppen kyrkport var av samma storlekordning som det uppmäta; dock klarade programmet inte av att hantera inverkan av vindriktning så väl, vilket pekar på en utvecklingspotential.

Avslutningsvis undersöktes vinddrivet flöde igenom portöppningar i en kyrkmodell i vindtunnel, där luftomsättningen mättes med hjälp av spårgasmetoden. Vid ensidig vädring observerades högre flöde vid högre vindturbulens och när öppningen var på vindsidan av byggnaden, i överensstämmelse med fältmätningarna. Dessutom var vädringsflödet vid tvärdrag i storleksordningen 15 högre än det vid ensidig vädring. Det verkar alltså som att man kan öka vädringstakten avsevärt om man kan åstadkomma tvärdrag. Kalibreringskonstanter presenteras också för en enkel ekvation för vinddrivet flöde genom portar. Vindtunnelstudien indikerar vidare att advektion genom turbulens är en viktigare vädringsmekanism än pumpning.

Föreliggande arbete bidrar med kunskap speciellt kring *luftinfiltration* och *vädring* genom portar i *höga en-zonsbyggnader*. Resultaten kan även vara tillämpliga på andra typer av höga en-zonsbyggnader såsom industrihallar, atrier/ljusgårdar och idrottshallar.

Nyckelord: Naturlig ventilation, Vädring, Luftinfiltration, Ensidig ventilation, Tvärdrag, Höga en-zonsbyggnader, Kulturhistoriska kyrkor, Modellutvärdering/optimering, Fältmätningar, Vindtunnel, Inomhusklimat och energisimulering, IDA-ICE, Spårgas teknik, Trycksättningstest.

Acknowledgements

Thank God for all his kindness and support to me during my life, and therefore I'm blessed with a wonderful family, awesome friends and everything I need and I have.

I am forever grateful to my main supervisors: Associate Professor Magnus Mattsson and Professor Mats Sandberg. Magnus, as a distinguished researcher, is a diligent, genius and compassionate person with a highly admiring and caring character. Mats, the living legend, is a humble, creative, and kind person. Magnus and Mats have kindly dedicated time and patience to my work and the quality of my research has been upgraded always owing to their comments and effort. I am very blessed and honored to have them as my main supervisors and mentors and I truly enjoyed the fruitful discussions and the challenging tasks. Their expertise and personality has shaped my career and has led me to accomplish my project.

Associate Professor Jan Akander at University of Gävle was my unofficial supervisor and mentor; he kindly put time and effort into my work and was always open to my debates. Thanks also to my administrative supervisor Professor Jens Fransson for his help.

Further, I am thankful for other teachers, lab technicians and colleagues. Special thanks to lab responsible and technical assistants and also my teachers and kind friends who gave me invaluable support during my measurements; therefore my thanks goes to Mr. Leif Claesson, Ms. Elisabet Linden, Mr. Svante Lindström, Mr. Mikael Sundberg and Mr. Hans Lundström with whom I spent great time during measurement and learned a lot. I would like to thank my teachers with whom I had great discussions and it is always joyful to meet them, therefore my special thanks goes to Associate Professors Taghi Karimipanah, Hans Wigö, Mathias Cehlin and Dr. Claes Blomqvist at University of Gävle and Professor Hazim Awbi at Reading University. Special thanks to Hans Wigö for all interesting and funny discussions at the lunch table during these years. Thanks also to other colleagues and previous teachers, Dr. Nawzad Mardan and Professor Björn O. Karlsson. I would like to thank the head of Energy systems department Mr. Ulf Larsson and the current and previous head of Academy for Built Environment, Associate Professor Gunilla Mårtensson and Dr. Bengt Eriksson. I am also thankful to Eva Wännström for administrative help and Staffan Nygren for IT-support during these years; and thank to Karin Meyer Lundén, Malin Almstedt Jansson and Lisa Grelsson Wiik for preparing and publishing my dissertation thesis.

Constructive comments and suggestions received at "IAQ2016 ASHRAE/AIVC conference" and "Cultural heritage preservation – 3rd European Workshop on Cultural Heritage Preservation" for previous versions of my studies are also gratefully acknowledged.

My study trip to Japan was really informative and inspiring and it was an honor for me to visit the lab facilities and discuss about my research topics;

and therefore I would like to express my gratitude to Dr. Kobayashi, Professor Hisashi, Dr. Momoi, Professor Yamanaka, Professor Sagara, Professor Kato and Professor Ito and Mr. Sakaguchi. In addition, I am grateful to PhD and master students at the departments I visited in Osaka University, Kyushu University, and Tokyo University for the great time and discussions that we had together. The conference in Osaka also led to meet successful Irish researchers, Dr. Paul O'Sullivan and Dr. Michael D Murphy, which made my trip even more fruitful.

I would also like to express appreciation for all my previous teachers, who's love, passion and effort has led me to this point. Especially, I would like to thank Mr. Yazdani, Mr. Nazarizadeh. Mahdi, Mr. Nazarizade. Mohsen, Mr. Ghajar, Mr. Rajabi, Mr. Bonakdar, Mr. Ghorbani, Mr. Moghadasian, Mr. Khayati, Mr. Akhbarieh, Mr Kaghazchi, Mr Jahromi, Mr Shaban, Mr Gholamhosseini, Mr Sanaye, Mr Faghiri, Ms. Esfehani, Ms. Davoodi, … the list could go on. Especial thanks also to all my dear teachers at the institute of "Daneshamuzan e Nemuneh", Amirkabir University of technology (Tehran Polytechnics), Emami Aleagha high school, Alborz high school, Bayat guidance school and Hurr elementary school.

I am one of the richest persons in the world because I have many great friends to whom I am grateful because of creating a friendly atmosphere like a family, providing useful advice and/or for being great supporters; my special thanks goes to Amirreza (for being always there, like a true brother), Jafar, Iman and all my friends/classmates especially at the third period of the institute "Daneshamuzan e Nemuneh". Further, coming to Sweden thankfully led to make forever friendship with Naeim, Taha, Mohammad Reza and Aliakbar who made the atmosphere in Gävle just like a family.

Moreover, I am thankful to the current and former PhD students at the University of Gävle for providing a friendly and stimulating work environment, so thanks to: Shahriar, Setareh, Abid, Jessika, Alan, Mohammad, Amir, Hossein, Arman, Huijuan, Harald, Ioana, Ida, Åsa, Mobashar, Gottfrid, … at HiG, Ali in Linköping and also Samer and Marc at KTH.

I am eternally grateful to my father Hassan (may he rest in peace), my mother Ameneh (may she rest in peace), my brother Mostafa (may he rest in peace) and my other brothers Saboktakin and Morteza. I have all happiness in my life having Saboktakin and Morteza who have always been my canny mentors with full support and kindness for which I am always thankful.

I am also thankful to my beloved wife, Reihaneh, without her love, positive encouragement and patience I could not make this happen. Thanks to her parents, Maryam and Bahram, as well for their understanding and support during these years. Especial thanks also to my brother in law, Mohammad, pushing me into sport and training during these years!

I am forever indebted to my aunt Marzieh for taking care of my brother and me during many years. Especial thanks to her family, my beloved cousins who are just like brothers and sisters for me; therefore I like to thank Nadi, Zari, Ashraf (and her husband Akbar), Ghasem, Alireza, Mehdi and Bagher as well as their beloved families.

Nomenclature

Latin Symbols

Symbols	*Description*	*Unit*
A	Opening area	m^2
A_{proj}	Projected area	m^2
B	Thickness of construction	m
b	Door width	m
B_0	Specific permeability of a material	m^2
C	Power law flow coefficient	$m^3s^{-1}Pa^{-n}$
C_1	Flow resistant coefficient	$Pa\ m^{-3}s$
C_2	Flow resistant coefficient	$Pa\ m^{-6}s^2$
C_d	Discharge coefficient	-
C_D	Drag coefficient	-
C_e	An empirically attained coefficient for the buoyancy driven flow through large openings	-
C_f	Flow coefficient	-
C_p	Wind surface pressure coefficient	-
d_{crack}	Depth of the crack	m
D_h	Hydraulic diameter	m
E	The amount of exchanged room air	%
F	Drag force	N
f	Geometry factor	$m^{0.5}$
Fr	Froude number	-
g	Gravitational constant	$m\ s^{-2}$
h	A certain vertical height along the opening or façade	m
H	Opening height	m
H'	Height of wind speed measurement site	m
$H_{building}$	Height of building	m
h_{crack}	Height of crack	m
H_{NPL}	The height of neutral pressure level (NPL)	m
k	Crack flow coefficient	$m^3s^{-1}m^{-1}Pa^{-n}$
L	Length of crack	m
l_{50}	Building air tightness value	$Ls^{-1}m^{-2}$

Symbols	*Description*	*Unit*
m	Correction factor	-
n	Flow exponent	-
P_s	Buoyancy or stack pressure	Pa
P_w	Wind surface pressure relative to outdoor static pressure of the undisturbed flow	Pa
$P_{w,i}$	Wind surface pressure inside the building envelope relative to outdoor static pressure of the undisturbed flow	Pa
Q	Flow rate	m^3s^{-1}
r	The ratio between the flow resistant coefficients	-
Re	Reynolds number	-
T	The average temperature between the indoor and outdoor temperatures	K
t	Duration of airing	h
T_i	Indoor temperature	K
T_o	Outdoor temperature	K
U	Undisturbed wind speed at the building height	ms^{-1}
u	Mean velocity of air through the porous material or through the opening/aperture	ms^{-1}
U'	Undisturbed wind speed at the height of the measurement site	ms^{-1}
Vol	Volume of indoor space	m^3

Greek Symbols

Symbols	*Description*	*Unit*
α	Terrain parameter	-
β	Interaction Coefficient in the AIM-2 model	-
γ	Terrain parameter	-
λ_f	The Poiseuille flow friction factor	-
μ	Dynamic viscosity of air	Pa s
ξ	Entry and exit loss term	-
ρ	Density of air at a reference temperature and pressure	kgm^{-3}
ρ_i	Indoor air density	kgm^{-3}
ρ_o	Outside air density	kgm^{-3}

Abbreviations

Letters	*Description*
ACH	Air change rate per hour
AIM-2	Alberta air infiltration model
CFD	Computational fluid dynamics
C.I.	Confidence interval
HVAC	Heating, ventilation and air conditioning
IR-Thermography	Infrared thermography
LBL	Lawrence Berkeley Laboratory air infiltration model
NPL	Neutral pressure level. The height above ground where the static pressure is the same on the indoor side of the building as on the outside.
PIV	Particle image velocimetry
SD	Standard deviation

Glossary

Explanation of some terms used in the present study.

Air change rate, ACH (h-1): Airflow rate in a zone divided by its interior volume.

Air infiltration: Unintentional airflow through adventitious leakages in the building envelope. Air infiltration can be caused by buoyancy, wind effect and the pressure induced by mechanical ventilation.

Airing: Intentional air exchange through large openings such as windows and doors. Airing can be either single-sided or cross flow.

Buoyancy effect: Also called stack or chimney effect, caused by thermally induced pressure difference between inside and outside. A temperature difference between indoor and outdoor air causes a density difference which results in the pressure difference, which varies with height.

Cross flow ventilation: Airing in which openings are located on two different walls; in this study being opposite to each other.

Draught lobby: Extended porch volume after the entrance, constituting "corridor" extending into the building, intending to reduce the inflow of cold outdoor air. During airing, both the porch and an inner door of the draught lobby need to be open.

Gravity currents: Also called buoyancy or density currents are primarily horizontal flows generated by small density differences (due to the temperature difference between the streaming flow and the stagnant body of fluid). As an example, a gravity current can be generated in a house by opening a front door and letting the incoming outdoor (colder) air propagate over the floor (Etheridge and Sandberg, 1996).

Guesstimated leakage distribution: An educated guess about likely leakage distribution, with the help of using different leakage identification techniques, including IR-Thermography, visual inspection, NPL assessment, and tracer gas measurements.

Leakage: Adventitious openings in the building envelope of which the size, shape and position of inlet and outlet are unclear and direct measurement of the opening area is not possible. Cracks and gaps in walls, floor, ceiling and at window and door frames are examples of the leakages.

Natural ventilation: Airflow through purpose provided opening such as open doors, windows and grilles (ASHRAE, 2013a). Natural forces such as the buoyancy and wind effect are used to introduce and distribute the outdoor air into the building (WHO, 2007).

Neutral pressure layer (NPL): The height above a reference plane in which there is not any indoor-outdoor pressure difference, and consequently no local air flow exchange between inside and outside at that height.

Open-door airing: Airing through outer doorways, either in the form of single-sided ventilation or cross flow.

Opening: A space or gap or an aperture in a building envelope that allows airflow passage. It can be divided into purpose provided and adventitious openings. Here, for the purpose provided ones, the size and position is known. Examples include windows, doors, porches, vents, stacks, chimneys, etc.

Porch: The door opening of a church or other monumental building.

Semi-empirical air infiltration or airing model: An analytical (or semi-analytical) superposition model, which is based on the fundamental flow equations that relates the flow to pressure, such as Bernoulli equation. Semi empirical models relate the total air infiltration or airing flow rates to each buoyancy and wind induced flowrate with help of empirical coefficients, gained from statistical fits of infiltration rate or airing data for some specific houses.

Single zone models: Models, in which the interior of the building is described by a single zone at uniform temperature and pressure, constituting a well-mixed pressure node.

Single-sided ventilation: Airing in which opening(s) are located on only one outer wall of a building. There can be one or several openings located on the same outer wall; however, here in this study single-sided ventilation is studied through only one opening (door) on the outer wall.

Superposition model: Once each wind or buoyancy induced flow rate is calculated, the total flow is often not a simple addition. Calculating the exact flow prediction is impossible and neither is it possible to measure the wind and stack induced flow rates separately. Therefore, the total flow is gained by the superposition equation or models aimed for combing the buoyancy and wind-induced airflows. The models can be then tuned by comparing the predictions with the measurement data.

Wind effect: Wind induces an indoor-outdoor pressure difference which causes air flow through possible openings in the building envelope. Wind effect is caused not only by the average wind speed but also by the fluctuations in the wind speed, i.e. wind turbulence.

Zone: A bounded or unbounded indoor space. Buildings can be divided into single- and multi zone spaces, where only one or more than one zone, respectively, are present within the building envelope.

List of Appended papers

Paper I

Abolfazl Hayati, Magnus Mattsson, & Mats Sandberg. (2014). Evaluation of the LBL and AIM-2 Air Infiltration Models on Large Single Zones: Three Historical Churches. *Building and Environment* nr. 81, pp 365-379. doi: 10.1016/j.buildenv.2014.07.013

Paper II

Abolfazl Hayati, Jan Akander, & Magnus Mattsson. (2016). Development of a Numerical Air Infiltration Model Based On Pressurization Test Applied On a Church. *IAQ 2016 conference co organized by ASHRAE and AIVC* September 12–14, 2016, Alexandria, VA

Paper III

Mats Sandberg, Magnus Mattsson, Hans Wigö, Abolfazl Hayati, Leif Claesson, Elisabet Linden, & Mubashar Ahmed Khan. (2015). Viewpoints on Wind and Air Infiltration Phenomena at Buildings Illustrated by Field and Model Studies. *Building and Environment* nr. 92, pp 504-517. doi: 10.1016/j.buildenv.2015.05.001

Paper IV

Abolfazl Hayati, Magnus Mattsson, & Mats Sandberg. (2017). Single-sided ventilation through external doors: measurements and model evaluation in five historical churches. *Energy and Buildings* nr. 141, pp 114-124. doi: 10.1016/j.enbuild.2017.02.034

Paper V

Abolfazl Hayati, Magnus Mattsson, & Mats Sandberg. (2016). A Study on Airing through the Porches of a Historical Church - Measurements and IDA-ICE Modelling. *IAQ 2016 conference co-organized by ASHRAE and AIVC* September 12–14, 2016, Alexandria, VA

Paper VI

Abolfazl Hayati, Magnus Mattsson, & Mats Sandberg. *A wind tunnel study of wind driven airing through doors*. (Submitted to journal for publication).

Reprints were made with permission from the publishers.

Table of Contents

1. Introduction

1.1. Natural ventilation history and application

Air exchange between indoors and outdoors can be separated into ventilation and infiltration. The main task of ventilation is to provide fresh air and remove air contaminants from the interior volume. As a completion to the ventilation system, heating and/or cooling systems can keep the air quality and thermal comfort at an acceptable level. Ventilation itself can be divided into mechanical, or forced, and natural ventilation. Mechanical ventilation supplies fresh air with the help of fans, ducts, inlet and outlet openings or vents. In case of natural ventilation, there is no mechanical fan but the outdoor air is brought in through purpose provided openings such as slots at windows, open doors and windows, grills, chimneys or stacks, wind towers and other intentional passages.

Natural ventilation is the oldest and most widely used sort of ventilation throughout the history. Even in ancient times, people had come up with ideas on how to capture the wind and buoyancy effect in order to maintain thermal comfort and ventilate their buildings. For example, the famous wind catchers “Baadgir” (BĀDGĪR), literally “wind-catcher”, in many regions in Iran such as the historic city of Yazd (inscribed on UNESCO's world heritage list), are brilliant examples of employing natural ventilation, especially wind driven airing. A typical wind catcher and the famous wind catcher of “Dolatabaad” garden are depicted in Figure 1. Such wind catchers are open in, one, two, four or eight sides at the top of the tower (Roaf, 1989), so that wind can push the air into the building in the windward side and exhale it out in the leeward side. Thus, they could capture the breeze from any direction. Normally, the airflow rates are mixed with the conducted air from water storages under the building and consequently a pleasant humidified air is introduced into the rooms. These types of wind catchers were commonly used in regions with hot arid climate. There are also some lids below each channel of the wind catcher in order to control the magnitude of the airflow. In addition, in these buildings the roof was normally built in semi-spherical (dome) forms, so that it was half-shaded most of the time. Beside there are some openings implemented in the top so that the extra overheat could be removed from the interior by stack effect. In addition, the wind catchers perform as stack chimneys; when there is not enough wind, and the walls of the wind catcher are warmed up by sun, the air is pushed up into the wind catcher and then ventilated out because of the buoyancy effect and instead cooler air is extracted from the basement or water

storages under the building. Moreover, the water reservoirs were chilled by the ventilation air through evaporative cooling. For more information on these type of wind catchers, see e.g. (Karakatsanis, Bahadori and Vickery, 1986; Bahadori, 1994; Montazeri and Azizian, 2009; Montazeri *et al*., 2010; Eiraji and Namdar, 2011; Montazeri, 2011; Ahmadikia, Moradi and Hojjati, 2012; Boloorchi and Eghtesadi, 2014).

Figure 1: Typical wind catcher “Baadgir” (left); the right picture shows “Dolatabaad” garden and the baadgir is positioned on the roof. Both baadgirs are located in the historic city of Yazd (inscribed on UNESCO's world heritage list), Iran. Photo with courtesy of the Administration of Cultural Heritage, Handicrafts and Tourism Yazd, http://ch.yazdcity.ir/.

Modern examples of combing natural and mechanical ventilation, i.e. hybrid ventilation (Heiselberg, 2002), can also be found; for instance commercial buildings in Osaka, Japan, in which wind and buoyancy driven ventilation is used when the outside weather is appropriate. Examples include high-rise office buildings in Umeda (Osaka), Japan (Sekkei, 2017).

1.2. Pros and cons of natural ventilation

Advantages of natural ventilation are that it is most of the time available and it saves energy by omitting fans in an alternative mechanical system and/or by providing cooling air. In a way, it is more sustainable as well. Another advantage by using natural ventilation is to temporarily achieve a high transient ventilation in order to remove particles emitted from people and lit candles (for instance in churches) or even from renovation activities in buildings (WHO, 2007).

Bearing in mind that the natural ventilation is very dependent on the outside condition, there is lack of control over its magnitude, except by opening or closing purpose provided apertures. On the other hand, in case the outside weather is too hot or cold, then costs of heating or cooling should be added as well.

Air flow rates and directions through building envelope vary a lot in an unpredictable manner. The flow rate through an opening depends on the wind speed, wind direction (which determines the wind pressure coefficient), and temperature differences between indoor and outdoor and the operating area. In fact, all of the above parameters are time dependent and the resulting flow rate changes in magnitude and direction, i.e. it becomes inward or outward. Moreover, all the individual flow rates depend on each other, i.e. the system is sensitive and design errors are difficult to correct. In natural ventilation, there is no need of space for ducts and HVAC (Heating, Ventilation and Air Conditioning) systems, while there may be needed some space for chimneys and stacks. However, there is lower investment, maintenance and operational costs in natural ventilation (WHO, 2007). In mechanical ventilation systems, flow rates are kept constant in magnitude as well as their direction and they are independent of each other considering negligible envelope leakage (Etheridge, 2012). The noise due to fans or air handling units is not present in a natural ventilation system; however, depending on the conditions in the outdoor environment the ingress of the outside noise (and also pollutants) might be an issue, e.g. due to nearby industries or vehicle traffic.

In natural ventilation, there is lower need for capital and operating costs regarding both maintenance and energy, i.e. the electricity for running an equivalent mechanical ventilation system is saved. However, in a mechanical ventilation system, a part of the heating energy can be conserved via heat exchangers implemented in the exhaust air system. Natural ventilation can be a reasonable system not only for residential houses but also for larger commercial buildings like atriums, shopping malls and airports. In such commercial buildings, natural ventilation can be used at least occasionally or in a mixed-mode together with other HVAC system. Because in non-domestic buildings other issues are of more importance such as maximizing the use of floor area, including ventilation system with heating and cooling, and precise control of processes and equipment. If the system is properly designed, it can be used in order to save energy and provide thermal comfort.

1.3. Motivation of this study

Historical and monumental buildings like churches in Sweden and other countries are mostly naturally ventilated by air infiltration and airing through the doors, porches or windows. The adventitious air infiltration happens unintentionally and possibilities of opening windows are often limited. Therefore, open door airing is often the only way to deliberately increase the ventilation. In old churches, air infiltration has a great impact on energy usage especially during the heating season. These buildings are often leaky and

there are limited possibilities of air tightening due to preservation and esthetical considerations. Due to the same reasons, possibilities to add mechanical HVAC installations to this kind of buildings are also limited. Even in case of having such systems available, the encountered natural ventilation and the air tightness characteristics are needed in order to tune the system.

Due to moisture generation from visitors and lit candles in a church, it can sometimes also be practical to extract humid air from the interior, because it might end up with material deformation, microbial growth and cause damage to art pieces, such as paintings and furniture. Studies have also shown that high candle emissions can affect the health of especially regularly present staff (Chuang, Jones and BéruBé, 2012). The concentration of indoor airborne particles and other contaminants are also affected by the magnitude of the natural ventilation flow rates. The gradual soiling of particle deposition can deteriorate the esthetical monuments on the interior surfaces. Especially in churches with limited air infiltration rates, extra fresh air can be introduced by venting (airing) the interior through open windows or doors and removing the particles emitted by people and lit candles. Airing is also mentioned as an important parameter for removing other indoor pollutants such as radon (Gerken *et al*., 2000).

Therefore, the magnitude of air infiltration and airing flow rate should be predicted accurately to have a better assessment of the energy saving, thermal comfort, preservation of the cultural heritage and also implementing appropriate renovation measures. Little guidance on this exists for large single-zone building envelopes like those of old churches. The airflow predictions can also have importance for residential and commercial buildings, which are ventilated by pure natural ventilation or in mixed-modes together with mechanical ventilation. Even in modern airtight buildings, airing can be used as a complementary system to save energy, provide thermal comfort and maintain a more sustainable system since no mechanical resources are needed.

1.4. Aim

The present study aims to increase knowledge on the issues of air infiltration and open-door airing in large single-zone buildings, with particular focus on historical churches. The historical churches are here thought to represent the vast number of old and relatively leaky churches and other buildings of similar construction, that are without mechanical ventilation and where, hence, little control is given regarding air change rate and effects on heating energy, air quality and humidity. Improved possibilities to calculate and control these qualities require enhanced knowledge of the mechanisms involved in air infiltration and airing. The study also intends to evaluate existing prediction models in this regard and possibly to improve them, but also to test an idea of a locally developed air infiltration model. Regarding airing, practically all previous studies concern airing through windows, whereas the present study focuses on doors, i.e. usually constituting somewhat larger

openings, placed at bottom level. One objective is to assess the practicability of open-door airing in such large spaces as churches, and to provide practical airing guidance.

1.5. Research process

The natural ventilation is investigated by field investigation, analytical model studies, numerical model investigation and wind tunnel model studies. Comprehensive literature study based on previous field and wind tunnel investigations and analytical model studies of air infiltration and airing are also compiled and included in the research. The measurement data are collected and recorded at different geographical positions and weather conditions. Because such measurements are costly and difficult to measure at longer periods, related analytical models for prediction of airing and air infiltration are investigated. Then, input from measurements is needed, and some of the results of this study can be used as template values to be used in similar buildings. An air infiltration model, developed based on detailed field observations, is also presented in this study. The models for airflow through large openings, used in IDA-ICE energy simulation program, are also examined here and compared with the field measurement of one of the case studies. Finally, the wind tunnel model studies are conducted for wind driven airflow through door openings. Based on the wind tunnel studies, tuning constants for a simple model for wind driven airing through doors are presented.

1.6. Methods

The current study is based on field measurements including pressurization tests, the so-called Blower door method, tracer gas decay method for quantifying the airtightness and airing flow rates. IR-Thermography and other leakage identification methods are also tested and utilized. Weather parameters are monitored and in one of case studies, a permanent weather mast is installed in the vicinity of a church as well as inside the church. Direct airflow velocity and smoke visualization is also measured during open-door airing in Hamrånge church. Different analytical air infiltration and airing model predictions are evaluated by comparing with field measurement in different churches. Some corrections are presented for the current air infiltration model improvement. Besides, an air infiltration model is being developed and a version is presented. The IDA-ICE indoor climate and energy simulation program is used in this study and its model for airflow through large openings is examined. Wind tunnel model studies including tracer gas and hot-film anemometry are performed for wind driven airing measurements. In addition, smoke visualization is used for analyzing the flow patterns.

1.7. Limitations

Field measurements are often costly and the measurement methods for air infiltration and airing suffer from some uncertainty. In addition, finding

appropriate time for the measurements regarding the availability of the investigation site, i.e. the churches, equipment and the technician staff was also limited, especially because the church buildings were in frequent use. Uncertainty sources include wind effect; extrapolation to realistically low pressure differences in pressurization tests; incomplete air mixing and air shortcutting in porch area during tracer gas tests. Analytical models suffer from great uncertainty because they are not designed for large, leaky single zones like churches but rather for normal residential buildings. Uncertainties in the input to the models also affect their predictions, for instance, exact estimation of the leakage distribution is impossible with the current measurement methods. However, the leakage estimation is in this study improved by field investigations including IR-Thermography. Regarding weather uncertainties, local weather masts have reduced these, although there is always some uncertainty in what the conditions are in the very vicinity of the buildings, and of open porches in particular. Reliable air change rate values from tracer gas decay method requires that the indoor air is well mixed. By measuring in several positions it became clear that this was practically always the case, since almost all measurements were performed when some indoor heating was taking place, yielding strong, natural convective air mixing currents. In a case with no heating, mixing was ensured by installing some powerful mixing fans during the measurements. Also in the wind tunnel model measurements, a small mixing fan was used to ensure the air mixing inside the model.

1.8. Outline of the appended papers

Confer "List of appended papers"

Paper I: The LBL and AIM-2 air infiltration models are examined and evaluated for large single zone building envelopes like churches. Both wind and buoyancy induced airflows are taken into account in the models. The model predictions are compared with tracer gas decay measurement in three different churches. Field measurement include pressurization tests as well as direct measurement of the weather parameters such as air temperature and wind speed at the buildings site. IR-Thermography was also used in order to locate the leakage and have a better guesstimation of the leakage distribution by field audit. Various versions of the models were used considering the position of Neutral Pressure Layer (NPL) as well as the crawl space in the model. A correction factor of 0.8 is also suggested in order to improve the model prediction, adjusting to large single zones.

Paper II: A numerical infiltration model is developed based on the NPL position. Both laminar and turbulent flow is considered via using the Poiseuille flow equation to model leakages. The model was calibrated by using NPL and pressurization test data. After calibration, the model was used in

order to predict the air infiltration rate within three different occasions, totally covering 90 hours period. The model functionality is proved by validating the model with measurement in one of the case studies.

Paper III: Wind induced ventilation and infiltration through the opening is investigated by Particle Image Velocimetry (PIV) measurements and wind tunnel model studies using a 1:200 scale model. The drag force induced by wind over the tested model, of a church, as well the wind blockage by the building body was investigated. It is shown that the number of stagnation point depends on the wind direction. The complexity of wind induced flow through an opening is investigated by showing that wind can flow through or around the opening. Pressure distribution on and around the building model is also monitored, because the distribution of the air streaming out over the windward façade depends on the distribution of the stagnation points over it.

Paper IV: Single-sided ventilation through porches of five different churches is investigated by field measurements including tracer gas decay method, direct air velocity measurement at the porch (in one of the cases) as well as air temperature and wind speed measurements. Flow pattern within the porch during the airing period is also illustrated by smoke visualization. The most common airing models for single-sided ventilation through large opening are examined and evaluated in this study. A practical diagram is also presented for buoyancy driven airing flows, which indicate the percentage of the exchanged air after a particular period of airing in a church with specific volume.

Paper V: The models used in IDA Indoor Climate and Energy (IDA-ICE) regarding the airflow through large vertical openings are examined by comparing with field measurements of single-sided airing through a porch of an ancient church. Such airing flows directly affect the thermal comfort, energy usage and the climate condition of the interior, and therefore should be predicted precisely by simulation programs. The simulated single-sided airflows through a side door of the church were of the same magnitude as the measured ones; however, the effect of wind direction was less present in the simulations.

Paper VI: Wind driven airing flow through porch openings is investigated by wind tunnel model studies. Tracer gas method was used in order to measure the flow rates and the method proved useful even in small scale models, set in the wind tunnel. The effect of a draught lobby and terrain roughness on the flow rates is also investigated. Fluctuations of the wind stream along the opening, flow pumping and the relative turbulence intensity is illustrated by smoke visualization in order to explain the driving mechanisms of the wind-induced flow. Tuning constants for a simple equation for wind driven flow through porches are presented.

1.9. Co-author statement

Confer “List of appended papers”

Papers I, IV and VI
The study was organized and planned by the author, Abolfazl Hayati, together with the supervisors, Associate Professor Magnus Mattsson and Professor Mats Sandberg. The field measurements and data collection were performed by the author together with Associate Professor Magnus Mattsson regarding Papers I, IV. The wind tunnel measurements and data collection were performed by the author regarding paper VI. Abolfazl Hayati did the literature review, analyzed and interpreted the data, presented the modelling results, wrote and revised the papers under supervision of the supervisors. Abolfazl Hayati is the corresponding author of the articles.

Paper II
The study was organized and planned by the author, Abolfazl Hayati, together with and based on an initial idea of Associate Professor Jan Akander. The field measurements and data collection were performed by the author together with the Associate Professor Magnus Mattsson. Abolfazl Hayati did the literature review, analyzed and interpreted the data, presented the modelling results, wrote most of the article and revised the paper under the supervision of the co-authors. Abolfazl Hayati is the corresponding author of the article.

Paper III
Abolfazl Hayati contributed in data collection, writing and revision of the paper.

Paper V
The study was organized and planned by the author, Abolfazl Hayati. The measurements were performed by the author together with the Associate Professor Magnus Mattsson. Abolfazl Hayati did the literature review, analyzed and interpreted the data, performed the numerical simulations, presented the results, wrote the article and revised the paper. Valuable advices and comments were given by Associate Professor Magnus Mattsson, Professor Mats Sandberg and Associate Professor Jan Akander. Abolfazl Hayati is the corresponding author of the article.

2. Literature review

2.1. Natural ventilation modelling

Natural ventilation, as the most available sort of ventilation, is the outdoor flow penetrating into a building through purpose provided openings on the building envelope. Generally there are different types of natural ventilation including single-sided ventilation, cross ventilation and stack ventilation (Awbi, 2008). Other sorts of natural ventilation are also found in the literature, such as corner ventilation but these are a kind of cross flow when the openings are located on the adjacent facades (Daish *et al*., 2016). In all sorts of natural ventilation, the size and characteristics of the opening is known and there is the least control over the flow, i.e. by closing or opening the vents otherwise it is totally driven by the climatic conditions (Awbi, 2003). Openings used for natural ventilation purposes can be divided into windows, doors, stacks, vertical flues, roof ventilators or wind catchers and other purpose provided/designed openings (ASHRAE, 2013a).

Airing, including both cross ventilation and single-sided ventilation, is inexpensive and often available. However the lack of control of natural ventilation system is also a major factor, the airflow rates are fairly uncontrollable due to high dependence on the outdoor conditions. The only controlling mechanism is to open or close the openings since there is no control over the outside weather conditions. In this regard, some references refer to building height/width ratio as a crucial parameter. According to Awbi (2003), single-sided ventilation through a simple opening like window is effective over an inner zone that stretches a distance of about 2.5 times the ceiling height. BRE Digest 399 (Building Research Establishment, 1994) recommends a window area of 1/20 floor area and room depth of up to 2.5 times the ceiling height for single-sided ventilation. The same reference recommends cross ventilation for depth of more than 2.5 H and up to 5 H, because wind pressure can provide larger flow rates (Awbi, 2003).

Stack ventilation is driven by the temperature differences between inside and outside and the cold outside air penetrating inside is extracted through a chimney or atrium or any other vertical path (Stabat, Caciolo and Marchio, 2012). Awbi (2003) has stated that the stack ventilation is mostly suitable for cold and windy conditions but in milder weather conditions it must be also provided with a form of single-sided ventilation, for example windows, in order to provide enough airflow rates.

Instead of using mechanical ventilation, in some buildings there are some openings implemented around windows in order to take benefit of natural ventilation driven by wind and temperature difference between inside and outside. Here by airing it means opening of windows or doors temporarily in order to refresh the inside air. Airing is an effective way to remove the air pollution from inside and it has an effect on the energy usage in case if it is needed for warming or cooling. Thus, it is more suitable for moderate climate not the cold ones regarding the energy point of view otherwise the incoming air should be warmed up. However, it can be used in any climates in order to refresh the inside air and remove the contaminants.

Airing is commonly used during summertime in milder climates for escaping overheating and taking benefit of natural colder air in order to save energy for cooling and maintaining thermal comfort (Stabat, Caciolo and Marchio, 2012). Cooling by natural ventilation especially diurnal airing is investigated by Barnard & Jaunzens (2001) and van Moeseke, Bruyère, & De Herde, (2007). Cooling capacity of the single-sided ventilation is lower than the cross ventilation since it provides less air change rate than the cross ventilation, but it is much more common especially in office buildings and cellular buildings which have the openings only in one side. Moreover, due to privacy and security concerns, fire safety requirements and control of air velocityit is difficult to implement cross ventilation despite its higher efficiency (Stabat, Caciolo and Marchio, 2012).

The driving forces for natural ventilation are the buoyancy effect, also called stack effect, and the wind effect. Air infiltration has these driving forces but deals with adventitious flow through leakages in the building envelope. Both air infiltration and natural ventilation are highly dependent to the weather conditions. Therefore, there are also mixed-mode or hybrid ventilation systems, which take benefit of natural ventilation when available for saving energy.

Different parameters can affect the natural ventilation flow rates like building height, location and the surrounding terrain, opening size and its position on the envelope, air tightness and the leakage distribution, weather conditions, wind characteristics such as speed, turbulence and direction. The building itself also affects the wind flow pattern around it. Besides, ingress of pollutants and noise can affect the natural ventilation strategy.

The largest difference between infiltration and airing is that air infiltration is the adventitious amount of air entering to the interior volume, whereas airing is done deliberately by opening a window or door and letting the fresh air come into the building. However, they are both affected by the building shape and governed by the weather conditions both inside and outside.

Adventitious ventilation such as air infiltration can be reduced by making the building envelope air tight, which is too challenging and often esthetically impossible in case of cultural heritage buildings. On the other hand, if the building is too tight, moisture and contaminant concentrations can increase and may cause health problems and mold problems. Especially in large single zone buildings like churches when occasionally there are many people

inside, for example in religious aggregations, it may be of extra importance to remove the air pollutants and introduce fresh air to the interior volume. A study performed by (Awbi, 2015) has shown that indoor pollutants can be noticeably increased in airtight buildings, leading to worsen indoor air quality; thus in turn it can cause health problems, especially with those suffering of asthma.

The mechanical ventilation is more common in the new buildings but especially in older buildings, natural ventilation dominates. According to an AIVC (Air Infiltration and Ventilation Centre) survey, carried out by using samples from 14 developed countries, the most dominating ventilation system in domestic buildings was natural ventilation (Limb, 1994; Awbi, 2003). Moreover, airing can be a completing solution also for mechanically ventilated buildings.

Airing has historically been treated for different purposes, for example minimizing energy use for cooling effect in moderate climates by opening the windows; refreshing the interior volume and maintaining thermal comfort in the offices exclusively in moderate climate or during summer conditions; providing fresh air in school rooms and maintaining the acceptable CO_2 level in classrooms. Airing is also studied as a supplementary to mechanical ventilation to fulfill the regulation demands regarding thermal comfort and CO_2 levels. In milder climates, window opening (both single-sided and cross flow) is often practiced to supplement the ventilation requirement (Awbi, 2003).

According to current literature, airing is mostly studied as airflow through windows, but in rare cases through internal doors, through which the flow is only thermally driven. Airing can also be conducted via controllable trickle ventilators, which are apertures or slots incorporated into window frames or other components of the building envelope. Airing through windows is likely to be practiced more often than through external doors, though doors might be used for occasional intensified airing. Particularly in multi-zone buildings like offices, schools and multi-family houses, windows are directly connected to the outside air, while there may be no direct external door.

One of the earliest reported studies on airing was performed by Rydberg (1945), who imitated airing through windows by using a scale model with saline water as working fluid. Eftekhari (1995) studied the thermal comfort by measuring the temperature and velocity at different positions in an office provided with single-sided ventilation through a window and found that the fresh air is generally well distributed and thermal comfort can be achieved during most of the summer days in small offices.

Heiselberg, *et al*. (2001) studied the characteristics of airflow through open windows, in particular the importance of window arrangement and its effect on draught and thermal comfort. They concluded that the top or bottom-hung windows are better for single-sided ventilation in winter for cold climates due to thermal comfort issues. In summer, however, side hung windows are preferable to provide enough airflow rate since the indoor-outdoor temperature difference (buoyancy force) is low. Stabat, Caciolo *et al*. (2012)

also studied single-sided ventilation through different type of windows; they tested horizontal and vertical sash window and top hung window.

There are several studies pointing out the necessity of window opening as a complementing method for airing at schools, for example (Liese and Usemann, 1980) concluded that without presence of mechanical ventilation, windows should be opened every 15 minutes in order to keep the CO_2 level in acceptable levels of below 1000 ppm during pupils' attendance. According to Swedish standards, concentration of CO_2 should not exceed 1000 ppm in schools and other work places (AFS 2009:2, 2009). Some studies have been performed in Sweden and also other countries in Europe in order to measure CO_2 level at schools. They frequently mention that the amount of ventilation flow rate is too low in schools during occupancy of pupils (Andersson and Sverdrup, 1992; Sundell and Kjellman, 1994; Nilsson, 1996; Harrysson, 1998; Wargocki *et al*., 2002). Nordquist (2002, 2007, 2008) found window airing a practicable complement to mechanical ventilation in schools.

Different methods are found in the literature for measuring the amount of incoming air both in air infiltration and airing cases. The concentration decay method measures the flow under the natural conditions (Magnus Mattsson, Lindström, Linden, & Sandberg, 2011; Abolfazl Hayati, Mattsson, & Sandberg, 2017). Besides, pressurization tests can give a value of the total leakage, i.e. the effective leakage area ELA, although the method suffers some uncertainties due to wind and stack effect (Mattsson *et al*., 2013). There are also methods for identifying the position of the leakage on the building envelope of churches, such as IR-Thermography (Mattsson *et al*., 2011a).

Tracer gas is a possible method for measuring the airing flow rate, in which the concentration of a tracer gas in the ventilated space is measured before and after airing, i.e. before and after opening and closing of the window or door; this has been practiced e.g. by (Nordquist, 2002). Another method is to measure air velocities at several positions in the opening, and multiply by associated sub-areas of the opening, thus giving the total amount of airing (Caciolo, Stabat and Marchio, 2011).

Blomqvist (2009) did measurements on buoyancy-driven air flow through indoor openings, both vertical openings as doors and horizontal openings as stairwells. Gravity currents propagate horizontally driven by the density difference. They propagate either as cold gravity currents along floors or as warm gravity currents along ceilings. Further, he performed both model tests with saline water as operating fluid and full-scale tests in an apartment of 70 m^2 floor area with the volume of 175 m^3. He concluded that the buoyancy driven bidirectional flow through vertical internal doorways often are greater than the flow rate generated by a mechanical ventilation system. Blomqvist concluded that in order to change the bidirectional flow into a unidirectional flow the flow rate generated by the ventilation system must at least be three times the flow rate through the door generated by buoyancy.

The general trend is to build more and more airtight buildings, and the need for airing as a complement to even mechanical ventilation is obvious regarding refreshing the interior volume. Therefore, the prediction of airing

flow is of extra importance for the natural ventilation design. Besides, prediction of the natural ventilation is also essential for calculating energy saving values, thermal comfort as well as for designing and tuning ventilation systems.

The indoor-outdoor pressure difference is a combination of the buoyancy and wind induced pressures in case of natural ventilation. The indoor pressure is also regulated by the total indoor-outdoor pressure difference maintaining a flow balance between the total air in- and exfiltration (Walker and Wilson, 1993). Therefore the total airflow through a leakage or an opening, as a result of the relation between the pressure difference over the opening or leakage, is dependent on the magnitude of the driving forces and also the shape, size, and position of the openings (ASHRAE, 2013a). The buoyancy induced pressure difference is dependent on the height of the opening relative to the position of the neutral pressure layer (NPL), at which there is no pressure difference in the absence of wind (ASHRAE, 2013a).

Different studies have been performed on the combination of wind and buoyancy effects, based on wind tunnel, tracer gas and PIV measurements, and also mockup or full-size model studies. Especially regarding airing through large openings, measured quantities include wind velocity, air velocity through entrance, turbulent intensity, air temperature, air change rate and air velocity inside the room (for thermal comfort purposes). Furthermore, Computational Fluid Dynamics (CFD) simulations considering wind and/or buoyancy effect are also found in the literature (Awbi, 1996; Cook, Ji and Hunt, 2003; Wang and Chen, 2012). For instance, Caciolo (2010) performed on site measurements including PIV measurements of the flow up till mid-height of a window and he realized that the averaged velocity field has a similar pattern to the buoyancy driven airflow. Different empirical models are found in the literature regarding combining buoyancy and wind effect. The models normally contain some empirical coefficients and correlations based on wind tunnel and or onsite measurements. Such models are fairly easy to use and implement in the building energy codes. For instance, De Gids and Phaff (1982) developed an equation for predicting what they call the effective air velocity and airflow through windows considering both buoyancy and wind effect based on field measurements from 33 buildings; their model is used in European standard, EN15242 (BSI, 2007).

Based on a similar study, Larsen and Heiselberg (2008) derived a rather more complex equation for combining airing flow due to buoyancy and wind including wind direction. They found that the most dominating force depends on the wind direction; for example on the windward side of the building wind is the dominating force while it is the temperature difference on the leeward side. They introduced three categories of constants in their model based on three different intervals of wind direction, i.e. windward, leeward and parallel to the building.

Caciolo (2010) developed a model for wind driven flow. Caciolo, Stabat *et al*. (2011) concluded that combination of the wind and buoyancy effect

depends on wind direction. They also concluded that wind velocities higher than 1.5 m/s can indeed increase the total air change rate.

Further, Chu, Chen and Chan (2011) investigated the effect of wind angle and concluded that the maximum air change rates can occur having wind directions between 45° and 67.5° oblique to the façade. On the other hand, having the opening on the leeward position, i.e. wind angles between 112.5° and 157.5°, leads to the minimum airflows.

2.1.1. Wind induced pressure

Wind induced pressure can be calculated by Bernoulli equation assuming that there is no pressure losses or height change (ASHRAE, 2013a), see Equations 1-4.

$$P_w = C_p \rho_o \frac{U^2}{2} \tag{1}$$

$$\Delta P_w = 0.5 \rho_o C_p U^2 - P_{w,i} \tag{2}$$

$$P_{w,i} = -0.5 \rho_o C_{pi} U^2 \tag{3}$$

$$\Delta P_w = 0.5 \rho_o (C_p - C_{pi}) U^2 \tag{4}$$

where P_w (Pa) is the wind surface pressure relative to the outdoor static pressure of the undisturbed flow; ρ_o (kg/m^3) is the outside air density and can be assumed as 1.2. Subscripts "*i*" and "*o*" refer to the parameters for inside the building and outside the building respectively. U (m/s) is the (undisturbed) wind speed and C_p [-] is the wind surface pressure coefficient. The magnitude of C_p at a point on the building surface depends on the building shape and geometry, wind speed and direction relative to building, building position and the topography and terrain roughness around the building (Awbi, 2003). In a building with sharp edges, flow separation occurs at the sharp edges and therefore the C_p value is independent of Reynolds number, i.e. wind speed. Typical values for the pressure coefficient can be gained in the literature (Liddament, 1986; ASHRAE, 2013b).

2.1.2. Wind speed

If the wind speed data is not gained by direct measurements at the building site, then the data from the weather station should be used. However, wind speed data are normally measured at the height of 10 meters above the floor/ground level. Therefore, the wind speed data should be converted to the position and height of the building considering the related terrain characteristics. For instance, Equation 5, which is a power law type formula, can be used:

$$\frac{U}{U'} = \alpha \left(\frac{H_{building}}{10}\right)^{\gamma} / (\alpha' \left(\frac{H'}{10}\right)^{\gamma'}) \tag{5}$$

where $H_{building}$ and H' (m) are height of building and wind speed measurement site respectively. α and γ are terrain parameters; primed values indicate parameters of the weather station and unprimed ones are for the location of building. Values for α and γ adjust the wind speed measured at the weather station to the related parameters at the specific terrain of the building location and can be gained from Table 1.

Table 1: Terrain parameters for standard terrain classes (Sherman and Grimsrud, 1980a).

Class	γ	α	Description
I	0.10	1.30	Ocean or other body of water with at least 5 km of unrestricted expanse
II	0.15	1.00	Flat terrain with some isolated obstacles (e.g. buildings or trees well separated from each other)
II	0.20	0.85	Rural areas with low buildings, trees, etc.
IV	0.25	0.67	Urban, industrial or forest areas
V	0.35	0.47	Center of large city

2.1.3. Stack induced pressure

The buoyancy, or stack induced pressure, P_s (Pa), is based on the height difference relative to the position of the neutral pressure layer, NPL, and can be calculated using Equations 6-9, assuming colder air outside:

$$\Delta P_s(h) = \rho_o g h \frac{\Delta T}{T_i} - P_{s,i} \tag{6}$$

$$P_{s,i} = (\rho_o - \rho_i) g H_{NPL} = \rho_o g H_{NPL} \frac{\Delta T}{T_i} \tag{7}$$

$$\Delta P_s(h) = (\rho_o - \rho_i) g (h - H_{NPL}) = \rho_o (\frac{T_i - T_o}{T_i}) g (H_{NPL} - h) \tag{8}$$

$$\Delta P_s(h) = \rho_o \frac{\Delta T}{T_i} g (h - H_{NPL}) \tag{9}$$

where T_o and T_i (K) are the outdoor and indoor temperatures, ρ_i (kg/m^3) is the indoor air density, g (m/s^2) is the gravitational constant, h (m) is a certain vertical height along the opening or façade and H_{NPL} (m) is the height of the neutral pressure level above reference plane, occurring without any driving forces except buoyancy.

2.2. Flow through individual opening or leakage

In general, air infiltration flows have relatively low values of Reynolds number, suggesting that viscous effects are dominant. However, flow through individual openings can be laminar or turbulent. Flow is laminar when velocity field does not have random components and just some random components from boundary conditions may arise. An example for the steady laminar flow is the buoyancy driven flow through an opening in the building façade. Laminar unsteady flow can also occur if the pressure is induced by turbulent wind. The turbulent flow can occur when the velocity pattern is unsteady and with variations around the average value. If the wind speed and direction is kept constant, the variation part will be also constant and then the turbulent flow is steady.

The airflow through an opening or a leakage in the building envelope is a complicated phenomenon and depends on the size and position of the leakage path as well as the pressure difference over them. By solving the air mass balance through the whole building envelope the total air inflow and outflow can be calculated. However, based on the opening type and type of the flow, being laminar or turbulent, there are some previously developed equations for calculating the flow rates (Awbi 2003).

Large openings

If the opening has a relatively large area, it can be considered in the category of the large opening, such as windows, doors, large vents, large cracks or holes in thin construction. Flow inside such opening tends to be approximately turbulent allowing for normal pressures. In such openings, flow is related to the square root of the pressure difference across the opening and the so called orifice equation, i.e. Equation 10, can be used (Awbi, 2003):

$$Q = C_d A \sqrt{\left(\frac{2\Delta P}{\rho}\right)} \quad \textit{(The orifice equation)} \tag{10}$$

where, Q (m^3/s) is the airflow rate, C_d [-] is the discharge coefficient, A (m^2) is the opening area, ρ (kg/m^3) is the density of air at a reference temperature and pressure. ΔP (Pa) is the pressure difference across the opening. For a single opening, ΔP can be assumed as the superposition of wind and stack induced pressures, i.e. the sum of Equations 4 and 9 (Awbi, 2003).

In case of sharp edge orifice flow, the discharge coefficient C_d is independent of Reynolds number and C_d can be assumed as 0.61 (Awbi, 2003). However, for building openings, the discharge coefficient is dependent on the geometry of the opening and the variation in pressure difference between inside and outside. According to the BS 5925 (BSI, 1991), Equation 10 is recommended for calculating the air flow through openings with a diameter larger than approximately 10 mm.

Small openings

The Couette equation can be used for laminar flow in very narrow openings like cracks with deep flow paths (Awbi, 2003), see Equation 11:

$$Q = \left[\frac{Lh_{crack}^3}{12\mu d_{crack}}\right]\Delta P \quad \textit{(The Couette flow equation)} \tag{11}$$

where L (m) is the length of the crack, h_{crack}, (m) is the height of the crack, d_{crack}, (m) is the depth of crack in flow direction, μ (N·s/m²) is the dynamic viscosity of air.

For wider cracks, in which flow is in the transition region, the crack flow equation can be used, i.e. Equation 12, which is a form of power law equation (Awbi, 2003):

$$Q = kL(\Delta P)^n \quad \textit{(Crack flow or power law equation)} \tag{12}$$

where k $(m^3s^{-1}m^{-1}\rho\alpha^{-n})$ is the crack flow coefficient, which is a function of crack geometry and the values can be chosen from tables in the literature (BSI, 1991). ΔP (Pa) is the pressure difference across the leakage. n [-] is the flow exponent and depending on the flow regime it can have a value between 0.5 (for fully turbulent flow) and 1 (for fully laminar flow). In practice, the value of n for cracks and adventitious leakages is between 0.6 and 0.7.

Mass flow through porous materials

Airflow through porous material is laminar and can be calculated by Darcy's law (White, 2011), see Equation 13:

$$u = -\frac{B_0}{\mu}\cdot\frac{dP}{dx} \quad (Q = u \cdot A) \quad \textit{(Darcy's law of porous flow)} \tag{13}$$

where u (m/s) is the mean velocity of air through the porous material or the aperture, B_0 (m²) is specific permeability of a material, and $\frac{dP}{dx}$ (Pa/m) is the pressure gradient over the porous material.

Airflow in cracks/cavities

The other equation for the airflow through cracks and cavities is the Poiseuille equation (White, 2011), see Equation 14, which is a form of quadratic equation and contains terms regarding both the laminar and turbulent flow:

$$\Delta P = \left(\xi + \lambda_f \frac{B}{D_h}\right)\rho\frac{u^2}{2} \quad \textit{(Poiseuille equation)} \tag{14}$$

where ξ [-] is the entry and exit loss term and can be set to 1.5, B [m] is the thickness of construction (or the crack depth), D_h (m) is the hydraulic diam-

eter, λ_f [-] is the Poiseuille flow friction factor which represents the laminar part of the flow. λ_f depends on the shape of the aperture or the leakage path and it can be set to 64/*Re* if the aperture is circular and 96/*Re* if the aperture is rectangular with infinite length. *Re* is the Reynolds number, see Equation 15.

$$Re = \frac{\rho u D_h}{\mu} \tag{15}$$

2.3. Air infiltration prediction and modelling

The air infiltration in the building cannot be gained only by visual inspection or from the building age. There are methods such as pressurization tests and tracer gas method in order to quantify the total amount of the air tightness and air infiltration (Cooper *et al*., 2011a). There are also some other leakage detection methods such as IR-thermography, using smoke as an indicator, or using particle counters (Mattsson *et al*., 2011a).

The other issue is that air infiltration is dependent to the weather conditions and the results of the pressurization or even tracer gas tests are limited to the measurement period. There are even passive tracer gas techniques, which can give a value over a time span of up to many days, but again the air infiltration result is an average over the whole period. Such methods are costly and the ability to perform the measurements over a larger time span is limited also due to fact that the building are in use, for example the doors, the windows or the ventilation ducts cannot be closed all the time for air tightness measurements.

The pressurization test, "Blower door", does not give a value for the air infiltration during natural conditions, because the building is pressurized to much higher levels than normally occurring. The value can be extrapolated to lower pressure differences, bearing in mind high uncertainty of extrapolating the Blower door test results to lower pressure differences of around 4 Pa (Mattsson *et al*., 2013). There are other pressurization tests such as pressure pulse method, in which the building is pressurized up to lower pressure differences of around 4-6 Pa, which is closer to natural conditions (Cooper *et al*., 2011a, 2011b). The pressure pulse method has been in the research level, however, the method is being developed and also commercialized by introducing more practical and portable equipment (Build Test Solutions, 2017).

In fact, air infiltration is a dynamic phenomenon and can vary a lot depending on the weather conditions. Therefore, some equations are developed based on the pressure flow relation considering both buoyancy and wind effects. These methods are not purely analytical and contain some coefficients by fitting the equation into the measurement data. Therefore, they are called the semi empirical models, intended to be used in order to predict the amount of the air leakage over longer periods. These models do need to be fed with some input data, such as the wind and temperature data, the leakage characteristics and their distribution on the building envelope, pressure distribution

and wind pressure coefficient (Awbi, 2003; ASHRAE, 2013a). Some models take also into account the mechanical ventilation, if the building is not only naturally ventilated. Some of the inputs are difficult to access, and therefore some assumptions may be assigned which affects the accuracy of the air exchange rate predictions (ASHRAE, 2013a). These sort of models are appropriate for adjusting the size of cooling and heating plants (Awbi 2003).

The air infiltration models can be divided into single-zone and multi-zone models (Awbi 2003). The common method for multi-zone models is the so-called nodal methods, in which each zone is considered as a separate temperate and pressure node and the nodes are connected in serial or parallel to each other, and there is the assumption that air is well mixed in each zone. The power law, or quadratic equation, i.e. Equations 16 and 17 respectively, are used for the air-pressure relation. The air infiltration is gained by solving the pressure of each zone considering the mass balance between the air in- and exfiltration in the nodal network. Multi-zone or multi cell models are used in airflow calculation programs like CONTAM and COMIS (Feustel, 1999; Dorer *et al*., 2001; Haas *et al*., 2002; Dols and Polidoro, 2015).

In single-zone models, the interior of the building is defined by a uniform temperature and pressure, i.e. air is considered as well mixed. The pressure node inside the zone is connected to the external pressure nodes. The well-mixed assumption implies that there is ignorable airflow resistance inside the zone and air can freely move inside (Awbi, 2003). In fact, single-zone model uses some functions for combining the wind and stack induced flow and often have some empirical coefficients based on special type of buildings. There are some examples of single zone models like the models developed by the Building Research Establishment (BRE) (Warren and Webb, 1980), the Lawrence Berkeley National Laboratory (LBL) (Sherman and Grimsrud, 1980a, 1980b), the University of Alberta (AIM-2) (Walker and Wilson, 1990). Other examples include British Gas model (VENT), ENCORE (Norwegian Building Research Institute model), Gas Research Institute/ Institute of Gas Technology model, Reeves, McBride, Sepsy and NRC (National Research Council Canada) air infiltration models (Liddament and Allen, 1983; Shaw, 1985; Reardon, 1989).

For the LBL and AIM-2 models, there are *basic* and *enhanced* versions, resp. (ASHRAE, 2013a). The basic versions uses the effective air leakage area at 4 Pa, estimated from an ordinary whole-building pressurization test. The enhanced models use pressurization test results to characterize the air leakage by the pressurization flow coefficient C and the flow exponent n, see Equation 16. Both versions also need input of assessed leakage distribution over the building envelope as well as weather parameters and information about wind shelter and terrain pattern around the building. The enhanced versions tend to yield better prediction accuracy, typically ±10% when the parameters are well known (Sherman and Modera, 1986; Palmiter and Bond, 1994; Walker and Wilson, 1998). All mentioned single-zone models can be sensitive to the input values, and these are sometimes difficult to determine.

Regarding air infiltration there are two widely used equations coupling the relation between indoor-outdoor pressure difference and flow rate:

- Power law equation:

$$Q = C\,\Delta P^{n} \tag{16}$$

- Quadratic equation:

$$\Delta P = C_1 Q + C_2 Q^2 \tag{17}$$

where C ($m^3 s^{-1} Pa^{-n}$) is the pressurization flow coefficient, in turn being equal to the total kL value in Equation 12. C_1 (Pa $m^{-3}s$) and C_2 (Pa $m^{-6}s^2$) are flow resistance coefficients in which $C_1 Q$ represents laminar flow and is more significant at low flow rates and $C_2 Q^2$ represents turbulent flow and is more significant at large flow rates. C_1 and C_2 can be gained experimentally for each opening and suggestions of their values can be found in the literature, see e.g. (Baker, Sharples and Ward, 1987).

The flow exponent, n, in the power law equation, Equation 16, can vary between 0.5 for fully turbulent flow, such as orifice leakage types, and 1 for fully laminar flow, such as the flows inside long and narrow leakage openings. A value of 0.67 has been suggested when there is a large variety of leakages of unknown nature (Walker and Wilson, 1993). Both laminar and turbulent terms are included in the quadratic equation, making it similar to the Poiseulle equation, Equation 14.

Equations 16 and 17 are used to extrapolate the leakage data of a pressurization test to actually encountered pressure differences, typically below 10 Pa. Some studies have used these equations to predict the air infiltration rate and compared results with measurement data. For instance Liddament (1987) reported that for a single family building in normal conditions, the two equations give similar results for pressure differences of more than 20 Pa, whereas for low pressures the power law equation gives better results. The validity of the power law equation has been tested through laboratory measurements, theoretical analysis of crack flow and field measurement of building envelopes, and it is indicated that the power law equation is valid for extrapolating the leakage data to ordinary (low) pressure differences (Walker, Wilson and Sherman, 1998).

However, David Etheridge compared the extrapolation results (using Equations 16 and 17) with CFD calculated leakage flows and reported that the quadratic equation, i.e. Equation 17, is preferable for extrapolating pressurization test results to lower pressure differences (for example 4 Pa) (Etheridge, 2012). Etheridge has also combined openings in parallel and in series and found indications of that the resulting flow characteristics were not quadratic for parallel leakages, and not according to the power law equation for either cases in series or in parallel (Etheridge, 2012).

Both forms of crack flow equation, i.e. the power law and the quadratic, are used in the models that use network of nodes for openings relating the external and internal pressure. An iterative process then solves the equations until the developed pressure difference satisfies the flow equation and yields a flow balance for the building.

Typically, the stack and wind induced pressures are determined via the formulas above and the total pressure is calculated by simple summation of the two pressures as well as the fan induced pressure (if available), see Figure 2. However, this is not the case regarding the total flow rate. Once each wind or buoyancy (or fan) induced flow rate is calculated by pressure flow relations (power law or quadratic form), the total flow is not a simple summation, see Figure 3. Sherman (1992) compared different superposition models and showed that the sum of stack and wind induced flow rates is always greater than the actually occurring total air infiltration rate. He suggested that in order to get the total flow rate caused by wind and stack effect, between 0 to 85%, on average 35%, of the lowest flow contribution should be added to the larger one.

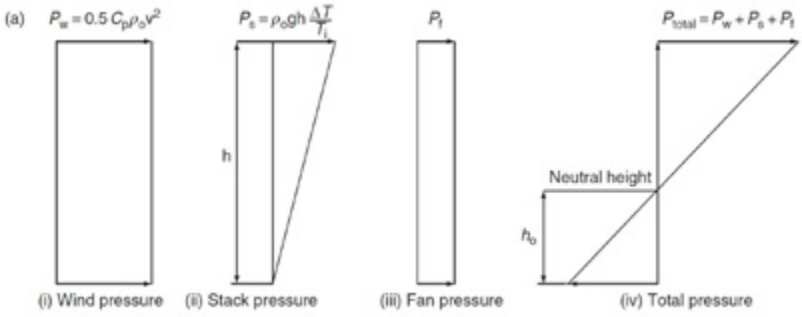

Figure 2: Total indoor-outdoor pressure difference across an opening or leakage resulting from summation of both stack, wind and fan induced pressures (Awbi, 2003).

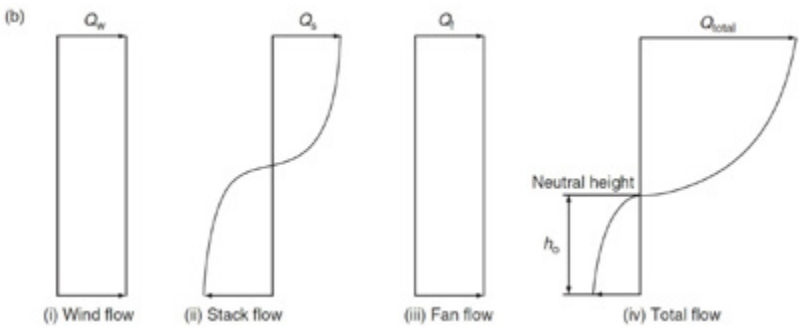

Figure 3: Total flow rate through an opening or leakage resulting from summation of both stack, wind and fan induced flow rates (Awbi, 2003).

Calculating the exact flow prediction is impossible and neither is it possible to measure the wind and stack induced flow rates separately. Therefore, different superposition methods have been developed to determine the total flow rates. In these, each wind and buoyancy (stack) induced flow, i.e. (Q_w) and (Q_s), is calculated separately with the help of power law or quadratic equation, i.e. Equations 16 and 17, and then the total flow, Q_t, is gained by the superposition. The models can be tuned by fitting to measurement data.

Below, five common superposition methods are presented:

1) The simple linearity method: The total flow is gained by the linear addition of the flow rates due to wind and stack effect (which will cause some over prediction and great errors), see Equation 18.

$$Q_t = Q_w + Q_s \tag{18}$$

2) The quadrature method: Adding wind and stack driven infiltration flow rates in quadrature (The stack and wind induced *pressures* are simply added, and then they are replaced with their equivalent flow rates, using power law equation with the assumption that flow is fully turbulent), see Equation 19. The method is also used in Lawrence Berkeley Laboratory (LBL) model (Sherman and Grimsrud, 1980a).

$$Q_t = \sqrt{Q_w^2 + Q_s^2} \tag{19}$$

3) The simple pressure method: Pressure addition was used by Shaw (1985) for a variable *n* model, the process is similar to the quadrature method but the flow exponent of *n*, gained from pressurization (Blower door) test is used in the equation, i.e. Equation 20, instead of using the fixed value of 0.5 for the flow exponent in the quadrature method, i.e. Equation 19.

$$Q_t = [Q_w^{1/n} + Q_s^{1/n}]^n \tag{20}$$

4) The method including interaction between stack and wind effects: interaction method or the AIM-2 model (Alberta Infiltration Model), see Equation 21:

$$Q_t = [Q_w^{\frac{1}{n}} + Q_s^{\frac{1}{n}} + \beta(Q_s Q_w)^{\frac{1}{2n}}]^n \tag{21}$$

in which, the $\beta(Q_s Q_w)^{\frac{1}{2n}}$ term identifies the interaction term between the wind and stack effect. β is a constant factor and is suggested a value of -0.33 (Walker and Wilson, 1990, 1993).

In case when either stack or wind effect dominates, β disappears, and if they both have identical infiltration effects, Equation 22 can be used:

$$\beta = (2^{(\frac{1}{2n})} - 2) \tag{22}$$

5) Etheridge's model (Etheridge, 1977; Walker and Wilson, 1993), see Equations 23-24:

$$Q_t = [\left(\frac{r}{2}\right)^2 + r(Q_w + Q_s) + Q_w^2 + Q_s^2]^{1/2} - r/2 \tag{23}$$

$$r = \frac{C_1}{C_2} \tag{24}$$

where r [-] is the ratio between the flow resistance coefficients C_1 and C_2, see equation 17; r can be set to zero in case of fully developed turbulent flow and is undefined for fully developed laminar flow since ($C_2 = 0$), in the latter case r should be set to one. Etheridge by using two reference pressures of 1 and 10 Pa, suggested that r can be gained via Equation 25:

$$r = \frac{C(1 - 10^{2n-1})}{(10^{n-1} - 1)} \tag{25}$$

Walker and Wilson (1993) compared different superposition models including Linear addition, Pressure addition, Quadrature (i.e. LBL model) and AIM-2. They concluded that the simple pressure addition, i.e. the LBL model is the best choice because it is simple and physically realistic. They compared the prediction results with air infiltration measured at two test houses and showed that the prediction errors for both LBL and AIM-2 models were up to 10% while for the simple addition method the error was up to 50%.

The Lawrence Berkeley Laboratory (LBL) model and the Alberta air Infiltration Model (AIM-2) are the two most advanced air infiltration models based on input from pressurization (blower door) test. The input to the LBL and AIM-2 models are flow coefficient and flow exponent gained from a pressurization test, the temperature inside and outside, building height, wind velocity and an estimation of the leakage distribution over the building envelope. Especially the latter is a great source of uncertainty in the models because there are no direct measurement methods for quantifying individual leakages in the building envelope. However, pressure measurements and IR-thermography can be useful to get an idea of the leakage distribution. More details on the LBL and AIM-2 models, and comparison with field measurements in churches, are given in (Hayati, Mattsson and Sandberg, 2014).

The leakage distribution is according to the effective leakage area in LBL model, while in AIM-2 model, it is according to the total flow coefficient gained from pressurization test. The AIM-2 model is a bit more developed because, for instance, the flow exponent of the power law equation, i.e.

Equation 16, is used in the AIM-2 superposition model, i.e. Equation 21, while in LBL model, the simple quadrature method with fully turbulent flow assumption, i.e. n=0.5, is used in the superposition equation, i.e. Equation 19. Further, an interaction term regarding the wind and buoyancy induced flows is considered in the AIM-2 model while the LBL model does not include such a term. In addition, flues are included as separate leakage site in the AIM-2 model, and separate pressure coefficients are allotted for crawl space and attic.

Some studies have validated the LBL and AIM-2 models. For instance, Sherman and Modera (1986) compared air change rate measurements from 15 building sites with LBL model prediction results. They conducted tracer gas and weather parameter measurements and found that the predicted air infiltration rates were on average within 2% of the measured ones with a standard deviation of about 20%. Another study on detached houses in central North Carolina showed well agreement between the LBL air infiltration model predictions with measurements (Breen *et al.*, 2010). Liddament and Allen (1983) also compared different air infiltration models, including the LBL model, (the AIM-2 model was not included) with the measured air infiltration results from three different houses and found good agreement between the LBL prediction with the measurement data.

Other studies have pointed to better prediction results of the AIM-2 model (Wang, Beausoleil-Morrison and Reardon, 2009). These compared air infiltration data from 16 detached houses and stated that AIM-2 model predictions showed 5% underestimation, while the LBL model had 7-15% overestimation. Their study showed that the models are significantly sensitive to the input data and the predicted results can significantly vary depending on the tested kind of house. Other studies have also pointed to the overprediction of the LBL model (Persily & Linteris, 1983; L. S. Palmiter, Brown, & Bond, 1991). Francisco and Paltimer (1996) also examined the LBL and AIM-2 model predictions with air infiltration data from ten residential houses. They showed that the AIM-2 model had slightly better predictions in comparison with the LBL model. They also pointed to the over prediction of the LBL model especially for the wind induced air infiltration.

2.4. Airing modelling

Airflow through large openings like windows and doors –airing – is a complex issue. It is driven by the average pressure differences between inside and outside, generated by temperature difference (buoyancy), average wind speed and also wind turbulence. Figure 4 illustrates what the air velocity pattern at an open window might look like (Awbi, 2003). There are several previous studies regarding thermally driven airflow through large openings; buoyancy effects are more well-known than wind effects. Recently, Andersen has done a literature study on semi-empirical models of buoyancy driven natural ventilation (Andersen, 2015). However, as to wind effects, it is not only the average value of the wind velocity that drives a flow but also wind

direction and turbulence plays a significant role (Allard and Utsumi, 1992; Fürbringer and Van Der Maas, 1995; Stabat, Caciolo and Marchio, 2012). Wind turbulence impact has in turn been divided into *turbulent diffusion*, occurring in a mixing layer, and *pressure fluctuations*, generating a pulsating flow at the opening, see e.g. (Haghighat, Rao and Fazio, 1991; Haghighat, Brohus and Rao, 2000; Larsen and Heiselberg, 2008; Stabat, Caciolo and Marchio, 2012). One of the first studies regarding the effect of the predominating wind and/or buoyancy effect on the total air change rate is performed by Dick (1950). Also, it appears that wind can both *boost* or *weaken* buoyancy induced flow, see e.g. (Li and Delsante, 2001; Larsen and Heiselberg, 2008).

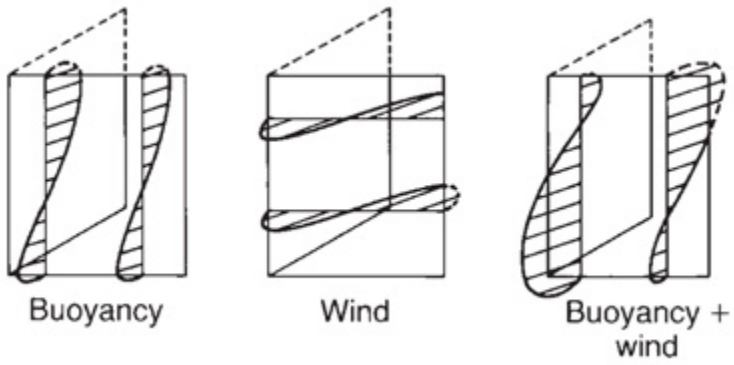

Figure 4: Buoyancy and wind induced flow pattern through a large window (Awbi, 2003).

Purely wind driven airing can occur in the absence of temperature difference, even if there is only one opening, i.e. single-sided ventilation. The mechanisms of wind driven single-sided ventilation are due to the mean airflow rates as well the fluctuation part. As just indicated, the fluctuation part consists of pulsation and the penetration of eddies (Malinowski, 1971). Pulsation is caused by fluctuating air pressure at the opening, which induces a back-and-forth because of the compressibility of the air inside the room. Therefore, the pulsation flow is dependent on the magnitude of fluctuating wind and the opening. Cockroft and Robertson (1976) studied the pulsation flow via single-sided ventilation through a single opening and concluded that a part of the incoming air is exhausted directly and therefore not all of the incoming air affects the air change rate of the whole indoor space. Based on their measurements, only 37% of the incoming air contributes to the air change rates. However, the ratio can vary depending on the frequency spectrum of the incoming turbulent air stream.

A *mixing layer theory* deals with eddy penetration into the openings. If the wind is turbulent or turbulence is produced within the opening area, then the external airflow can be conveyed indoors by eddies penetrating into the building, or, vice versa, the internal air can be extracted from the building

(Malinowski, 1971). Eddies penetrating the openings are of a smaller scale than the opening size and are less dependent on air compressibility according to (Haghighat, Brohus and Rao, 2000). Wang and Chen (2012) used CFD simulation to develop empirical models for wind driven single-sided ventilation. They used spectrum analysis and showed that with wind parallel to the opening surface, the flow is governed more by the eddy penetration. They found that with zero wind incidence angle, i.e. wind directly (perpendicularly) towards opening, the eddy penetration is zero since there is no parallel element of the wind.

Assuming only buoyancy driven airflow, Equation 26 can be used, which is very similar to the orifice flow Equation, i.e. Equation 10, considering only buoyancy induced pressure (Blomqvist, 2009):

$$Q = C_e A \sqrt{g \frac{|T_i - T_o|}{T} H} \tag{26}$$

Where H (m) is the opening height, C_e is an empirically attained coefficient and T (K) is the average temperature between the indoor and outdoor temperatures, i.e. T_i and T_o. Different values for C_e are suggested in the literature, gained from full scale and model studies; for example Van der Maas (1992) obtained 0.15 from several test arrangements. Allard, et al. (1990) performed full scale laboratory tests and gained 0.27. Lane-Serff (1989) performed model studies using saline water and gained 0.207 ± 0.005 for C_e. Kiel and Wilson (1989) performed a test arrangement with two adjacent rooms and reported $0.13 + 0.0025\Delta T$ for C_e.

Considering only wind driven airing, a simple equation was introduced by Warren (1977) based on the mixing layer theory. That theory assumes an air exchange due to the mixing layer between the outside and inside air at the opening, and that the flow can be defined by Equation 27:

$$Q = C_f A U \tag{27}$$

where C_f is a flow coefficient. Equation 27 expresses the fraction of the flow towards the opening (AU) that flows through it and therefore is a so-called catchment model (Sandberg *et al*., 2015). Different values are suggested for C_f, for example, Warren (1977) investigated the single-sided flow through one window by wind tunnel studies and field measurements using tracer gas, and suggested 0.025, if a reference wind speed at the standard height is used, and 0.1 if the wind speed within the vicinity of the window is used in Equation 27. He also showed that the flow coefficient could vary between 0.023-0.026, without having a turbulence-producing grid, and 0.034-0.035 in case of having such a grid. The value of 0.025 is used in the empirical model of the British standard model, BS 5925, for the single-sided flow through one window (BSI, 1991).

Kato and colleagues (2006) studied single-sided ventilation by model studies in wind tunnel using tracer gas; they found that the flow coefficient is equal to 0.015 for the case of one square window, located in the middle of the facade parallel to the wind when the porosity of the opening (opening area divided by façade area) was 6.25%. They also reported 0.020 for the same case but with a larger opening, with the porosity of 12.25%.

Yamanaka, *et al*. (2006) investigated single-sided flow rates through a window opening via wind tunnel model studies, CFD simulations and PIV measurements. The window opening had a circular shape and was located in the middle of a façade, having the porosity factor of 1.40%. They concluded that the pulsation theory is not applicable to all wind directions because of the ignorance of the wind incidence angle. Instead, they advocated the existence of a mixing layer. Based on the wind tunnel measurements, they suggested 0.06 for C_f, with the local wind speed along the facade as the reference U.

Other (rule of thumb) values are found in the literature (Wouters, P., De Gids, W. F., Warren, P. R. and Jackman, 1987; Riffat, 1991), suggesting 0.1 to 0.25 for C_f in case of single-sided ventilation and 0.4 to 0.8 for cross flow through windows, having the wind speed at the building height as the reference U.

A common theoretical approach to fluid flow through openings is based on the Bernoulli equation and the assumption that the so-called *orifice equation*, i.e. Equation 10, is valid (Awbi, 2003). The total pressure difference over an opening is considered being a superposition of the wind and buoyancy induced pressures, i.e. Equations 4 and 9 (Awbi, 2003). Based on the same equations, there are also some models for calculation of the airing flow rates considering both wind and buoyancy effects, designed especially for single-sided ventilation. These models include some empirically attained coefficients for trying to fit Equation 10 into measured airing flow rates. The most referred models are presented in Table 2. Further explanation of the models and test of their applicability to large single zones like churches are presented by (Hayati, Mattsson and Sandberg, 2017).

Table 2: Models for prediction of single-sided ventilation flow rates through large vertical openings.

Model developers	Main equation
British standard model BS 5925 (BSI, 1991)	$Q = Max\left(\frac{1}{3}C_d A\sqrt{g\frac{(T_h - T_c)}{T}H}, 0.025AU\right)$
De Gids and Phaff (1982)	$Q = 0.5A\sqrt{0.001U^2 + 0.0035H\Delta T + 0.01}$
Larsen and Heiselberg (2008)	$Q = A_{eff}\sqrt{C_1 f(\beta_v)^2\lvert C_p\rvert U^2 + C_2 H\Delta T + C_3\frac{\Delta C_{p,opening}\Delta T}{U^2}}$
Caciolo (2010)	$Q = \frac{1}{3}C_d A_{eff}\left(\frac{g\Delta T\Delta T^* H}{T}\right)^{0.5} + q_{wind}$

3. Method

In this part, the field study objects, i.e. the studied churches, and the conducted field measurement are presented. The methods used in the wind tunnel studies are explained thereafter. The validated analytical air infiltration and airing models are mentioned in the next part as well as the developed numerical air infiltration model. And last, the IDA-ICE simulation model is presented.

3.1. Field study objects

The field study was conducted in five historical stone churches located in Hamrånge, Söderfors and Valbo, all in Gävleborg County, Sweden, as well as Ludgo, south of Stockholm in Nyköping County, and Visby cathedral located in Visby, Gotland island, Sweden. The churches were constructed in the 13th century (Valbo), 16th century (Ludgo), 1792 (Söderfors), 1851 (Hamrånge) and mid-12th century (Visby cathedral). However, minor or major renovations have been conducted in all churches. All studied churches constitute hall churches with thick stone walls, plastered on both inside and outside, and with double outer doors to enter their large halls. They have gable roofs and inner ceilings that are plastered on the inside and insulated on the outside towards a naturally ventilated attic. The windows are double-glazed and weather-stripped. All churches are naturally ventilated without any flues and Hamrånge church has furthermore a naturally ventilated crawl space underneath a wooden floor, consisting of double boards with a ~15 cm layer of lime sand in between. Söderfors, Valbo and Ludgo churches and Visby cathedral all have stone slab floors, with some wooden inlays (Hayati, Mattsson and Sandberg, 2017).

Hamrånge church, Figure 5, located on top of a hill and much exposed to wind, has its main porch facing North but also one porch in the middle of each long side, facing West and East, respectively. Ludgo church has a main porch that is highly wind exposed, Figure 6. Söderfors church, Figure 7, has a main porch facing South and Valbo church, Figure 8, has a main porch facing North, as well as a side porch in the main hall, facing East. In addition, these churches are fairly wind exposed. Visby cathedral has a large main hall, with inner doors to some side rooms. The cathedral has, besides the main porch, several side porches, including a large (“wedding”) porch door; the latter was used for airing in this study, Figure 9. Visby cathedral is surrounded by 2- and 3-storey buildings, but there is some open space surrounding it, making also this church fairly wind-exposed. For the wind direction of the measurements, the horizontal distance between the cathedral

and the surrounding houses was around 10 times the height of those buildings; thus, the rooftop wind direction ought to be sensed also in the porch area (Hayati, Mattsson and Sandberg, 2017).

All church constructions are naturally ventilated without any flues. The churches differ significantly in volume and height/floor area ratio; additional information in this regard is summarized in Table 3. The interior zone of the churches is not perfectly cuboid since the ceilings are vaulted and resemble semi cylindrical or semi-spherical shapes. As a result, the ceiling height is not a fixed value, which the studied models presuppose. Therefore, an average ceiling height is used in the calculations relating to building envelope areas. The average height is attained by using the quotient "Room volume"/"Floor area". The calculation of building volumes and envelope areas was complicated due to the structure of ceilings and walls. In case of Hamrånge church, 3D Laser scanning is used for volume calculation, which showed 0.5% discrepancy with the calculated one (Hayati, Mattsson and Sandberg, 2014).

Figure 5: Hamrånge church, side porch visible centrally (Hayati, Mattsson and Sandberg, 2014).

Figure 6: Ludgo church, main porch on tower (Hayati, Mattsson and Sandberg, 2017)

Figure 7: Söderfors church, main porch on tower
(Hayati, Mattsson and Sandberg, 2017).

Figure 8: Valbo church, main porch on tower
(Hayati, Mattsson and Sandberg, 2017).

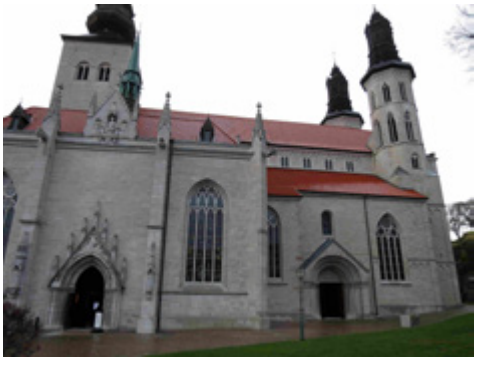

Figure 9: Visby cathedral, side porch used for airing visible
on the right (Hayati, Mattsson and Sandberg, 2017).

In Table 3, the properties regarding the size of the studied churches are presented.

Table 3: Dimensions of the studied churches and their porches

Location (Latitude, Longitude)	Volume (m^3)	Floor area (m^2)	Ceiling area (m^2)	Max ceiling height (m)	Average ceiling height (m)	Porch position	Porch size		
							Area (m^2)	Height (m)	Porch direction (°)
Hamrånge (60°55′37″N, 17°2′20″E)	7620	695	862	13.7	11.0	Side porch	5.47	2.92	250
Ludgo (58°54′58″N, 17°7′60″E)	1960	302	410	9.5	6.5	Main porch	5.38	3.02	290
Söderfors (60°23′6″N, 17°13′56″E)	4564	350	494	14.5	13.0	Main porch	5.04	2.32	260
Valbo (60°39′52″N, 17°4′12″E)	2631	349	523	9.7	7.5	Main porch	3.83	2.44	286
Visby (57°38′30″N, 18°17′51″E)	11080	902	1936	14.2	12.3	Side porch	7.28	3.57	180

The “Porch direction” in Table 3 is the horizontal angle of the normal of the porch’s outer surface against North, in clockwise direction. Having the wind and porch direction, the incidence angle can be calculated, i.e. the difference between the porch direction and wind direction. That is, at an incidence angle of 0 degrees the wind is perpendicularly towards the porch surface, while at 180 degrees the surface is on the leeward side of the building.

3.2. Field measurements

Weather data was recorded at a portable weather station (WXT520, Vaisala Oyj, Finland), placed within one km of the church, with the weather sensor at the approximate height of the church roof, see Figure 10. Weather data used in this study was outdoor air temperature, wind speed and wind direction, recorded at 5 min intervals. For Visby cathedral, however, wind data was attained from a 4 km distant weather station of the Swedish Meteorological and Hydrological Institute (SMHI). In addition, air temperature and humidity was measured with a logger (SatelLite TH, Mitec Instrument, Sweden) placed within 50 m from the church, at about 2 m height above ground.

Figure 10: Portable weather mast, with Valbo church in the background (Hayati, Mattsson and Sandberg, 2014).

Indoor air temperature was measured using gold-sputtered NTC thermistors (Ø 0.47 mm, 4 mm long) distributed at different heights centrally in the church hall. At the airing calculations, the height weighted average temperature between floor and porch height was used to represent the indoor air temperature (Hayati, Mattsson and Sandberg, 2017). For air infiltration calculations, the height weighted average temperature (floor to ceiling) was used to represent the indoor temperature, although an analysis of the impact of a noted temperature stratification proved this to have an insignificant effect (Hayati, Mattsson and Sandberg, 2014). The temporarily installed measuring mast set inside the Hamrånge church is shown in Figure 11. In case of Hamrånge church, another, permanent, measuring mast was also installed.

Figure 11: Measuring mast set inside the Hamrånge church. Photo: M. Mattsson

Leakage characteristics of the churches' building envelope were attained through pressurization tests, "blower door" (European committee for standardization, 2000) (using two 2200-Fans with DM-2A manometers, Retrotec Energy Innovations Ltd.), with the fan-screen placed in a smaller outer doorway, see Figure 12. These measurements have an estimated uncertainty of about 10%. Additional, more precise measurements of the indoor-outdoor pressure difference were performed using a separate manometer (FCO44, 0-60 Pa, Furness Controls Ltd, East Sussex, UK). During long term logging (several days) with this manometer, occasions with very low wind speed were identified, which, together with simultaneous indoor-outdoor temperature data could be utilized to assess the NPL (Neutral Pressure Level) (Hayati, Mattsson and Sandberg, 2014), see Figure 12.

Figure 12: Blower door test setup with the side porch of Valbo church.
Photo: M. Mattsson.

The air change rate, ACH, caused by air infiltration was measured by the tracer gas decay method (see e.g. ISO 12569 (European Committee for Standardization, 2012)), i.e. by spreading an instantaneous dose of tracer gas (in this case SF_6) inside the churches and measuring the concentration during the decay caused by infiltrated outdoor air. In general, the natural room air mixing proved good enough for using one- or two-hour portions of the decay data to calculate time-resolved air change rates. More details on these measurements can be found in (Mattsson *et al*., 2011b; Hayati, Mattsson and Sandberg, 2014). An example of the tracer gas measurement setup in Hamrånge church is shown in Figure 13.

Figure 13: Tracer gas measurements set-up in Hamrånge church.
Photo: M. Mattsson.

Tracer gas decay method was also used for determining the air change rate during the airing. The method involved spreading of an instantaneous dose of tracer gas (SF_6) inside the churches, awaiting well mixing with the room air, and measuring the concentration in the room air just before and after the airing period. From the change in concentration, calculation was enabled of how much fresh air had entered during the airing period. In general, heating units such as radiators and/or bench heaters tend to cause large enough convective air movements in church halls for tracer gas to be well mixed into a uniform concentration (Mattsson *et al*., 2011b). This was confirmed in the present study. Importantly, good room air mixing (homogeneous tracer gas concentration) was observed just before the airing periods, and again fairly soon after the airing periods. During non-heating conditions in Hamrånge church, however, three powerful (1500 W) mixing fans were utilized temporarily to attain good air mixing before and after the airing (Hayati, Mattsson and Sandberg, 2017).

In Hamrånge church, the airflow in the open porch was also measured temporarily by 21 omnidirectional constant-temperature anemometers (CTA 88, Swedish National Institute of Building Research), distributed over a vertical plane in a 7x3 array, as shown in Figure 14. The measurement range of the anemometers was 0.05-3 m/s and their response time 0.2 s at a 90% step change (Lundström *et al*., 1990). After being newly calibrated (in air flowing perpendicular to the sensor shaft), the uncertainty of the anemometers was estimated at ±5% (95% C.I.). Some directional sensitivity adds another ±10% for non-perpendicular airflows; flow visualization by smoke (Figure 31) indicated, however, that the flow was essentially perpendicular in this test case (Hayati, Mattsson and Sandberg, 2017).

Figure 14: Anemometer installation at the porch in Hamrånge church, in front of the inner doors of the draught lobby. (Hayati, Mattsson and Sandberg, 2017).

Other conducted field measurements include IR-Thermography, CO_2 concentration, relative humidity inside and outside, the crack size at some leakages and electricity power used for heating (bench heating and radiators).

3.3. Wind tunnel model studies

The experiments were carried out at the closed-circuit wind tunnel of the University of Gävle (see Figure 15), having a working section 3.0 m wide, 1.5 m high and 11 m long, and with a maximum wind speed of 27 m/s. The tested building model was mounted on a 2.85 m diameter turntable, the center of which was located 8.5 m downstream of the entrance to the test section. Besides varied wind speed, the tests included two levels of air turbulence, attained with and without roughness elements placed in the wind tunnel; see Figure 16. The roughness area in the working section of the wind tunnel was 7 m long, starting with five upstream spires, followed by W*D*H=50*50*80 mm^3 cubes, which, after about 1/3 of the roughness area, were substituted by 30*30*30 mm^3 cubes. The horizontal areal density of the roughness elements was 6.4%. The distance between the final row of roughness elements and the center of the model was 1.4 m.

The wind tunnel studies were performed on a 1:100 scale model of an existing church, Hamrånge, situated in mid Sweden. For simplification, the model consisted of the main hall of the church, but the tower was omitted, see Figure 16. The model had a pitched roof and one or two opposing porches as the only opening(s). Each porch opening had the area of W*H=19*29 (=551) mm^2, and the whole façade area was 683.40 cm^2; thus the net porosity – the ratio between the opening area and the area of the façade in which the opening was located – was 0.81%. The porches in the model were equipped with removable draught lobbies, visible in the lower picture of Figure 16. These mimicked existing draught lobbies in Hamrånge church, and it was hypothesized that they might affect airing through the porches. Such draught lobbies are common in Swedish churches, but also elsewhere, and serves to *prevent* cold outdoor air from coming in; an additional door at the inner end of the lobby completes the construction. The models' internal volume was 9342.5 cm^3; see more measures in Figure 16. The walls were of 3 mm thick Plexiglas and the draught lobbies were 20 mm deep, extending into the building. The ratio between the wall thickness and the hydraulic diameter of the opening area was 1.00 for the case with the draught lobbies and 0.13 for the case without the draught lobby. Thus, the current study includes four different configurations of with and without the draught lobby and roughness elements in the wind tunnel. In addition, four different wind speeds were attained by varying the speed of the wind tunnel fans, including 100, 200, 300 and 400 revolutions per minute (RPM). By rotating the turntable, nine different wind directions were tested: 0, 22.5, 45, 67.5, 90, 112.5, 135, 147.5 and 180°; where 0° is streamwise direction in the wind tunnel. Further, the undisturbed wind stream Reynolds number, assuming hydraulic diameter of the porch (approximately 23 mm) as the characteristic length and the

wind speed at 15 mm above the floor (approximate mid height of the porch opening) as the characteristic speed, was 2100, 4400, 6700 and 9200 for the different wind speeds in the wind tunnel, *with* the roughness elements. *Without* the roughness elements the corresponding Reynolds number was 3000, 6500, 10400 and 14100.

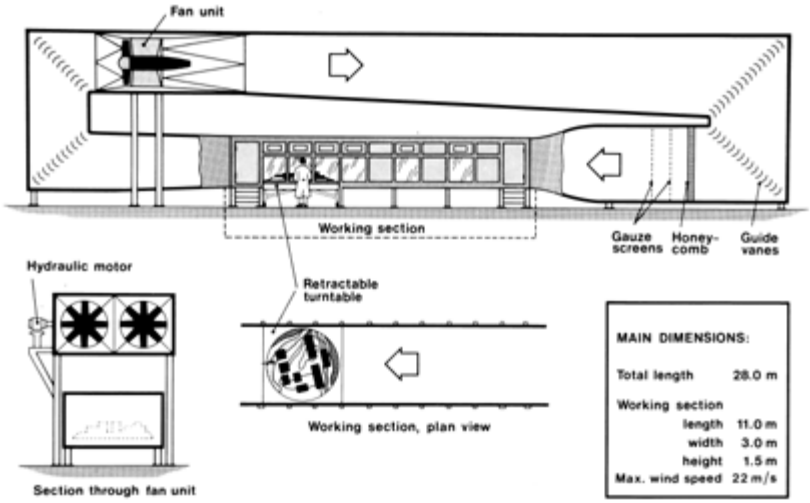

Figure 15: Schematic view of the wind tunnel located in Gävle, Sweden.

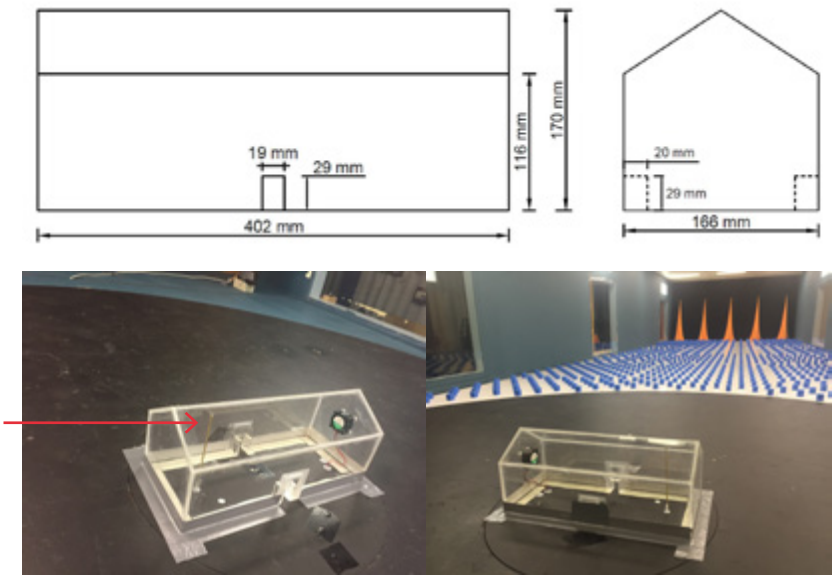

Figure 16: Tested model in the wind tunnel. The draught lobbies are indicated with dashed lines in the right upper picture. The red arrow points at the sampling tube. Roughness objects visible: Blue cubes and orange spires.

Tracer gas decay method was used for determining the air change rate during airing experiments. The method was conducted by spreading an instantaneous dose of tracer gas (N_2O) inside the model and measuring the concentration decay with a gas analyzer, (Binos 1.1), by sampling at different heights in one horizontal position during the airing period; see Figure 16. The decay method is widely used in field and model studies (Warren & Parkins, 1977; Etheridge & Sandberg, 1996; Yamanaka *et al*., 2006; Kato *et al.*, 2006; Larsen & Heiselberg, 2008; Abolfazl Hayati *et al*., 2017). A small electric fan was used inside the models in order to mix the air inside the interior volume and create a uniform concentration of the tracer gas. The fan, visible in Figure 16, was positioned on one sidewall, blowing air horizontally along the ceiling, with no direct air jets directed towards porch areas. Pre-measurement of the concentration at different heights and positions in the model indicated that the air was well mixed during the airing period.

The vertical wind speed profile was measured in the wind tunnel by using a hot-film anemometer (TSI 1054B, with a 20 µm wire, platinum deposited on quartz substrate). This was done without the building model in place, both with and without roughness elements, in order to characterize the airflow that the building model and its openings were exposed to. The anemometer was pre-calibrated, yielding an uncertainty of about ±3% (95% C.I.) for wind speeds over 0.5 m/s, excluding directional error. The anemometer wire was oriented horizontally, perpendicularly to the main flow direction, and since smoke visualization indicated an airflow with insignificant lateral components (when no model was present), the directional error is considered marginal.

The drag force of wind on the model was also attained by measuring the vertical component of wind-induced force on the model, i.e. F (N) in Equation 28. Drag coefficient, C_D , is a dimensionless number defined as the ratio between the drag force and (the stagnation pressure ($0.5pU^2$) times the projected area (A_{proj})) and can be calculated by Equation 28. The drag force measurements were conducted without having the roughness elements inside the wind tunnel and also within different wind directions toward the model.

$$C_D = \frac{F}{0.5\rho U^2 A_{proj}} \tag{28}$$

Flow visualization in both horizontal and vertical center plane of the model was performed to detect the flow direction and turbulence pattern in- and outside the models. The laser beam then used as light source had λ=523 nm wavelength and 9.25 mW power. Smoke was injected both inside and outside the model, and pictures were taken for different configurations of both single-sided and cross flow cases.

3.4. Semi-empirical (analytical) model studies

3.4.1. Modeling of air infiltration in large single-zone buildings

In order to use the LBL and AIM-2 infiltration models, two different assumptions of the leakage distribution at the building envelope were tested; one assuming even distribution (the uniform case) and the other with "guesstimated" leakage distribution. The leakage value or flow coefficient, in the uniform case, was proportional to its area for each building envelope. An educated guess about likely leakage distribution, in the case of guesstimated leakage distribution, was done by using different leakage identification techniques, including IR-Thermography, visual inspection, NPL assessment, and tracer gas measurements. For instance, previous studies showed that the wooden floor in Hamrånge church is a major leakage area (Mattsson *et al*., 2011a). Examples of IR-Thermography pictures are provided in Figure 17. The assumed leakage distributions in the studied churches are presented in Table 4.

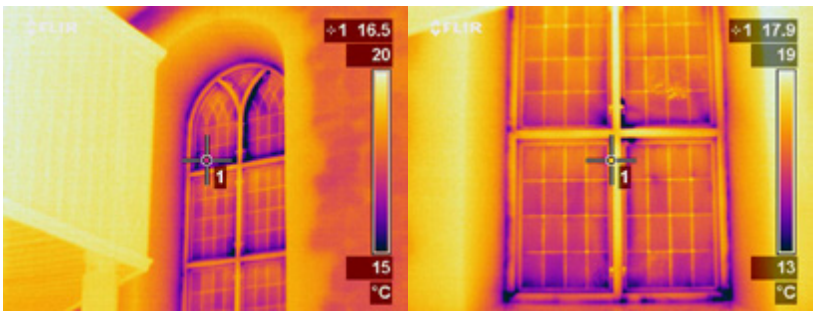

Figure 17: IR-Thermography pictures showing the leakage around the windows in Valbo church under pressurization test.

Table 4: Assumed leakage portion (in percentage of the total leakage area) (Hayati, Mattsson and Sandberg, 2014).

Location	Leakage assumption	Floor	Ceiling	Walls
Hamrånge	Uniform	25	25	50
	Guesstimated	50	25	25
Söderfors	Uniform	20	20	60
	Guesstimated	5	25	70
Valbo	Uniform	30	30	40
	Guesstimated	0	43	57

Froude number is used to investigate the dependency on prediction errors of wind and stack dominated conditions. The Froude number, Fr [-], indicate the relationship between kinetic vs. buoyancy forces of fluids, i.e. the ratio between the wind speed and a buoyancy-defined velocity, see Equation 29:

$$Fr = \frac{U}{\sqrt{gH\frac{|T_i - T_o|}{T_i}}} \tag{29}$$

In addition, a correction factor *m*, see Equation 30, is introduced to the AIM-2 final superposition equation, according to Equation 21, for tuning the model results for large single zone buildings like churches.

$$Q_t = m\left[Q_w^{\frac{1}{n}} + Q_s^{\frac{1}{n}} + \beta(Q_s Q_w)^{1/2n}\right]^n \tag{30}$$

3.4.2. A developed numerical air infiltration model

A proposed numerical single zone air infiltration model consists of a cuboid on top of a crawlspace, including a leaky floor towards a naturally ventilated crawl space. The air temperature inside the crawlspace was assumed as the outdoor air temperature. Some leakage areas were identified and put into the model and the flow due to each leakage was calculated. The total pressure difference caused by buoyancy, wind or/and fans, was calculated as a function of NPL. The NPL was gained by solving the continuity equation for the total flow, so that the sum of all in- and exfiltrating air of the zones become zero. The wind pressure coefficients at the facades have been measured in wind tunnel experiments (see e.g. Mattsson *et al*., 2013).

The Poiseuille's equation, i.e. Equation 14, was used for the air leakage paths considering both laminar and turbulent flow. The leakage characteristics, such as the size and position, were detected by field audit and IR-Thermography. The leakage assumed in the simulation model are presented in Table 5. The neutral pressure layer at natural conditions was also used for model calibration. The leakage lengths were adjusted by comparing the simulated neutral pressure layer with the measured ones (Hayati, Akander and Mattsson, 2016). Two sets of blower door tests were used (where the vents of the crawlspace were sealed and opened, resp.) in order to tune the model.

In order to improve correspondence between simulated and measured results, hydraulic diameters and lengths of the leakages were varied in multiple runs. These variations ("calibrating" input data to improve accuracy) were not performed in a systematic way; they were made on basis of trial and error with guidance of flow characteristics as described above. Table 5 shows final input data. After implementing the calibrations above, the developed model was used for prediction of air infiltration.

Table 5: Leakage characteristics used in the developed numerical air infiltration model (Hayati, Akander and Mattsson, 2016).

Envelope component	Description	Amount	Height (m)	Length (m)	Thickness/ depth (m)	Width/ radius (m)	Low position (m)
Southern wall	Gap around door	2	2.9	1.70	0.10	0.006	0.0
	Circular opening	1			0.10	0.005	1.5
	Gap around door	1	2.9	1.7	0.10	0.006	0.0
Western wall	Gap around window	12	4.7	1.0	0.10	0.001	2.0
	Circular opening	1			0.10	0.005	1.5
Northern wall	Gap around window	12	4.7	1.0	0.10	0.001	2.0
	Gap around door	1	2.9	1.7	0.10	0.006	0.0
Eastern wall	Gap around window	12	4.7	1.0	0.10	0.001	2.0
	Circular opening	1			0.10	0.005	1.5
	Horizontal gaps	2		65.0	0.15	0.003	11.0
Ceiling	Circular opening	15			0.15	0.0075	11.0
Floor	Horizontal gaps	1		220.0	0.045	0.002	0.0

3.4.3. Modeling of airing through porches

Four models of single-sided ventilation were evaluated against measurement data, i.e. the models developed by British standard (BSI, 1991), De Gids and Phaff (1982), Larsen and Heiselberg (2008) and Caciolo (2010), as listed in Table 2. Besides, examples of practical airing diagrams are presented in this study, considering buoyancy driven airing. The aim is to facilitate for e.g. building caretakers to estimate how much time that is needed to refresh a certain percentage of the building volume. The practical diagram is based on the size characteristics of the building, summarized in a geometry factor, $f = \frac{Vol}{bH^{3/2}}$ ($m^{1/2}$); where Vol (m^3) is the church volume, b (m) is the door

width and H (m) is the opening (door) height. Here, T is assumed as 288 K. Having calculated the geometry factor, f, Equation 26 can be transformed into the following equation 31 for assessing the air change rate that results from airing, indicated by ACH_{Airing}:

$$ACH_{Airing} = \frac{C_e}{f}\left(\frac{\Delta T}{T} g\right)^{1/2} \tag{31}$$

where C_e is the above mentioned empirical coefficient based on the discharge coefficient, here taken as 0.15; this is indeed the average value obtained also when fitting measurement data of the present study into Equation 26. The practical diagram shows the amount of exchanged room air, E, in percentage of the whole volume, see Equation 32. Assuming fully mixed room air yields:

$$E = (1 - e^{-ACH_{Airing} \cdot t}) * 100 \tag{32}$$

where t (h) is the duration of airing.

3.5. IDA-ICE simulation of the airing flow rate

A model of Hamrånge church was built in IDA-ICE simulation program version 4.6.2. The IDA-ICE model for airflow through large opening was examined by comparing with tracer gas measurement of two different airing occasions, when the porch was located in the windward and leeward side. The model was consist of six different zones, including main hall, crawl space, main entrance and the tower, sacristy, attic room and the storage room, see Figure 18. The allocated leakage area, presented in Table 5 is also considered and put into the simulation model (Hayati, Mattsson and Sandberg, 2016).

The weather data were gained from a portable weather station, placed within one km of the church, with the weather sensor (WXT520, Vaisala Oyj, Finland) at the approximate height of the church roof. Weather data used in this study were outdoor air temperature, relative humidity, wind speed and direction, recorded at 5 min intervals. The data for solar radiation and relative humidity as well as the data for the rest of the year was gained from Swedish Meteorological and Hydrological Institute (SMHI) available at (Lundström, 2016).

The 0.85 m thick external walls consist of stone with an assumed U-value of 0.4 W/(Km^2) and the rest of the walls were taken as default walls for roof, floor and inner walls in IDA ICE. Each window is 2.6 m times 4.7 m large and has three panes with assumed U-value of 1.9 W/(Km^2), solar heat gain value of 0.68 and solar transmittance value of 0.6. The side porches used for airing are 1.9 m long and 2.9 m wide. The building is quite wind exposed. The default values of pressure coefficient (varying with wind direction) for

wind exposed building in the program were used in this study, gained from handbook data set of the Air Infiltration and Ventilation Centre, see e.g. (AIVC, 1984; Orme, Liddament and Wilson, 1998).

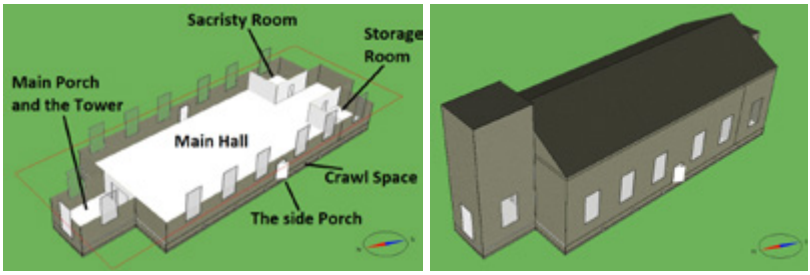

Figure 18: Hamrånge church model in IDA-ICE (Hayati, Mattsson and Sandberg, 2016).

The occupancy schedule for the main hall was set as 20 people present on Sundays from 10:00 to 12:00 and 2 people present during the rest of the days from 8:00 to 16:00 with half an hour lunch break. The activity level was assumed as 1 MET and clothing was assumed as 0.85±0.25 Clo for all occupants. No occupancy was assumed for the rest of the zones. The only heating units were in the main hall consisting of 20 electrical bench heaters with 120 kW total power. The heaters were controlled by thermostats working between 15 and 16 °C. Total lighting of 2 kW and equipment of 1 kW power was set for the main hall with the same schedule as for the occupants. For sacristy and storage room 0.5 kW electric heaters as well as 0.2 kW lighting was assumed (Hayati, Mattsson and Sandberg, 2016).

4. Results and discussion

Results are divided into two major parts, i.e. for air infiltration and airing. In each part, the results from field measurement are brought forth following by model prediction. In the part for airing, results from IDA-ICE simulations and wind tunnel studies are also presented.

4.1. Air infiltration

4.1.1. Typical air tightness of church envelopes

Air tightness, measured by pressurization (Blower door) tests in different church buildings are presented, in Table 6. In the table, the building envelope air tightness is presented both as air change rate per hour (ACH_{50}) and as air tightness value l_{50} ($L/s \cdot m^2$); the latter is defined as how many liters of air infiltrate the building envelope per second and per square meter of the enclosing building envelope area at a pressure difference of 50 Pa (Bankvall, 2013). With enclosing building area, in the denominator of l_{50}, means the enclosing parts/walls, which confines the heated interior against the outdoor climate, i.e. roof ceiling, floor and the surrounding walls of a building envelope.

Table 6: Typical values of air tightness for the studied church buildings.

Location	q_{50} (L/s)	Enclosing area (m^2)	Volume (m^3)	Flow coefficient, *C* ($m^3/(sPa^n)$)	Flow exponent, *n*	l_{50} ($L/s \cdot m^2$)	ACH_{50}
Hamrånge	6770	2745	7620	0.550	0.64	**2.47**	3.20
Hamrånge (closed crawl space openings)	4220	2745	7620	0.284	0.69	**1.54**	1.99
Söderfors	1119	1900	4564	0.088	0.65	**0.59**	0.88
Valbo	959	1527	2631	0.087	0.61	**0.63**	1.31
Bomhus	4240	1000	2000	0.238	0.74	**4.24**	7.63

According to Table 6, high discrepancy regarding air tightness can be observed in the churches; varying from 0.59 (L/s·m^2) (equivalent to 0.88 ACH) to 4.24 (L/s·m^2) (equivalent to 7.63 ACH) at 50 Pa pressure difference between inside and outside. The leakiest church, Bomhus, is of wooden construction; i.e. more leakages could be expected. From Table 6, an average air tightness of 1.89 (L/s·m^2) is gained regarding the studied church envelopes, which can be compared with 0.3 (L/s·m^2 with 50 Pa indoor-outdoor pressure difference) for the passive house (Passivhuscentrum, 2012). The flow exponents gained from the blower door test, are very similar for different churches, varying from 0.61 to 0.74 (0.67 on average). This is in agreement with previous studies that point to an average flow exponent of 0.65 for the residential buildings (Orme *et al*., 1994). The attained value of 1.89 (L/s·m^2) can also be compared with the airtightness demand of 0.6 (L/s·m^2 with 50 Pa indoor-outdoor pressure difference) for detached houses and non-residential premises (with heated (more than 10ºC) floor area of < 50 m^2) according to the Swedish building regulations (Boverket, 2016). For other types of buildings and buildings with larger heated floor area there is not any specific air tightness demand but the building should be tight enough to fulfil the requirements for building specific energy use and installed electric input for heating (Boverket, 2016). However, the Swedish Building Regulation also states that air tightness should not affect the moisture level, thermal comfort, ventilation and the heat loss of a building. There are extra air tightness rules to prevent the spread of fire (Boverket, 2016).

The NPL height depends on the leakage distribution over the building envelope. With the help of pressure measurements, in relatively wind still conditions the NPL level is measured as approximately 25%, 50% and 75% of the ceiling height, above the floor, for Hamrånge, Söderfors and Valbo churches, representing three different churches with low, intermediate and high NPL position. This gives a hint on the leakage distribution, which can be complemented by field investigations such as IR-thermography. For instance, the lower NPL position in Hamrånge church implies that there are larger leakage areas in the lower parts of the building; for example, obvious leakage were observed in the wooden floor of Hamrånge church.

4.1.2. Examples of measured air change rates and weather data

An overview of the pairwise temperature and wind data with the related air infiltration rate is shown in contour diagram of Figure 19, for Valbo church. In general, a positive correlation between the wind speed, temperature difference and the air infiltration rates, measured by tracer gas can be observed, however with some variations, perhaps due to uncertainties like different wind directions.

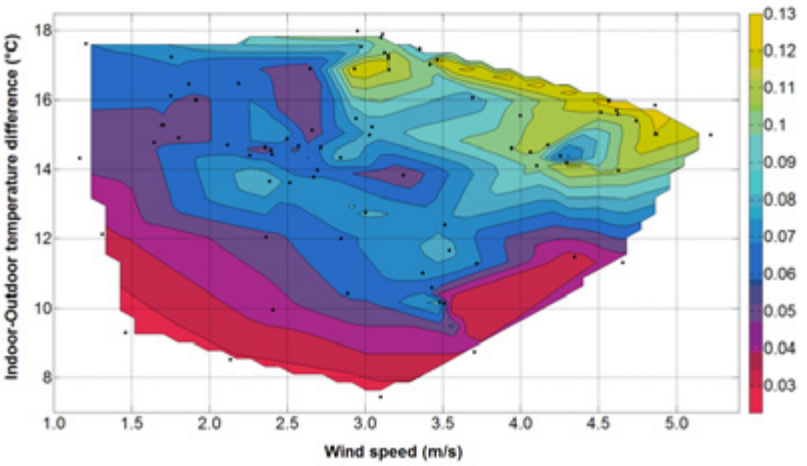

Figure 19: Pairwise wind and temperature data (dots) attained at Valbo church and contours for measured ACH. Color scale indicates the ACH (1/h). (Hayati, Mattsson and Sandberg, 2014).

4.1.3. Validation of the air infiltration models

The LBL and AIM-2 model and their other variants, considering NPL (LBL_{NPL}) and crawlspace ($AIM\text{-}2_{Crawl}$), are validated and presented in this part. As the model predictions are dependent on the leakage distribution, two different scenarios are assumed, a uniform distribution and one with a better, "guesstimated" leakage distribution (see Table 4). Table 7 indicates the model prediction error, comparing with the tracer gas measurements for Hamrånge, Söderfors and Valbo churches.

Table 7: Median ACH prediction error (%) of the four tested models, assuming the uniform and guesstimated leakage distribution assumptions (Hayati, Mattsson and Sandberg, 2014).

	Hamrånge		Söderfors		Valbo	
Infiltration model	Uniform	Guesstimated	Uniform	Guesstimated	Uniform	Guesstimated
LBL	+38	+33	+43	+37	+60	+50
AIM-2	+28	+36	+39	+31	+46	+22
$AIM\text{-}2_{Crawl}$	+22	+22	-	-	-	-
LBL_{NPL}	+17	+14	+13	+10	+15	+19

According to Table 7, air infiltration is overpredicted by all models. However, inclusion of the crawl space in the AIM-2 model for Hamrånge church slightly improves the prediction. The LBL_{NPL} model generated slightly better predictions together with the AIM-2 model; however, because NPL measurements are rather cumbersome, the AIM-2 model is preferred. Bearing in mind that to get better results, measurement of the NPL position is recommended.

The reason for the observed overprediction in the models can be because of the fact that the models are not developed for such large single-zone building like churches but instead they are based on data from normal residential buildings with ceiling height of up to 3 m (Walker and Wilson, 1990).

An example of the time-history diagram of the measured weather parameters and the measured air infiltration rates, with tracer gas decay method, is shown in Figure 20 for Valbo church. The weather parameters include a 3.5 day span including wind speed and the temperature difference between the interior and the outside, which are the driving forces for the air infiltration. The resulting air infiltration rates are the one-hour moving average of the air change rates together with other curves demonstrating ± one standard uncertainty. Moreover, the prediction results of the LBL, LBL_{NPL} (the LBL model assuming the NPL level) and AIM-2 model are also depicted in Figure 20, assuming guesstimated leakage distribution. Apparently, the models show consistent overpredictions comparing with the tracer gas measurements.

The standard uncertainty for the air infiltration rates, measured by tracer gas, was in average 3% for Valbo and Söderfors churches and 9% for Hamrånge case. The quite low uncertainty is corroborated by the strong positive correlation with the driving forces, especially with the temperature difference.

The models do not consider wind direction, while, in practice, the pressure difference induced by wind is dependent on the wind direction. Finding exact value of the leakage distribution is also an impossible mission. Another uncertainty source is the temperature stratification in the churches, while only a single room temperature can be fed to the models. A temperature difference of up to 3 K, between the ceiling and floor was measured inside the studied churches, with larger stratification close to the floor. However, the temperature stratification inside the church is assessed to cause minor error in air infiltration predictions, if the height averaged temperature is used in the calculations, as was the case in this study.

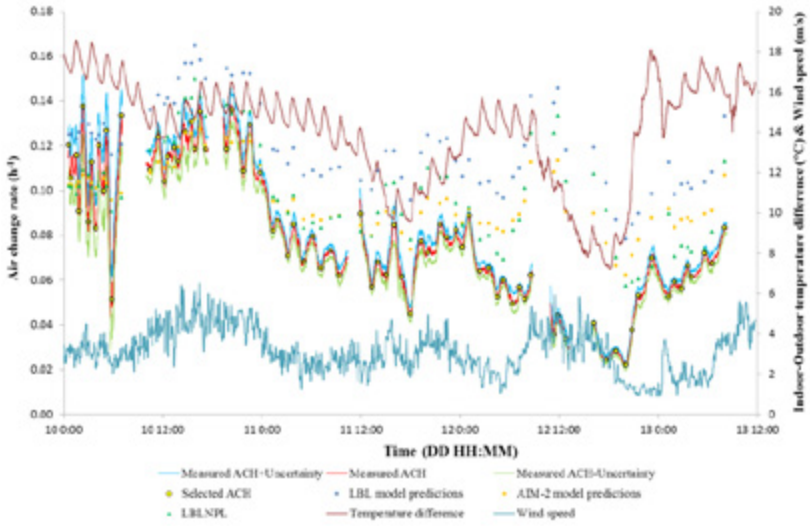

Figure 20: Time history of measured and modeled air change rate in Valbo church, and the corresponding climate data (Hayati, Mattsson and Sandberg, 2014).

4.1.4. Prediction dependency on wind vs. buoyancy forces

The relation between the model predictions and the relative effect of the driving forces, i.e. wind and buoyancy effect are examined here. The ratio between the predicted and measured air infiltration rates are depicted versus the Froude number and the difference between the wind and buoyancy induced infiltration terms (Q_W - Q_S), in Figures 21-22 respectively. The AIM-2 model predictions with guesstimated leakage distribution are presented in the figures. The difference between wind and buoyancy (stack) induced air infiltration rate in the abscissa of Figure 22, i.e. (Q_W - Q_S), is gained from the related terms predicted by the AIM-2 model (using guesstimated air leakage distribution), see (Hayati, Mattsson and Sandberg, 2014). Noticing Figure 22, the negative (Q_W - Q_S) values indicate a dominate buoyancy induced infiltration term. In order to fit high values of Hamrånge church in the same diagram, its (Q_W - Q_S) values have been multiplied by a factor of 0.5 in Figure 22, and the Fr numbers in Figure 21 have been multiplied by a factor of 0.125. The trend lines in both figures shows that the air infiltration prediction for the Söderförs church is more affected by the difference in the wind and buoyancy induced air infiltration, especially larger overpredictions can occur with higher wind speeds. A tendency to similar trend can be observed for the Hamrånge church, but on the whole the prediction dependency on the wind/buoyancy ratio seems rather small.

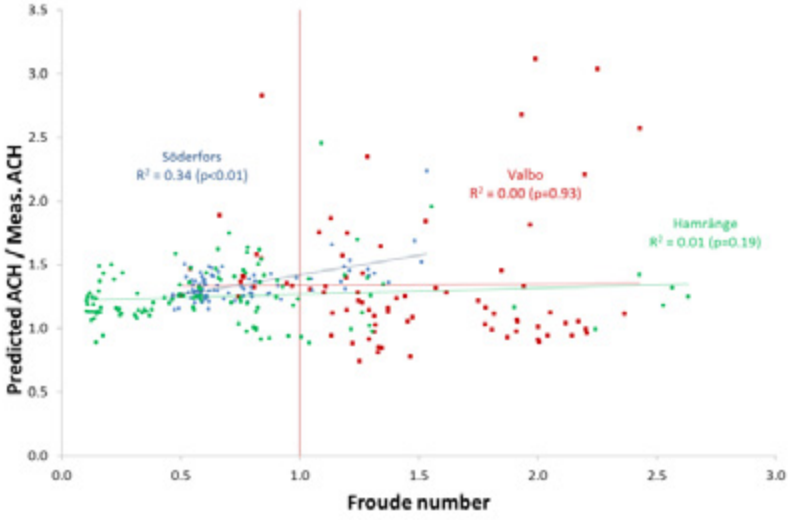

Figure 21: Modelled ACH predictions vs. Froude number (Hayati, Mattsson and Sandberg, 2014).

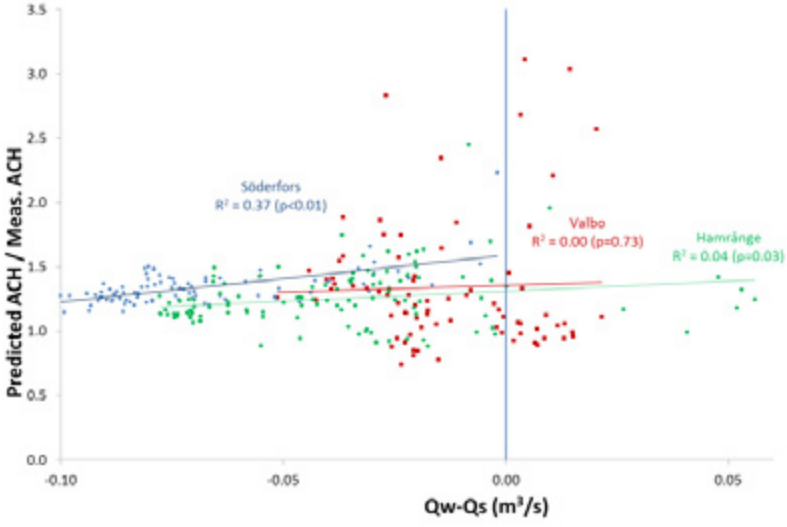

Figure 22: Modelled ACH predictions vs. difference in wind and stack induced air infiltration (Hayati, Mattsson and Sandberg, 2014).

4.1.5. Model adjustment for better predictions

Based on the measurements and analyses of the present work, the AIM-2 model is tuned for better prediction for large single-zones like churches. The interaction term β used in the AIM-2 model, i.e. Equation 21, is fixed at -0.33 and the flow exponent, n, in the same Equation is fixed at 0.64, 0.65 and 0.61 for Hamrånge, Söderfors and Valbo church gained from individual "Blower door" tests, see Table 6. The correction factor m in Equation 30 is tested for model tuning. The optimum m are 0.84 (Hamrånge), 0.75 (Söderfors) and 0.86 (Valbo) respectively, for an average of 0.82. AIM-2 model predictions with the correction m-factor of 0.8 and the guesstimated leakage distributions are shown in Figure 23. The air infiltration rate for Hamrånge church, shown in Figure 23, are predicted by the AIM-2_{Crawl} model, i.e. the AIM-2 model considering a crawl space.

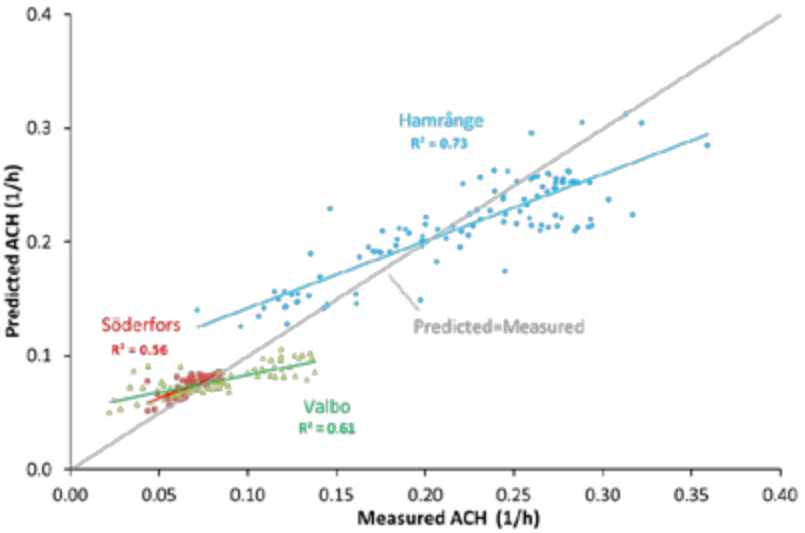

Figure 23: AIM-2 model predictions with correction factor m = 0.8 (Hayati, Mattsson and Sandberg, 2014).

According to Figure 23 the model predictions are improved by introducing the correction m factor of 0.8. The median prediction error is 0% in average, having -2% (Hamrånge), +4% (Söderfors) and -3% (Valbo). However, the trend lines are not perfectly overlapped with the perfect prediction line; and the median of the *absolute* prediction errors is 11% in average, having 10% (Hamrånge), 5% (Söderfors) and 17% (Valbo), which indicates the approximate error of a single predicted value. According to Table 7 the averaged absolute prediction error is 25% before adjusting with the m-factor. Thus, the AIM-2 model overprediction is significantly reduced by introducing the correction factor of m=0.8, however there is still potential for the improvement of the prediction patterns.

4.1.6. The developed air infiltration model

As explained in section 3.4.2, a numerical model is developed by allocating leakage in various parts of the building envelope. The leakage allocation, presented in Table 5, is based on visual inspection and IR-thermography observations. The air change rates predicted by the developed air infiltration model are presented in this part. In order to calibrate the model, the blower door air change rates are also predicted by the model for Hamrånge church. The results are depicted in Figure 24.

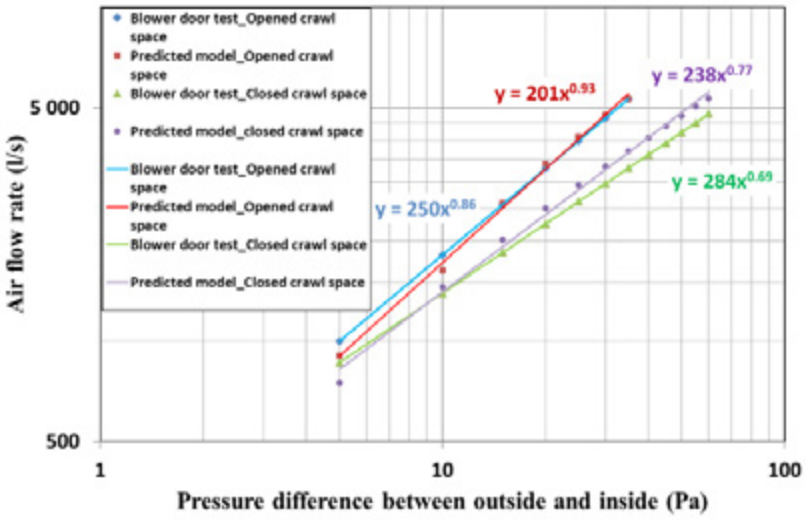

Figure 24: Blower door and prediction results for two cases: the vents of the crawlspace are opened and closed, resp. Power law relationship between pressure difference and airflow rate are presented for each case (Hayati, Akander and Mattsson, 2016).

According to Figure 24, higher flow exponents (steeper slopes) are predicted by the model in comparison with the pressurization (Blower door) test. One reason for this can be that the shape of the modelled leakages and gaps are assumed straight and smooth, while this is not the case in reality. In field, flow is more turbulent and the related flow coefficient is likely to be closer to 0.5. Another reason can be the discrepancy between the total modelled leakage area, 1.15 m² (of which 38%, 34% and 28% are distributed on floor, ceiling and surrounding walls, respectively,) and the effective leakage area with 4 Pa, 0.32 m². This is due to Poiseuille's equation, Equation 14, used in the model, which consists of non-linear entry and exit pressure loss terms, and a linear pressure loss inside the leakage. The effective leakage area, gained from Blower door test, does not include a linear pressure loss term and therefore is smaller than the one calculated with Poiseuille's equation, see (Hayati, Akander and Mattsson, 2016). A part of the calibration is to com-

pare the NPL level from the program with measured NPL during a non-windy day. If the program's NPL is lower than the measured, the leakage below NPL is too large and must be redistributed above NPL whilst fulfilling Blower door results. The redistribution can be made on basis of crack lengths (which are difficult to assess); however not by relocation (since the location has been observed during audits and Bloower door tests).

After model calibration, the developed model is used for prediction of air infiltration. The measured air infiltration rates during three different periods, including 90 hours in total, are compared with the model prediction, see Figure 25. The predicted air infiltration rates are almost evenly distributed around the perfect prediction line with a coefficient of determination (R^2-value) of 0.61. The model performance is in agreement and even somewhat better, comparing with the AIM-2 and LBL model predictions, because they normally overpredicted the airflow rates, see Table 7. However, with calibration (m=0.8), AIM-2 predicts slightly better (R^2=0.73) according to Figure 23. An advantage of the model developed here is that it is based on assumptions that are physically correct and the model is still being developed and evaluated with larger weather data variations.

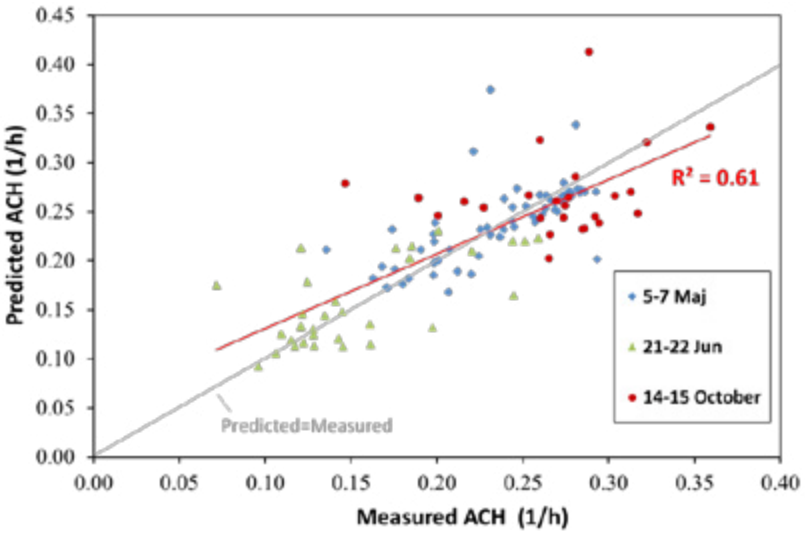

Figure 25: Predicted (simulated) and measured infiltration rates during 5-7 May, 21-22 June and 14-15 October. Data from 5-7 Maj adapted from (Hayati, Akander and Mattsson, 2016).

4.1.7. Energy loss due to air infiltration

Air infiltration in churches depends on the type of the construction; for instance, a church with wooden façades can be significantly leakier than a church with stone walls, as was shown in Table 6. Typically, according to previous tracer gas measurements, a church has an air infiltration rate of 0.1 ACH (1/h), considering a temperature difference of 15 °C and wind still conditions (Sandberg *et al*., 2014). However, air infiltration rate varies depending on the temperature difference and also wind speed.

The quite low air infiltration has its benefits regarding the energy usage, because less air volume should be heated. The tuned AIM-2 model is used for a church (with stone structure) with 2600 m^3 volume, to predict the air infiltration assuming two different inside temperature of constant 20 °C during the weekdays or with intermittent heating of 10 °C during the weekdays and 20 °C during the weekends when the church is in use. In addition, it is supposed that the church is located in different positions in Sweden thus has different outside weather conditions. For the energy calculation, weather data gained from Swedish Meteorological and Hydrological Institute (SMHI) is used from 2004 to 2014 for Nattavaara (north), Örebro (mid) and Hörby (south).

Predicted air infiltration and the related heating demand are depicted in the upper and the lower diagrams of Figures 26-27 for a stonewall church with 2600 m^3 volume, placed in Hörby, Örebro and Nattavara the inside temperature is considered as 20 °C. In the first case with the constant inside temperature during the whole year, Figure 26, on average 20600 kWh is gained for the annual energy usage. Tightening of the leakages might halve the energy usage and lead to an annual energy saving of around 10000 kWh for a typical Swedish church. Assuming the total 3500 churches in Sweden this might lead to around 35 GWh in total energy saving. However, intermittent heating is common in churches, with inside temperature kept at e.g. 10 °C during the weekdays, when the church is not in use, i.e. Figure 27. Thus, the annual energy usage and the related energy saving potential is decreased by 40-50%, so that a total energy usage of 10 GWh is assumed reasonable by tightening Swedish churches (Sandberg *et al*., 2014). However, higher energy saving potential can be expected in windy conditions as wind can induce even more air infiltration and result in more energy losses, which is neglected in the presented numbers.

According to Figures 26-27, stronger variation is observed in energy rate than in the air infiltration because the outside temperature affects the temperature difference, which is directly proportional with the energy usage, while the air infiltration is roughly proportional to the square root of the temperature difference.

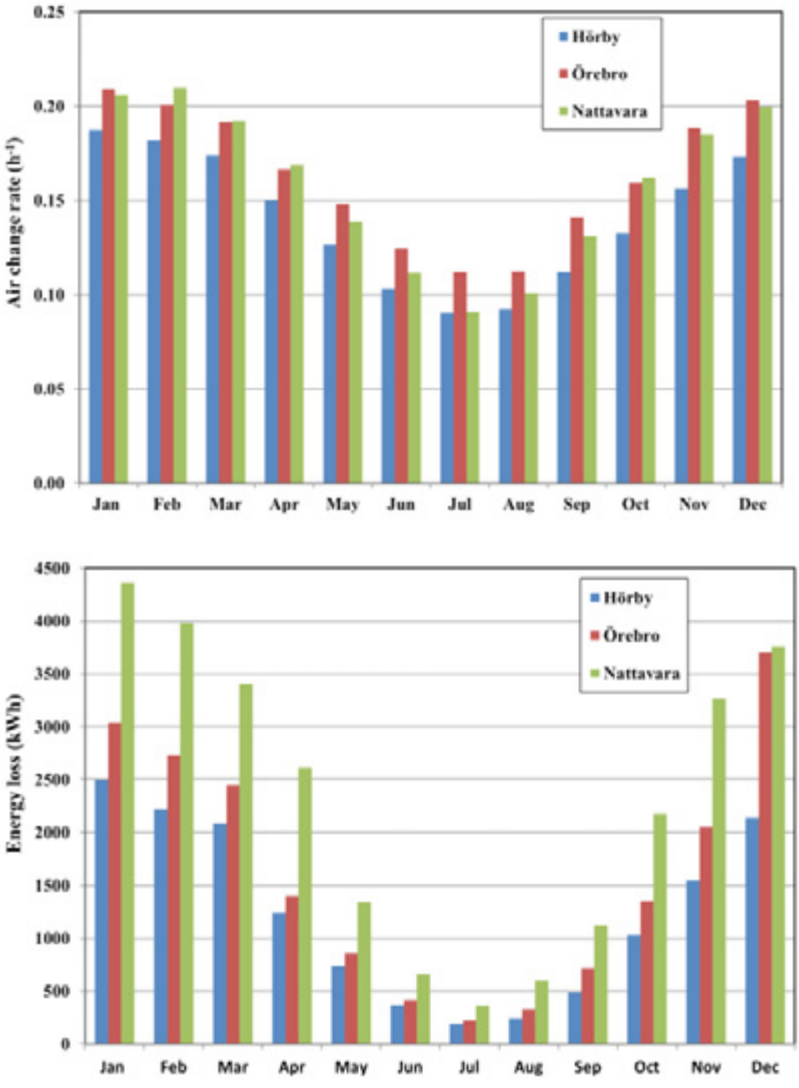

Figure 26: Predicted air infiltration (the upper diagram) and the related heating demand (the lower diagram) for a stonewall church with 2600 m^3 volume, placed in Hörby, Örebro and Nattavara. The inside temperature is considered as 20 °C (Sandberg *et al*., 2014).

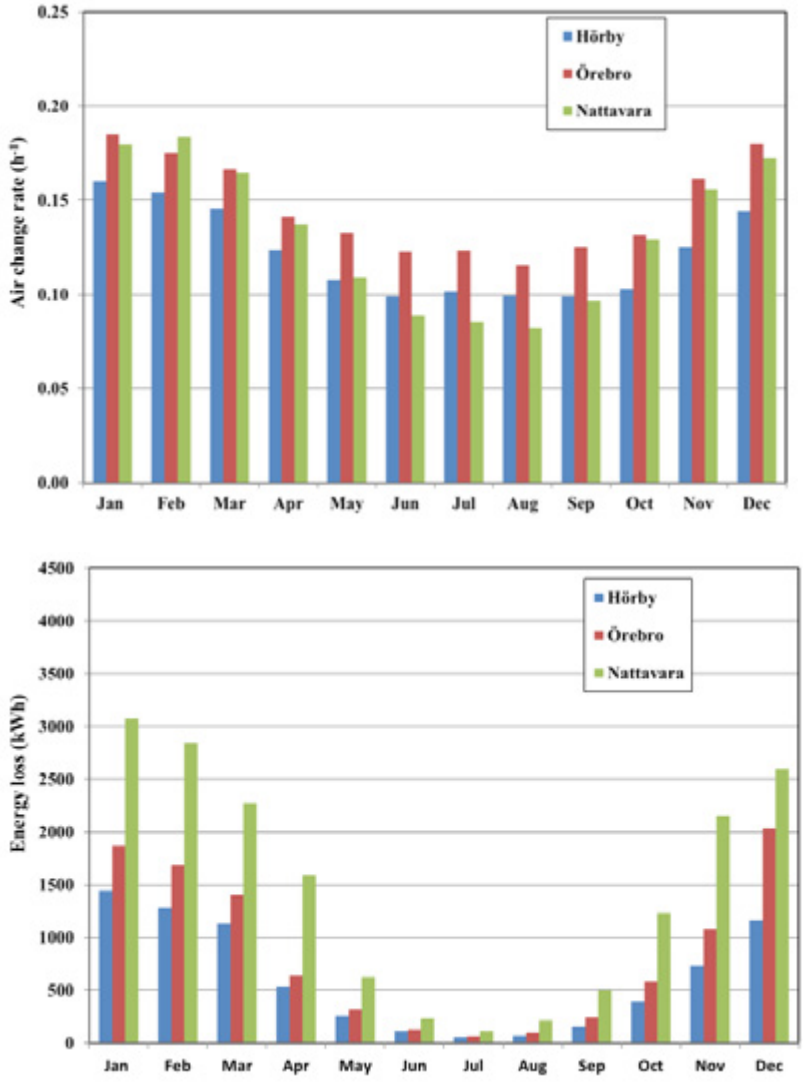

Figure 27: Predicted air infiltration (the upper diagram) and the related heating demand (the lower diagram) for a stonewall church with 2600 m^3 volume, placed in Hörby, Örebro and Nattavara. The inside temperature is considered as 10 and 20 °C during the weekdays and weekends respectively (Sandberg *et al*., 2014).

4.1.8. Examples of leakage detection methods

Besides quantifying the air infiltration, different methods can be used in order to detect the leakage positions. IR-Thermography is a common method of detecting the leakage, thermal bridges, and even moisture damage in building context. One way to distinguish the problems is to get pictures both before and after a pressurization test, trying to see traces of the incoming colder flow rates, which point to a leakage problem. Examples of such pictures are provided in Figure 28; the leakages can be clearly identified in the pictures (on the right hand side) during the pressurization test, i.e. the incoming colder flows are visible by the darker tails around the window frame.

IR-Thermography, as a non-destructive method, can give a hint on the location of each leakage and perhaps some idea of its size, which can be helpful for allotting leakage distribution in the prediction models. This also points to the ratio between the buoyancy and wind effects on the total air infiltration. For instance, detecting more leakage on windows, porches and the surrounding facades suggests that the wind induced flows are dominating. On the other hand, if more leakage is detected on the floor or ceiling, then buoyancy induced flow might be more dominating. However, exact size characteristics of the leakage still cannot be measured. To get a clearer IR-Picture, it is important also that the outdoor be cold enough, maintaining enough in- and outdoor temperature difference to be detected by IR-camera.

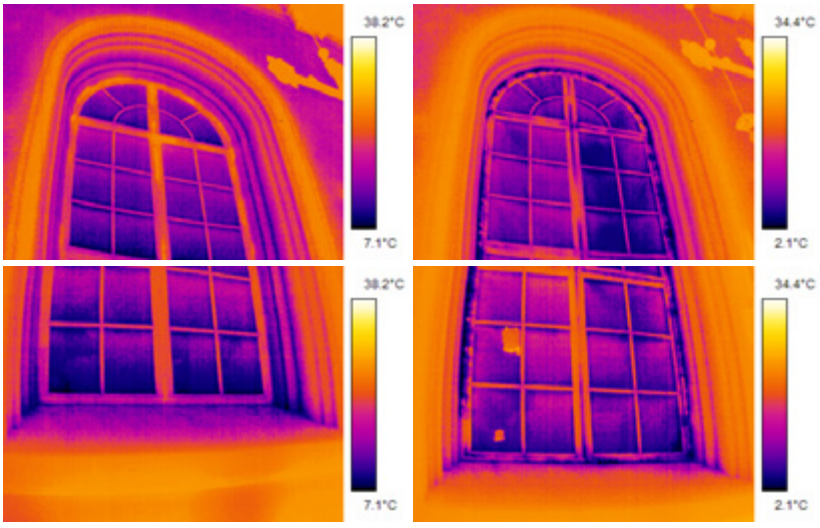

Figure 28: IR-Thermography pictures showing the leakage around the windows in Hamrånge church before and during depressurization test (the left and right pictures, respectively). Photo: S. Lindström & M. Mattsson.

One can also emit particles with help of e.g. a lit candle and look after leakage positions with the help of a portable particle counter device. For example, lighting ten candles over a ten minutes period is typically enough for producing small-scale particles (<0,1 µm) (Sandberg *et al*., 2014) in concentrations well above the outdoor level. Sufficient air mixing can be achieved either by the help of mixing fans or by the operating heating system inside the church. Then the places where it is suspected that air is leaking in can be investigated by checking if the particle concentration is lower around those positions, see Figure 29.

Figure 29: Looking after leakages with particle counter,
Photo: M. Mattsson

4.2. Airing

The results of open-door airing are divided into measurements and modelling. The IDA-ICE simulation results are brought next, and at last the results of wind tunnel model studies are presented.

4.2.1. Tracer gas measurements

The tracer gas results and the related weather data for all studied churches are summarized in Table 8.

Table 8: Open-door airing results from tracer gas measurements and the related conditions during the airing experiments (Hayati, Mattsson and Sandberg, 2017)

Location	Duration of Airing (min)	ΔT (°C)	Wind Speed (m/s)	Wind Incidence Angle (°)	Pressure Coefficient, C_p	Air Infiltration, ACH	Airing Rate, ACH
Hamrånge	30	3.1	2.4	29	0.33	0.06	**0.49**
Hamrånge	25	2.6	2.7	188	-0.23	0.06	**0.22**
Ludgo	57	10.0	0.0	-	-	0.08	**0.99**
Söderfors	60	14.8	2.0	0	0.56	0.07	**0.81**
Valbo	60	11.5	3.9	34	0.27	0.06	**0.52**
Visby	30	9.2	7.0	210	-0.36	0.05	**0.62**

The positive values of the temperature difference, ΔT in Table 8, indicate warmer air indoors than outdoors in all the studied churches. The studied cases include a wide variety of windward and leeward airing cases with different duration and weather parameters such as temperature difference and wind speed. The results presented in Table 8 show that opening of a porch in a large single zone like a church typically lead to an air change rate of 0.2-1 ACH, depending on the conditions; an average of 0.6 ACH is attained here. Comparing the two airing cases at Hamrånge church shows that with almost the same temperature difference and wind speed, having the porch positioned windward can lead to double flow rate in comparison with the leeward positioned porch. Table 8 indicates that single-sided open door airing through a porch results, on average, in a 9-fold increase in the air change rate (range: 4-12), compared to the air infiltration rate when the porches were closed. Thus, open-door airing seems to be an effective method to refresh the interior and remove particles and other contaminants produced e.g. by many people and lit candles during church services. Furthermore, inserting the averaged 0.6 ACH into Equation 32 shows that almost 50% of the indoor air is exchanged after one hour airing through an external porch.

An example of open-door airing measured by the tracer gas decay method for the Valbo church is depicted in Figure 30.

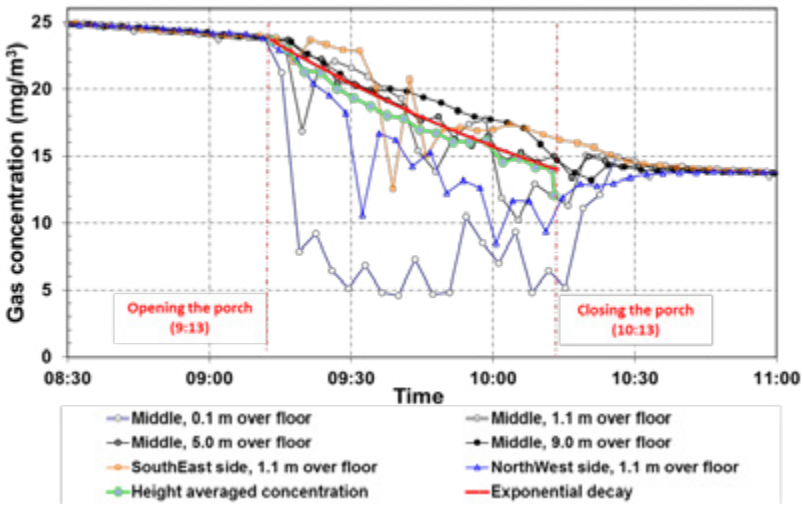

Figure 30: Tracer gas decay in Valbo church (Hayati, Mattsson and Sandberg, 2017).

The overlapping of the tracer gas concentration at different positions indicates it is well mixed before opening the porch, see Figure 30. Then, during the airing period, there are larger variations in the gas concentration, with a substantial drop at lower levels. Moreover, the quick drop in tracer gas concentration at lower levels shows that the fresh outside air reaches these lower levels first, which is as could be expected since the incoming air is colder and therefore heavier than the inside air and thus presumably flows over the floor as a gravity current. After closing the porch, the concentration curves converge again, and a homogeneous concentration appears to be attained after around 20 min. This rather fast mixing is likely to occur due to convective air currents at the heating units inside the church (or due to the mixing fans, in case of Hamrånge church). The room-average gas concentration at the moment of the door closing was assessed by extrapolating backwards the decay curve after the 20 min point where the concentrations were homogeneous again.

Moreover, the height averaged tracer gas concentration (using "Middle" data) which is shown by a green line in Figure 30 is close to the exponential decay curve, i.e. the red line (calculated by fitting an exponential curve to the average concentrations before and after opening the porch). Thus, the exponential decay assumption seems reasonable for measuring the airing flow rates by using the tracer decay method. The overall uncertainty in the airing measurements, using tracer gas concentrations before and after airing, is estimated at ±10-15% (95% C.I.).

4.2.2. Air velocity measurements in porch opening

Air velocity measurements in the porch of Hamrånge church, during the same time of the tracer gas measurements (presented in Table 8), are presented here. The installation of thermal anemometers is shown in Figure 31 and the red dashed line in Figure 31 indicates the position of the Neutral Pressure Layer (NPL), where there is a change in flow direction. The airflow pattern and direction is visualized using smoke as it is depicted in Figure 31. According to the picture, there is inflow at the lower part and outflow at the upper, indicating bidirectional airflow through the porch.

Figure 31: Smoke visualization of open-door airing, with the indoor-outdoor temperature difference of around 5 °C and wind speed of 1 m/s (blowing from the leeward side). Red dashed line indicates approximate height of the Neutral Pressure Layer, NPL (Hayati, Mattsson and Sandberg, 2017).

The recorded air velocity profiles are depicted in Figure 32 for both windward and leeward case. As the sensors were omnidirectional, flow direction (inflow or outflow) was evaluated from the smoke visualizations together with temperature measurements of the anemometers. The average temperature between the highest and lowest point is used as threshold; comparing with the threshold temperature, flow rates with lower temperature are considered as inflow, having a temperature closer to the outdoor air. Vice versa, the airflows with higher temperatures are considered as outflowing air, having a temperature closer to the indoor air. The bidirectional flow depicted

in Figures 31-32 does show that flow through the porch is significantly governed by buoyancy. The horizontal fluctuation bars in the middle of Figure 32 indicate high turbulence engaged with the in- and outflow interface, which can be caused by the shear stresses in that region.

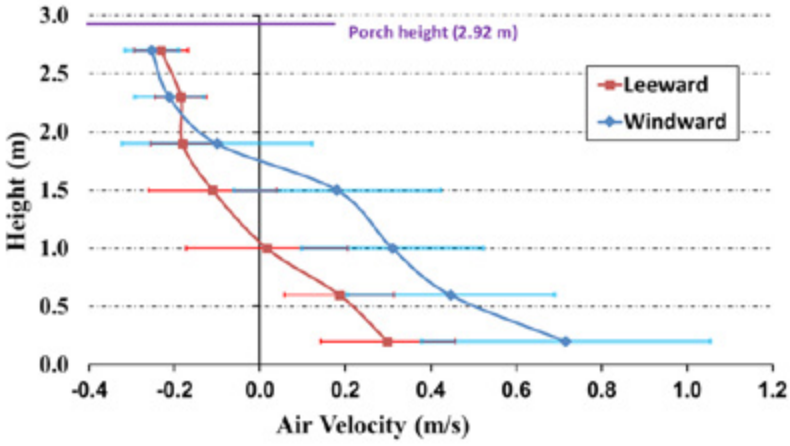

Figure 32: Air velocity profiles (average ±one standard deviation) in the porch of Hamrånge church; windward and leeward case, resp (Hayati, Mattsson and Sandberg, 2017).

The air velocity measurements are used to calculate the airing flow rates, by summing up all air velocities times their related subarea of the porch opening. The resulting porch-airing flow rates are presented in Table 9:

Table 9: Airing rates at the two single-side test cases in Hamrånge church, assessed from air velocity measurements (Hayati, Mattsson and Sandberg, 2017).

	Duration of airing (min)	In-flow (m^3/s)	Out-flow (m^3/s)	Airing rate, ACH
Hamrånge Case 1 (windward)	30	*1.368*	0.517	0.65
Hamrånge Case 2 (leeward)	25	0.477	*0.639*	0.30

The difference in the in- and outflow rates are due to air in- and exfiltration through the adventitious leakages in the rest of the building envelope; with the open porch on the windward side, more exfiltration than infiltration can be expected, and *vice versa* with the porch on the leeward side. Therefore, the resulting air change rates are calculated based on the highest values between in- and outflows. Comparing airing flow rates in Table 9 with the tracer gas ones in Table 8, both indicate that airing in the windward case

is almost double the leeward one. In addition, the airing flow rates gained by tracer gas method are 33% and 36% lower comparing with wind- and leeward cases of Figure 32. One reason for the overprediction of the airing flow rate assessed from the air velocity measurements in the porch, i.e. the Σ(velocity x sub-area) method, is the shortcutting of the incoming air with the entrance; i.e. a part of the incoming air might be withdrawn from the interior by the outgoing flow at the porch area due to a non-perfect air mixing inside the church or due to turbulence at the porch. Another reason is that a perfect result with the direct air velocity measurement method using the omnidirectional anemometers would require the flow to be perpendicular to the anemometers, which might not be always the case. Shortcutting of the airflow in the opening area is reported by previous studies; for instance (Cockroft and Robertson, 1976) also reported that only 37% of the incoming flow through the opening contributed to effective air change rate.

4.2.3. Air temperature variations during airing

Air temperatures during an airing occasion, measured at different heights from 0.1 m to 8.0 m over the floor, are depicted in Figure 33, for a windward case in Hamrånge church (Hamrånge Case 1 in Table 9).

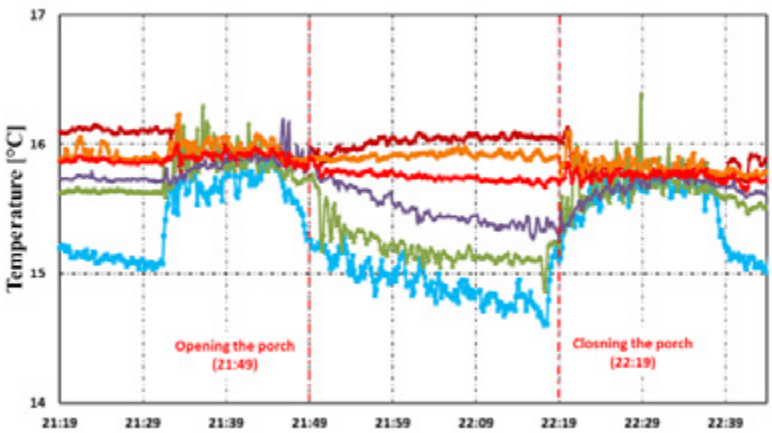

Figure 33: Time history of measured air temperatures at different heights in Hamrånge church, during 30 min single-sided airing test, windward case. Outdoor temperature = 12.2 °C (Hayati, Mattsson and Sandberg, 2017).

A clear temperature stratification can be seen during the airing period in Figure 33, with colder air in the lower levels and warmer air close to ceiling. However, the temperature stratification is more or less eliminated just before and after the airing period, owing to the mixing fans. As soon as the mixing fans are turned off, the stratification tends however to be reestablished fairly quickly. The outside temperature was 12.2 °C pointing to the limited in-outside temperature difference, however it is clear from Figure 33 that the

temperatures below the porch height of 2.9 m are the most affected ones by the incoming colder airing flows.

4.2.4. Results from modeling

Models for airing through large openings are evaluated by comparing with the tracer gas measurements. The studied models are mentioned in Introduction, see Table 2, and include the British standard model BS 5925 (BSI, 1991) (model 1), the model developed by De Gids and Phaff (1982) (model 2), the model presented by Larsen and Heiselberg (2008) (model 3) and the model by Caciolo (2010) (model 4). Figure 34 shows predicted vs. measured airing data, including a line indicating perfect agreement between the measured and predicted airing flow rates, plus two dashed lines showing a range of ±25%.

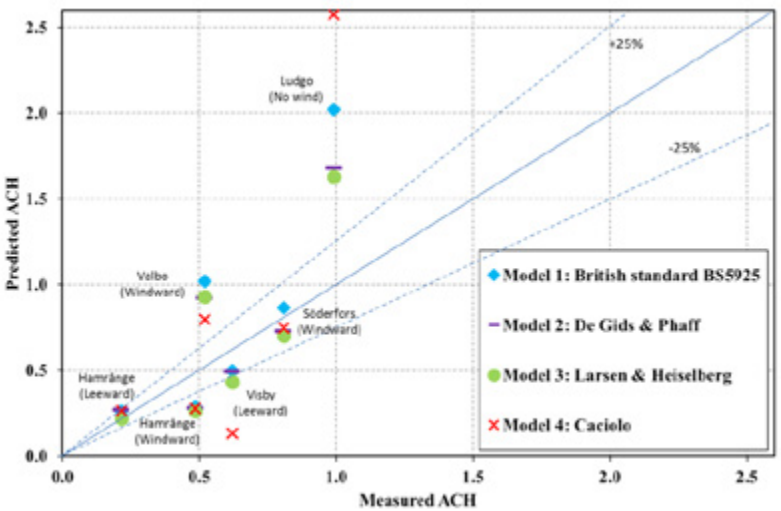

Figure 34: Predicted vs. measured open-door ACH for all the case studies (Hayati, Mattsson and Sandberg, 2017).

Figure 34 shows that there is a positive correlation between predictions and measurements, with three cases of under-prediction by all models and three cases of over-prediction. Modelled airing rates deviate from measurements by a factor of between 0-2.6. The predicted flows are in the same range for all models, with exception of the model 4 results for Ludgo and Visby churches. Therefore, the results from model 4 may have lower reliability. Highest predicted values are observed for the British standard model (BS 5925) while the lowest predicted airing are observed for the model developed by Larsen & Heiselberg. The largest modelling deviation is observed for the airing in Ludgo church, where there was not any wind effect and the airing was purely buoyancy driven. There is no apparent tendency for the prediction deviations to be due to wind direction, i.e. windward/leeward

positioned porches. Airing flows predicted by the models developed by De Gids & Phaff and Larsen & Heiselberg, are within the ±25% region in half of the cases and display the smallest prediction deviations. The slightly better predictions of these models can be due to including terms for wind turbulence, which are based on wind tunnel studies and site measurements. The current study indicates viability of the models for *rough* estimation of open door airing, although they are not specifically developed for airflow through doors but through windows or openings in general. However, the residuals in Figure 34 indicate a potential for model improvement.

4.2.5. The practical airing diagram

Practical airing diagrams, as described in Method, are presented in Figures 35-37 showing the magnitude of the exchanged room air (in percentage of the church volume), i.e. Equation 32. The diagrams are based on size characteristics of the church, indicated by the geometry factor ($f = \frac{Vol}{bH^{3/2}}$) and are depicted for different in- outdoor temperature differences, i.e. ΔT (considering warmer inside air). For instance, f equal to 500, see Figure 36, represents a typical church with the volume of 5000 m^3 and a door size of 5.8 m^2.

If several openings are opened simultaneously, their size term, i.e. $bH^{3/2}$, can be added in the denominator of the formula for *f*. The diagrams do however not include wind cross flow effects, and in those cases, larger flow rates can be expected. The practical diagrams, Figures 35-37, also include a line for typical air infiltration of 0.1 ACH in churches (Sandberg *et al*., 2014) for the sake of comparison between the airflow through leakage and via the porches.

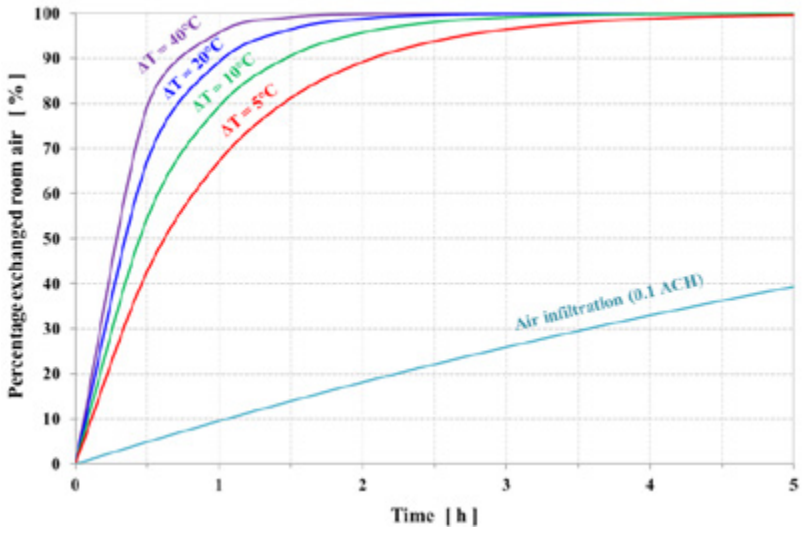

Figure 35: Practical diagram of airing for a church with geometry factor *f*=200.

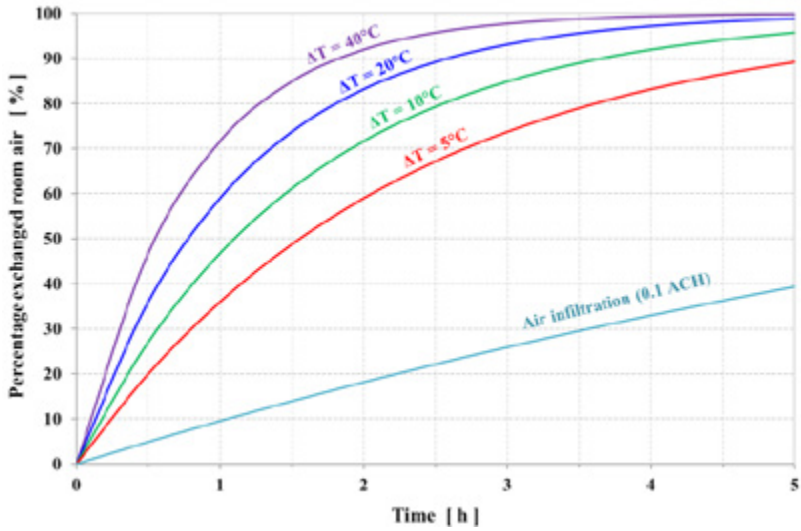

Figure 36: Practical diagram of airing for a church with geometry factor *f* =500 (Hayati, Mattsson and Sandberg, 2017).

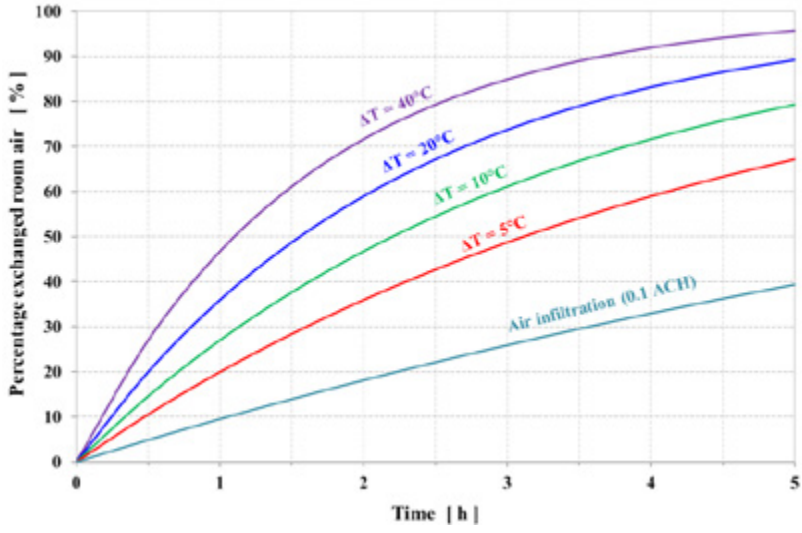

Figure 37: Practical diagram of airing for a church with geometry factor *f* =1000.

It is shown in Figures 35-37 that the percentage of exchanged air decreases with increasing geometry factor. In other words, it takes more time for the air in a *larger* church with *smaller* opening to be exchanged through airing, as would be expected. For instance, approximately one hour airing is needed in order to refresh more than 40% of the interior space of a church with *f* equal to 500. As another example, in case of having a geometry factor equal

to 200, practically all the air in the interior volume will be exchanged after 2-3 hours, depending on the temperature difference, while this would take almost double the time for a church with a geometry factor of 500. Further, according to Figures 35-37, open-door airing can provide larger airing flows comparing with only air infiltration, also for a relatively large building with small door. Thus, given a specific geometry factor for a specific church, one can use Equations 31-32 to calculate the airing rate, or interpolate between values attained from Figures 35-37.

As mentioned, wind effect is not considered in the practical airing diagrams, i.e. Figures 35-37. Therefore the airing rate in windy conditions are underestimated calculating with the diagrams; consequently the calculated airing period for exchanging a certain amount of interior air is the *maximum* airing periods needed.

As the modern buildings are equipped with tight façades, occasional airing can be a complement to the mechanical ventilation system, especially for removing the extra contaminants produced by people and lit candles like in churches or during breaks at schools. Especially churches, but also most of the existing dwellings, are however only naturally ventilated. Therefore, the results of this study can be useful, for providing airing guidelines. Single-sided ventilation through doors or windows is mostly available and extra ventilation can be provided in case it is needed and appropriate regarding comfort aspects and outside air quality conditions. The heat loss during the airing occasions of Table 8 is roughly calculated as 1-13 kWh (6 kWh on average) for one hour airing; which can be considered as a relatively small portion of the total energy use.

Assuming 600 people at the same time in a church, which is the maximum capacity of Hamrånge church, and an initial indoor CO_2 concentration of 400 ppm (=outdoor concentration), the guideline value 1000 ppm is reached within 26 minutes, assuming 0.1 ACH ventilation due to air infiltration only; this seems to be a typical value in historical Swedish churches (Sandberg *et al*., 2014). In the assumption it is supposed that the only CO_2 emission source is by people and each person releases 18 L/h (Awbi, 2003). In such building, where there is no mechanical ventilation or the possibilities of adding that is limited, the only way to introduce fresh air is opening the porches or if possible the windows. In case if implementation of cross flow is possible, even larger flow rates can be gained. Thus, airing is recommended after or sometimes during each aggregation in churches and similar buildings especially if naturally ventilated via air infiltration. The risk of draught must however be considered when airing during occupation. Further, in churches and other spaces that have culturally and esthetically valuable artefacts, airing may be especially motivated for removing particulate contaminants released by visitors, candles, incense, etc, which otherwise will cause surface soiling.

4.2.6. A discussion on pressure and flow distributions

As noted above, the air change rate inside a church can be significantly increased by airing, in comparison with air infiltration. Because the area of the door or windows in general is much larger than the total leakage area of a building envelope. In case it is colder outside, the outside air flows in through the lower parts of the porch and the indoor air flows through the upper parts of the porch, as it is illustrated by smoke visualization in Figure 31. Therefore there is bidirectional flow and assuming a relatively tight building, opening a porch (single-sided ventilation), the NPL will be positioned around half the porch height (Sandberg *et al*., 2014), see Figure 38. However, a far as the opening area is far larger than the leakage area, the flow exchange through the porch is the dominated flow and depending on the leakage distribution over the rest of the building envelope, the NPL position can be shifted somewhat up or down around the middle of the porch height.

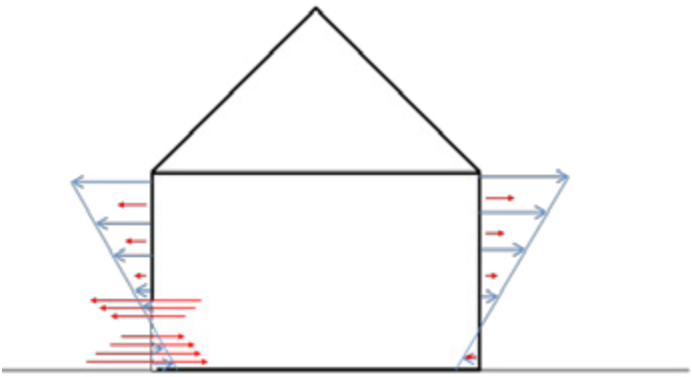

Figure 38: Schematic view of the buoyancy induced in- and outdoor pressure difference (the blue arrows) and the airflow (the red arrows) in a single-sided ventilation case, the porch on the left side is opened (Sandberg *et al*., 2014).

In a cross flow case, when two opposing porches are opened simultaneously, the airflow will be one directional through the porches, i.e. air enters through the whole area of one porch and exits via the other porch, see Figure 39. Obviously, there will be a minor air exchange also through the leakages, but the absolutely dominating flow is the cross flow through the porches. Cross flow rates are normally much larger than the single-sided ventilation, because wind induced flow is more effective and can be peneteratd into the building in a much easier way. Therefore, in order to provide a given amount of extra ventilation, shorter airing periods are needed copared with single-sided ventilation (Sandberg *et al*., 2014).

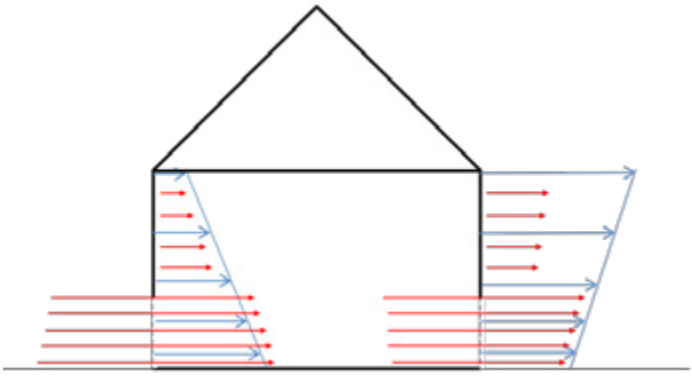

Figure 39: Schematic view of the buoyancy and wind induced in- and outdoor pressure difference (the blue arrows) and the airflow (the red arrows) in a cross ventilation case. Both porches on the right and left side are opened and wind is blowing from leftside (Sandberg *et al*., 2014).

4.2.7. A discussion on dryness and condensation risks

In a church, humidity is emitted to the air from people and lit candles. Consequently, the relative humidity can be increased with condensation risks if the surface temperatures are low enough, i.e. lower than the related dew point. The relative humidity can often be even higher in the attic space because the humid warmer air will issue up into this space. During the winter season, when the outside air is drier, it is advised to keep the airing relatively short, otherwise the indoor relative humidity might be too dry, which can cause deformation of valuable wooden constructions and different pieces of art. On the other hand, during spring and early summer, the relative humidity is higher outside, and airing in these seasons can lead to condensation on interior heavy surfaces like thick stone walls which still are bit cold. This is an important issue in churches and similar cultural heritage buildings, where condensation might destroy wall paintings, furniture or other artefacts. In order to assess the condensation risks, the maximum dew point for five different regions in Sweden is calculated throughout the year. The dew point data are mean values of the monthly registered maximum temperature over a ten-year period, between 2004 and 2014, gained from Swedish Meteorological and Hydrological Institute (SMHI). The regions include Nattavaara in the North, Göteborg in the Southwest, Hörby in the South, Gävle in the East and Örebro in the mid region of Sweden. The dew points are presented in Table 10. Thus, condensation might occur if the surface temperatures are lower than the dew point temperature during an airing occasion in a particular position and month, given in Table 10. Airing in such circumstances should be avoided. The porches in churches are often opened before the services in order to welcome people. Therefore, in case of condensation risk, the church should be warmed up in an appropriate time before each

occasion, so that the surface temperatures does not fall below the dew point temperatures. The data given in Table 10 can be useful for such estimations in these situations (Sandberg *et al*., 2014).

Table 10: The maximum dew point temperature (°C) of the outdoor air at different cities in Sweden; mean of ten-year period (Sandberg *et al*., 2014).

	Gävle	Hörby	Göteborg	Nattavaara	Örebro
Jan	3.2	5.5	8.2	-0.7	4.3
Feb	2.3	5.5	9.4	-0.4	3.4
Mar	3.2	*7.9*	15.8	0.4	5.2
Apr	8.5	10.1	*21.7*	2.9	9.4
May	12.9	15.4	23.0	9.7	13.6
Jun	16.2	17.2	24.9	14.1	15.2
Jul	18.6	19.6	25.5	16.7	17.4
Aug	18.8	19.3	24.0	16.0	17.6
Sep	13.9	14.8	19.5	11.0	12.7
Oct	10.3	12.3	14.7	6.6	10.2
Nov	7.0	9.2	10.7	2.1	7.1
Dec	3.9	6.7	8.3	0.5	5.1

During services in Swedish churches, the indoor temperature is usually close to ordinary indoor conditions, or a few degrees lower, typically around 18-20 ºC. Especially in intermittently heated stone churches, surface temperatures are often a bit lower than this. Still, when comparing with the dew points in Table 10, the overall condensation risk appears small. An exception is the Göteborg region, next to the sea, where the outside humidity often is high; there it seems sensible to be particularly attentive to condensation risks.

4.2.8. The IDA-ICE computed results

The wind- and leeward airing cases for Hamrånge church, as shown in Table 8, were simulated with the IDA-ICE software for the same airing periods. The measured weather parameters as well as the simulated indoor air temperature and the airing flows are depicted in Figure 40.

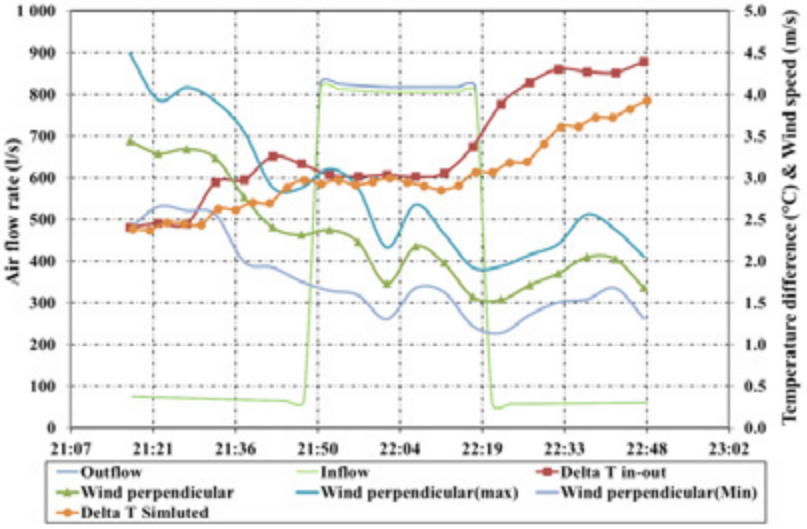

Figure 40: Weather and airing data for the windward airing case of the Harmånge church (Hayati, Mattsson and Sandberg, 2016).

"Outflow" and "Inflow" in Figure 40 are the total airflow, flowing out from or into the main hall of the church. The average Perpendicular component of the wind, perpendicular to the façade, is shown in Figure 40. Besides, the minimum and maximum wind variations are also shown in the figure pointing to the wind dynamics. "Delta Tin-out" and "Delta T Simulated" are the measured and simulated temperature differences between inside and outside respectively. The model verification is proved by having good agreement between the simulated indoor air temperature and the measured ones, particularly during the airing period. The simulated airing flow rates are rather constant or have minor increase because the driving forces are almost constant; i.e. there is slightly increase in the wind speed while the temperature is constant during the airing period.

The simulated airing flow rates are depicted in Figures 41-42. Both in- and outflows through the porch and through the envelope leakages, i.e. airing and air in- and exfiltration are depicted. Besides the wind- and leeward cases of Hamrånge church, other cases are simulated with No wind, Fixed wind (2.4 m/s wind speed and 29° wind incidence angle) during the whole simulation period. All the simulated cases share the same outside temperature.

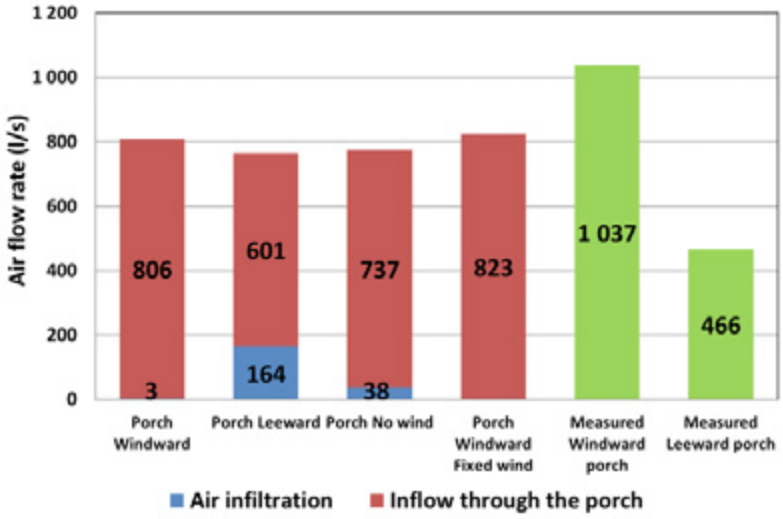

Figure 41: Air inflow to the main hall (Hayati, Mattsson and Sandberg, 2016).

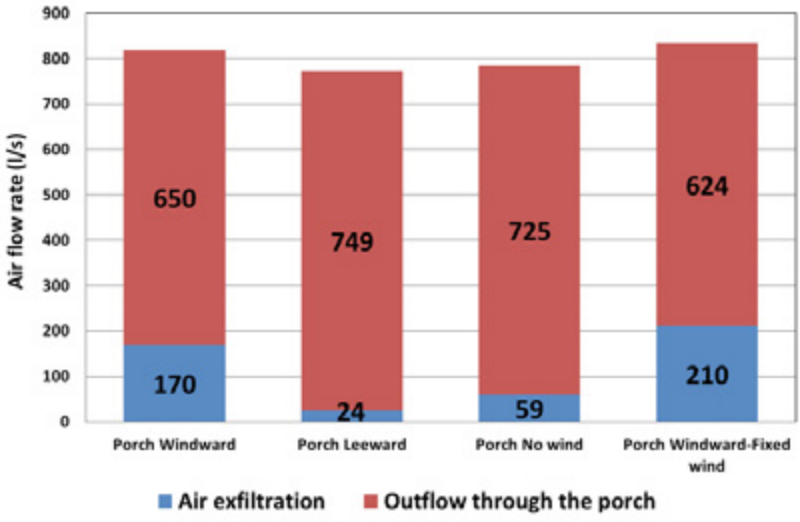

Figure 42: Air outflow from the main hall (Hayati, Mattsson and Sandberg, 2016).

The green bars in Figures 41-42 depict the measured airing flow rates when the porch was located in the wind- and leeward side. These values are the purging or effective air change rates gained by tracer gas and include airflows both through the side porch as well as through the adventitious leakages in the building envelope. The simulated total air in- and outflow for the Windward, Leeward, with No wind at all and with Fixed wind are not varying significantly. The reason can be that the driving forces for airing, i.e. wind speed and the temperature difference do not differ dramatically between the cases. However, the percentage of air infiltration show a discrepancy between different cases; for instance for the windward cases, air infiltration is lowest and flow through the porch is mostly dominated. Because, there is a positive pressure inside the church, in the windward case, caused by the incoming airflow that increases the air exfiltration through the leakages. In the leeward side, airflow is pulled out from the interior, which makes a negative pressure inside and cause infiltration through the leakages.

IDA-ICE program has been validated generally in different studies, which have tested the program's reliability and functionality (Achermann, 2000; Kropf and Zweifel, 2001; Kalamees, 2004; Sahlin *et al*., 2004; Moosberger, 2007; Hilliaho, Lahdensivu and Vinha, 2015). The functionality of the program is also considered reasonable here since, according to Figure 41, the simulated airing flows are of similar magnitude as the measurement data. However, the measured windward airing flow is almost double the leeward flow and this is not well predicted by the simulation. The reason can be the turbulence ignorance in the models used in IDA-ICE, and, as will be shown in Ch. 4.2.11, turbulence appears to be important at open door airing. Further, there are more options for the air rather than penetrating into the opening: it can be blown around the façade walls or the roof (Sandberg *et al*., 2015), which is ignored in the orifice equation, i.e. Equation 10. The orifice equation, used in IDA-ICE, is more aimed for airflow in ducts, where air does not have any other options. Other reasons for the discrepancy can also be the inaccuracy of input data such as the leakage allocation over the building envelope.

4.2.9. Drag force measurements on wind tunnel model

The drag force over the wind tunnel model used for airing measurements, i.e. Figure 16, was measured in the wind tunnel and the resulting drag coefficients, calculated by using Equation 28, is presented in Figure 43. The wind tunnel was not equipped with the roughness terrain in these measurements.

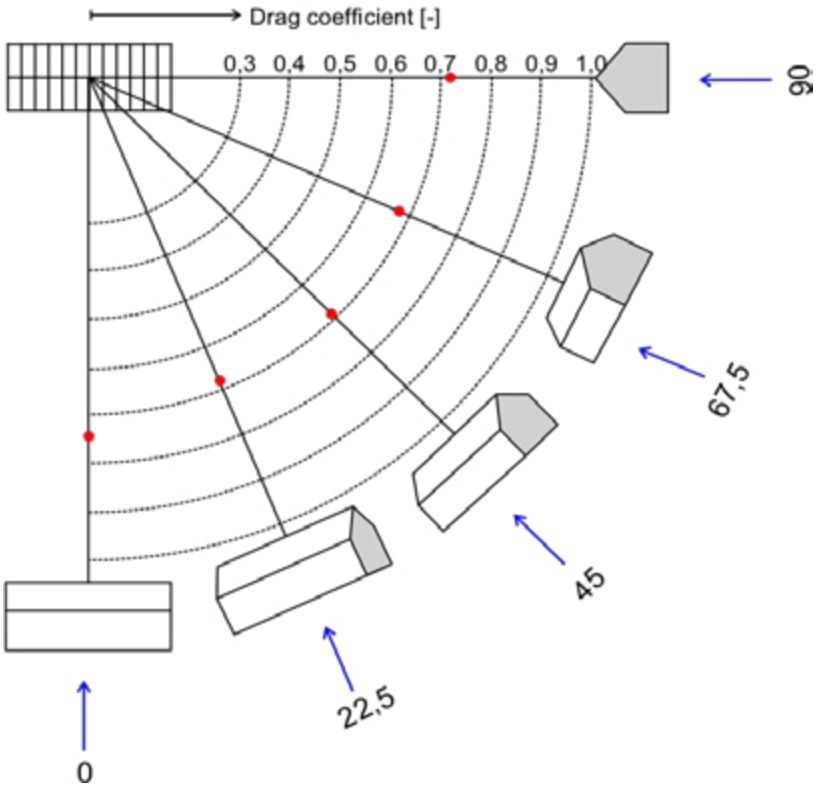

Figure 43: Drag coefficient over the model with different wind directions and fixed wind speed of 14 m/s at the model height.

According to Figure 43, drag coefficient variates somewhat within different wind directions, i.e. different projected area, and in average 0.70 can be gained. In other wind tunnel studies, when there was not any opening, the measured discharge coefficient, Cd was attained as 0.73 (with the wind speed of 14 m/s, blowing perpendicular towards the porch façade). The same cases were repeated having the porches with different opening sizes and the attained drag coefficient was in averaged 0.74, showing that having the porches opened or closed has practically no effect on the drag coefficient.

4.2.10. Smoke visualization of the wind driven airing flow in wind tunnel

Examples of smoke visualization of the wind driven airing through the porch(es) of a model, set in wind tunnel, are presented in Figures 44-46 for single-sided and cross flows.

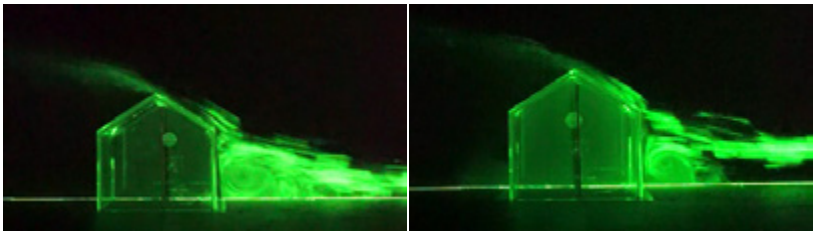

Figure 44: Smoke visualization (side view) of the *single-sided Windward flow* (left) and *cross flow* (right). Wind blowing from the right. Wind tunnel is equipped *with the roughness elements*, and fans' speed at 100 RPM.

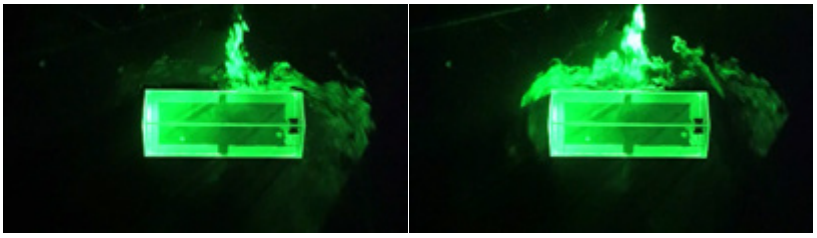

Figure 45: Smoke visualization (top view) of the *Cross flow case (both pictures, openings visible)*, with smoke injected upstream. Wind tunnel is equipped *with the roughness elements* and fans' speed at 50 RPM.

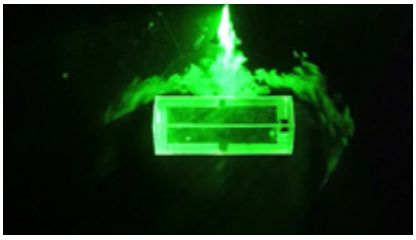

Figure 46: Same as Figure 45, but *without* the roughness elements.

Wind flow behavior regarding an opening is a complicated phenomenon and wind flow can be conducted through the opening and/or around the envelope. As can be observed in the smoke visualization Figure 44, there is a vertical standing vortex in front of the windward façade, with a diameter of about 75% of the façade height; and some part of the flow is clearly directed around the building and above the roof. The flow through the porch openings is however hardly discernable in the figures. The fraction of the wind that is conducted via the openings depends on many parameters, such as building shape, the opening size and position on façade, wind characteristics including turbulence, speed and direction, and location of the openings relative to the location of the stagnation points (Sandberg, Mattsson *et al*. 2015).

As indicated in Figure 45, the case of higher upwind air turbulence (*with* roughness elements) involved a more unsteady flow at the building model, with a greater proportion of the oncoming air alternating between flowing to the right and to the left of the building. However, for the case without the roughness elements, see Figure 46, the flow was more steady and distributed more evenly around the building. More oscillations of the wind stream at the opening, when the wind tunnel was equipped with the roughness element, can lead to more flow pumping at the opening, and as a result, more air can penetrate into it. In Hayati, Mattsson and Sandberg (n.d.), a calculated pumping volume of about 1.03 cm^3 (for wind tunnel fan speed of 200 RPM) is compared with the porch volume of 12.67 cm^3 *with* draught lobby, and 1.65 cm^3 *without* the draught lobby, resp. That is, the assessed pulsating volume is of the same magnitude as that represented by the wall thickness, but less than 1/10 of the draught lobby volume. This suggests that, especially for the draught lobby case, other mechanisms than pulsation are likely to dominate the air transfer, like advection by turbulence vortices.

4.2.11. Airing flow coefficient based on tracer gas measurements in wind tunnel

The vertical profiles of the free wind stream and the relative turbulence are presented in Figures 47-48 for both cases with and without the roughness elements (see Figure 16). The cases include different fan speeds of 100, 200, 300 and 400 RPM in the wind tunnel.

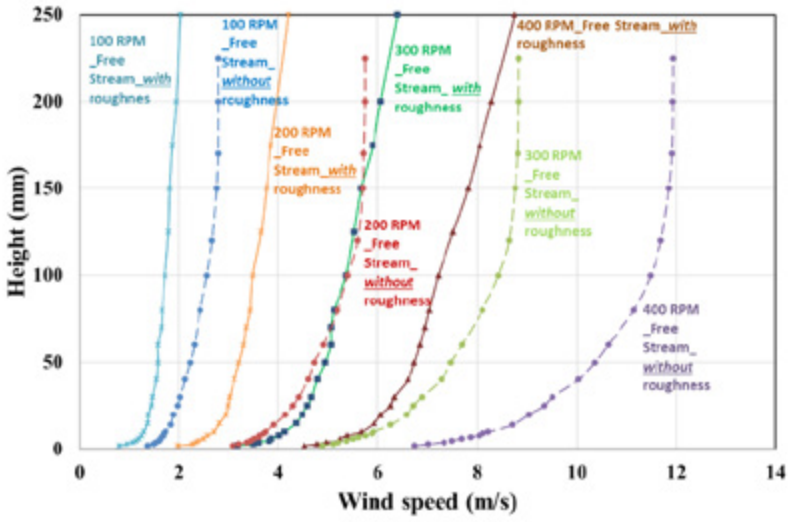

Figure 47: Vertical profiles of free wind stream (mean velocity) both with and without roughness elements at different wind tunnel fan speeds. The dashed line indicates the cases without having the roughness elements in the wind tunnel.

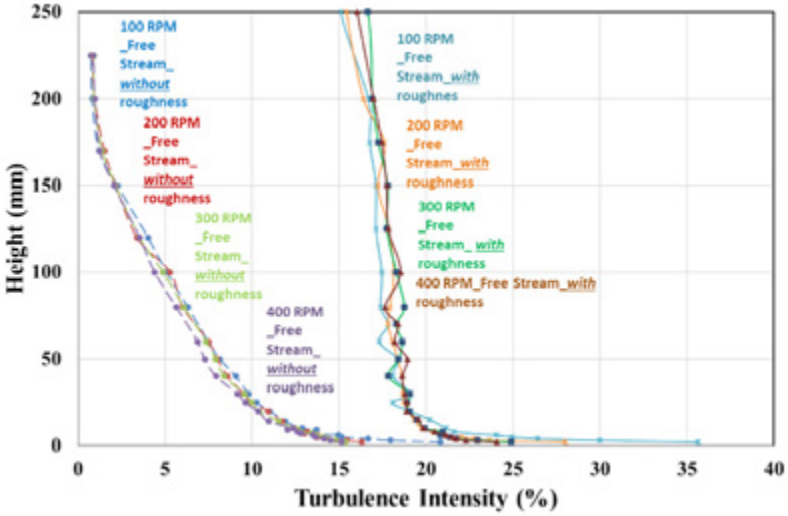

Figure 48: Relative turbulence intensity profiles of free wind stream both with and without roughness elements at different wind tunnel fan speeds. The dashed line indicates the cases without having the roughness elements in the wind tunnel.

In practice, the boundary layer gets thicker in case of having the roughness elements in wind tunnel. According to Figure 47, the wind speed becomes constant approximately above 170 mm height in cases *without* having the roughness elements in wind tunnel. While, according to measured wind profiles (up to 900 mm height), in case with having the roughness elements, the air velocity increases even beyond mid-height of the wind tunnel, i.e. 750 mm due to a thicker boundary layer. Comparison with patterns given in the guideline VDI 3783/12 (VDI, 2000) indicates that the relative turbulence intensity is equivalent to *rough* terrain for the case *with* the roughness elements and *slightly rough* terrain for the case *without* the roughness elements.

The flow coefficient, C_f, explained in Equation 27, is assessed based on the tracer gas measurements performed in the wind tunnel. The vertical profiles of the free wind stream and the relative turbulence are presented in Figures 47-48 for both cases with and without the roughness elements. The fan speeds 100, 200, 300 and 400 RPM were used in the cases *without* the roughness elements, while *with* the elements, the fans were speeded up a bit, to yield the same mean air speed at mid-height of the façade of the building model. This was done in order to better detect the effect of turbulence level on airing. The resulting flow coefficients are presented in Figures 49-50 and Table 11.

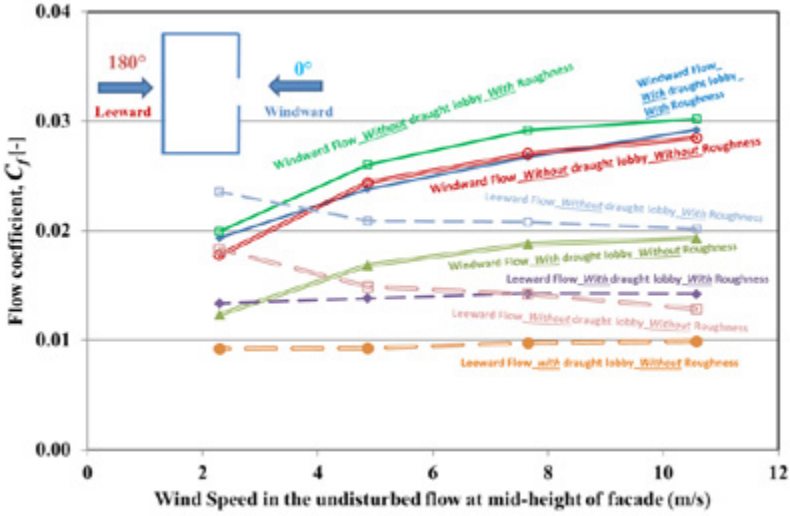

Figure 49: Flow coefficient, C_f, related to wind speed at mid-height of façade, calculated for *single-sided* airing. Cases with/without roughness elements in the wind tunnel are indicated with filled/hollow lines, cases with/without draught lobby are indicated with filled/hollow markers, and the windward/leeward cases are indicated with solid/dashed lines.

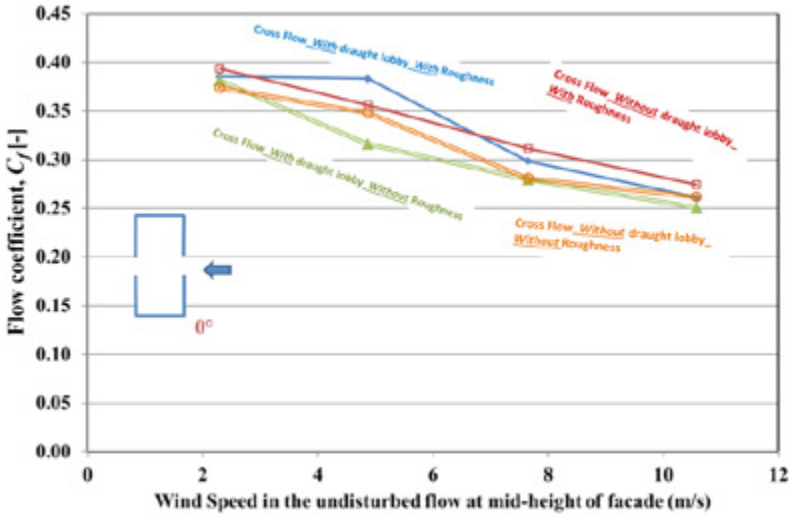

Figure 50: Flow coefficient, C_f, related to wind speed at mid-height of façade, calculated for *Cross flow* airing. Cases with/without roughness elements in the wind tunnel are indicated with filled/hollow lines, cases with/without draught lobby are indicated with filled/hollow markers.

Figure 49 indicates that, at single opening airing, a higher turbulence level (*with* roughness elements) on average yields higher airing rate, and that the existence of a draught lobby results in lower airing rates. Also at cross-flow, Figure 50, the higher turbulence level tends to yield a bit higher airing rate, whereas there is no apparent effect of the draught lobby. The area used at the cross flow coefficient calculations is that of only one opening, and the two openings are equally large. The flow coefficients, presented in Figures 49-50, are calculated considering the wind speed at mid-height of the model façade, while the results in Table 11 include C_f-values attained also at height averaged wind speed up to both the façade and porch height. The data in Table 11 are averaged over both turbulence conditions (with and without the roughness elements) and only includes the cases without draught lobby. "Windward cases" and "Leeward cases" means strict wind- and leeward direction, i.e. wind incidence angles of 0° and 180°, resp.

Table 11: Flow coefficient, C_f-values, calculated from the tracer gas measurements at the model in the wind tunnel.

	Reference wind speed definition		
	Mid facade	**Facade height averaged**	**Porch height averaged**
Windward cases	0.025	0.024	0.029
Leeward cases	0.018	0.015	0.019
Crossflow cases	0.325	0.334	0.401

From Table 11, as an average, a flow coefficient of 0.022 for the single-sided cases and 0.325 for the cross flow can be gained. This indicates that only 2% of the free stream wind flow contributes to the induced single-sided flow while the ratio is 33% for the cross flow. Noticing Table 11, the flow coefficients are quite similar considering different wind speeds as the reference in Equation 27. Thus, using wind speed measured at the mid-height of the façade seems reasonable for prediction of the wind driven flows.

Regarding single-sided ventilation the attained flow coefficients here can be compared with 0.025 (Warren and Parkins, 1984), 0.015 and 0.020 for parallel single-sided flows and opening porosity of 6.25% and 12.25% (Kato *et al*., 2006) and 0.0175 (Chu, Chen and Chen, 2011). Regarding cross flow, a value between 0.4 to 0.8, as a rule of thumb, is suggested by Riffat (1991). The difference in the coefficients can partly be due to the fact that other studies are performed for window type of the opening, while flow through porches and the effect of the draught lobby is investigated in the current study. Another reason can be differences in type of flow at the façade. For instance, some studies have only considered that flow attaches to the building and therefore only the flow that is parallel to the opening is considered developing the flow coefficient.

5. Conclusions

The present study has penetrated the issues of air infiltration and open-door airing in large single-zone buildings, with particular attention to historical churches. These represent old and relatively leaky buildings without mechanical ventilation, where the air change rate affects heating energy, air quality and humidity. In addition to health concern, the air quality issue includes in these buildings the critical problem of particle deposition, which causes gradual soiling of indoor surfaces, including paintings and other pieces of art. Some of the soiling particles are infiltrated, but significant amounts are also emitted from visitors and from candles, incense, etc. Enhanced knowledge of air infiltration and the possibilities to temporarily enhance ventilation through airing is of importance for these reasons. The current study investigates these air flow matters regarding mechanisms, prediction models and possibilities in open-door airing. The study methods involve field measurements, experiments in wind tunnel and computer modelling. Below, conclusions regarding air infiltration and airing are presented separately.

5.1. Air infiltration

Two of the most established models for predicting air infiltration rate in buildings were evaluated against measurements in three historical stone churches. The two models were the Lawrence Berkeley Laboratory (LBL) model and the Alberta air Infiltration Model (AIM-2). These were originally developed mainly for dwellings, and their applicability to church-like buildings was tested. The somewhat more developed AIM-2 model yielded slightly better predictions than the LBL model. There is also an AIM-2 model that includes a parameter for the existence of a crawl space, this model yielded still a bit better results for the church having such a crawl space. However, an LBL version that allows inclusion of the Neutral Pressure Level (NPL) of the building envelope produced even better predictions, and also proved less sensitive to assumptions on air leakage distribution at the building envelopes. All models yielded however significant overpredictions of the air infiltration rate, when compared to tracer gas measurements in the field. Since NPL may be difficult to attain in practice, the AIM-2 model was chosen for model modification to improve predictions. Tuning of this model by varying its original coefficients yielded however unrealistic model behaviors and the eventually suggested modification implied introducing a correction factor of 0.8. This reduced the median absolute prediction error from 25% to 11%. Thus, especially when the NPL is not at hand, this modification of

the AIM-2 model may suit better for air infiltration assessment of churches and other buildings similar to the tested kind. The biggest challenge in using these air infiltration models is to estimate the leakage distribution parameters, allotting leakage area between floor, ceiling and the surrounding walls. Guesstimated leakage distribution was achieved by field audit, using IR-Thermography and pressure measurements for assessing NPL. However, these measures only marginally improved the model predictions (Hayati, Mattsson and Sandberg, 2014).

Guesstimated leakage distributions, achieved in field audits similar to above, was used in combination with blower door measurements to develop a numerical model for computerized air infiltration calculations. The physical relationships for the flow through leakage paths, i.e. Poiseuille's equation (Equation 14), were used in the model, and the pressure difference caused by buoyancy and wind were considered as a function of NPL. Summation of all inflows through each modelled leakage path should equal the total air infiltration; this is solved iteratively. After initial calibration of the model, comparison with field measurements indicated reasonable prediction (R^2=0.61) of the airing rates recorded during totally 90-hours. A more systematic calibration process is however being developed, as well as testing of the model with various types of buildings and weather data.

5.2. Airing

Similar to the air infiltration study, some previously developed models for single-sided airing were investigated and validated through field measurements in five historical churches, where open-door airing was practiced. Tracer gas was used for measuring the airing rates and the results were compared with model predictions. Of the tested models, those developed by De Gids and Phaff (1982) and Larsen and Heiselberg (2008), which are more developed and include terms for wind turbulence, yielded somewhat better predictions than the other. Of those two, the model by De Gids and Phaff (1982) is judged preferable due to its relative simplicity to use.

It is concluded that single-sided open-door airing is a workable method to enhance the ventilation rate, even in large single zone buildings like churches. In the test cases of the present study, measurements of airing rates indicated that one hour single-sided open door airing in a church yielded around 50% air exchange, being almost 10 fold the air *infiltration* rate at the same conditions. For buoyancy induced open-door airing, practical diagrams to facilitate estimations of appropriate airing period for a particular situation are presented in this study. Airing can also be useable in atriums, sport halls, schools and similar mechanically ventilated buildings, where temporarily extra ventilation might be needed.

Air velocity measurements and smoke visualization were found useful together with tracer gas measurements to determine the in- and outflows during airing occasions. According to the current study, the neutral pressure layer, NPL, is not necessarily located at mid height of an opened door; it

might be shifted a bit vertically due to wind effect together with considerable air leakages in the rest of building. Further, the airing rate measured at windward positioned open porch indicated higher airing flows than when the same porch was located on the leeward side. Therefore, wind direction should be included in airing models.

The airflow at airing affects thermal comfort and energy usage and needs to be reliably treated by numerical simulation programs. Therefore, the airing models used in IDA Indoor Climate and Energy (IDA-ICE) simulation program were examined. A church model was then simulated in IDA-ICE to evaluate the flows through large vertical openings, such as doors. Measured weather data at the site of the real church were used in IDE-ICE and the simulation results were compared with tracer gas measurements of the single-sided airing flow via the church porch. Compared with the measured airing rates, the simulated ones were overall of the same magnitude. However, the effect of wind direction seemed not to be well predicted in the simulations. A possible reason for this can be the ignorance of wind turbulence in the simulation model; and turbulence appears to be important according to the wind tunnel tests presented below.

Further investigations and model improvement is recommended for the models used for airing and air infiltration predictions. For instance, implementing turbulent related coefficients can be useful regarding the flow through large vertical opening on a building envelope. Such coefficients can be gained via wind tunnel model studies. The key values of the field and modeling studies performed here is that they add knowledge on airing through *external porches*, and considers both *buoyancy* and *wind effects* with the focus on *large single zones*, like *historical churches*.

Finally, the airing studies included wind driven airing through external porches of a church model in a wind tunnel. Here, the effect of wind direction, turbulence level (roughness elements in the wind tunnel) and the existence of a "draught lobby" at the porch were investigated. Tracer gas method proved useful in measuring the airing flow rates also in such scale (1:100) models. For single-sided airing, the results pointed at higher flow rates with a windward positioned opening in comparison with a leeward positioned; thus in agreement with field measurements. With a draught lobby (extended entrance space) the airing rate was somewhat lower.

Analysis of the pumping effect entailed by wind fluctuations outside the single opening indicated that this effect is comparatively small, especially in case of a draught lobby, and it is suggested that advection through turbulence is a more important airing mechanism. More investigations of wind driven airing mechanisms are intended in future studies.

For rough estimations of wind induced airing flow rate, Q (m^3/s), a simple formula seems useful: $Q=C_f AU$, where C_f is a case-dependent flow coefficient (-), A (m^2) is the opening area and U (m/s) is wind speed. Averaged over wind directions, the present study suggests $C_f \approx 0.022$ for single-sided airing and $C_f \approx 0.32$ for cross flow. This suggests that the airing rate is on the

order of 15 times higher at cross flow than at single-sided airing. Realization of cross flow thus seems highly recommendable for enhanced airing. It must however be kept in mind that in practice *buoyancy* (indoor-outdoor temperature differences) often will be at least as important as wind as airing driver, especially in single opening cases and especially in large (high) single zone buildings. The buoyancy mechanism was however outside of the scope of the wind tunnel study, but is recommended to be included in future studies, including CFD simulations.

6. Future research

The current study is one of the first of its kind regarding investigation of the air infiltration and airing flows in large single-zones like churches. The methods include analytical and numerical model studies, field measurements and wind tunnel model studies. However, there are always need for continuing the current research and correspond to the remaining questions. For instance, the current measurement methods, especially for air infiltration, should be developed. Still there is no direct measurement method for charactering the leakage properties and estimations are uncertain. However, efforts like using radar systems, IR-Thermography or developing pressure pulsation methods might shed new lights over this topic.

The current study can be developed in numerous ways. Regarding air infiltration, more field measurement for various building types in different weather conditions can be performed in order to make a national air infiltration database. Such data could be used in providing guidelines for energy and indoor climate calculation, especially for historical buildings and renovating projects. The presented air infiltration model in this study is being developed and seems very promising if a more systematic calibration method can be implemented. Furthermore, more precise infiltration and airing models are also recommended in energy simulation programs. A further step to continue this study is to investigate the multizone models for predicting the air infiltration rates.

Airing through external porches in large single zones like churches is investigated in this study, probably for the first time, considering both wind and buoyancy effects. The literature includes airing mostly through window type of opening, placed in more modern buildings. Further field measurements are needed to evaluate the airing models for different types of buildings and weather conditions. Moreover, wind tunnel studies with different types of openings and building structures, and comparison with field measurements are suggested for further investigation and development of the models. Especially, further fundamental research should be performed in order to explore the wind induced flow via various types of openings and envelopes.

The current study of airing flow rates recognizes the great potential of natural ventilation to be used alone or in mixed mode ventilation systems. This can result in energy savings, e.g. by reducing cooling demand, while providing thermal comfort and fresh air. More detailed guidelines for practicing airing can be developed with the help of the current results. Further studies are however recommended considering the outdoor environmental conditions, besides weather also infiltration of outdoor pollutions and noise.

Another issue is draft – thermal discomfort that needs to be prevented. Moisture content and condensation are other concerning issues, especially in historical buildings like churches, where wall paintings, furniture and other artefacts might be deteriorated. The issue is addressed to some extent in the present study, but further research about these issues is needed, including more detailed guidelines regarding airing practices. Also the presented kind or practical airing diagrams of this study would be good to develop by considering also the wind effect, so far it only includes buoyancy driven flows.

As measurement procedures are costly and cumbersome, computational fluid dynamics (CFD) simulations are often used to study ventilation in buildings. The complexity of air infiltration and airing calls however for an elaborate validation work against measurements to increase reliability in these numerical tools.

7. References

Achermann, M. (2000) *Validation of IDA ICE, Version 2.11.06 With IEA Task 12 - Envelope BESTEST*. Horw: Hochschule Technik+Architektur Luzern. Available at: http://www.equaonline.com/iceuser/validation/old_stuff/BESTEST_Report.pdf.

AFS 2009:2 (2009) *Arbetsplatsens utformning: Arbetsmiljöverkets föreskrifter om arbetsplatsens utformning samt allmänna råd om tillämpningen av föreskrifterna [Design of the workplace: Work Environment Administration´s regulations on the design of the workplace and general advice for application of the regulations]*. Stockholm: Arbetsmiljöverket. Available at: https://www.av.se/arbetsmiljoarbete-och-inspektioner/publikationer/foreskrifter/arbetsplatsens-utformning-afs-20092-foreskrifter/.

Ahmadikia, H., Moradi, A. and Hojjati, M. (2012) 'Performance Analysis of a Wind-Catcher With Water Spray', *International Journal of Green Energy*, 9(2), pp. 160–173. doi: 10.1080/15435075.2011.622019.

AIVC (1984) *'Wind pressure workshop proceedings'*, in AIVC Technical Note 13.1. Brussels, Belgium: Air Infiltration and Ventilation Centre (AIVC).

Allard, F., D. Bonnotte, and K. L. (1990) 'Air flow through large openings: experimental study of the discharge coefficient', in *Internal Report CETHILL-URA CNRS 1372*. Lyon: CETHIL.

Allard, F. and Utsumi, Y. (1992) 'Airflow through large openings', *Energy and Buildings*, 18(2), pp. 133–145. doi: 10.1016/0378-7788(92)90042-F.

Andersen, K. T. (2015) 'Semi-Empirical Models for Buoyancy-Driven Ventilation-A Literature Study', *International Journal of Ventilation*, 14(1), pp. 77–90.

Andersson, S. and Sverdrup, C. (1992) *Klimatet i den inre miljön: Kartläggning och sambandsanalys av inomhusmiljön på 74 förskolor, 48 skolor i Malmö kommun [The climate in the indoor environment: Mapping and correlation analysis of the indoor environment at 74 preschools, 48 schools in Malmö municipality]*. Statens råd för byggnadsforskning.

ASHRAE (2013a) 'Chapter 16: Ventilation and Infiltration', in *ASHRAE HANDBOOK: Fundamentals 2013*. Atlanta, GA: American Society of Heating, Refrigerating, and Air-Conditioning Engineers.

ASHRAE (2013b) 'Chapter 24: Airflow Around Buildings', in *ASHRAE HANDBOOK: Fundamentals 2013*. Atlanta, GA: American Society of Heating, Refrigerating, and Air-Conditioning Engineers.

Awbi, H. (2015) T*he future of indoor air quality in UK homes and its impact on health.* Reading: British Electrotechnical and Allied Manufacturers Association. Available at: http://www.myhealthmyhome.com/downloads/Indoor-Air-Quality-Future-Scenarios-Report.pdf.

Awbi, H. B. (1996) 'Air movement in naturally-ventilated buildings', *Renewable energy*, 8(1), pp. 241–247. doi: 10.1016/0960-1481(96)88855-0.

Awbi, H. B. (2003) *Ventilation of Buildings.* London: Spon Press.

Awbi, H. B. (2008) *Ventilation systems: design and performance.* London: Taylor & Francis.

Bahadori, M. N. (1994) 'Viability of wind towers in achieving summer comfort in the hot arid regions of the Middle East', *Renewable Energy*, 5(5), pp. 879–892. doi: 10.1016/0960-1481(94)90108-2.

Baker, P. H., Sharples, S. and Ward, I. C. (1987) 'Air flow through cracks', *Building and Environment,* 22(4), pp. 293–304. doi: 10.1016/0360-1323(87)90022-9.

Bankvall, C. G. (2013) *Luftboken: luftrörelser och täthet i byggnader [The air book: air movements and tightness in buildings]*. Lund: Studentlitteratur.

Barnard, N. and Jaunzens, D. (2001) *Technology selection and early design guidance.* Construction Research Communications Limited.

Blomqvist, C. (2009) *Distribution of Ventilation Air and Heat by Buoyancy Forced Inside Buildings*. PhD. Thesis, Centre of Built Environment, University of Gävle and KTH.

Boloorchi, H. and Eghtesadi, N. (2014) 'Investigation of the Middle East Windcatchers and (Comparison between Windcatchers in Iran and Egypt in Terms of Components)', *International Journal of Architecture and Urban Development*, 4(1), pp. 87–94. Available at: http://ijaud.srbiau.ac.ir/article_2502_515.html.

Boverket (2016) *Swedish Building Regulations BBR 24. BFS 2016:13 (In Swedish).* Karlskrona: Boverket-National Board of Housing, Building and Planning.

Breen, M. S., Breen, M., Williams, R. W. and Schultz, B. D. (2010) 'Predicting residential air exchange rates from questionnaires and meteorology: model evaluation in central North Carolina', *Environmental science & technology*, 44(24), pp. 9349–9356. doi: 10.1021/es101800k.

BSI (1991) *Code of practice for ventilation principles and designing for natural ventilation, BS 5925:1991*. London: British Standards Institution (BSI).

BSI (2007) *Ventilation for buildings: Calculation methods for the determination of air flow rates in buildings including infiltration (EN15242:2007)*. London: British Standards Institution (BSI).

Build Test Solutions Ltd. (2017) *PULSE Air Test*. Available at: http://buildtestsolutions.com/pulse/

Building Research Establishment (1994) *Natural ventilation in non-domestic buildings.* DIG 399. Bracknell: IHS BRE Press. Available at: https://www.thenbs.com/PublicationIndex/Documents/Details?Pub=BRE&DocId=84454.

Caciolo, M. (2010) *Analyse expérimentale et simulation de la ventilation naturelle mono-façade pour le rafraîchissement des immeubles de bureaux*. École Nationale Supérieure des Mines de Paris.

Caciolo, M., Stabat, P. and Marchio, D. (2011) 'Full scale experimental study of single-sided ventilation: analysis of stack and wind effects', *Energy and Buildings*, 43(7), pp. 1765–1773. doi: 10.1016/j.enbuild.2011.03.019.

Chu, C. R., Chen, R.-H. and Chen, J.-W. (2011) 'A laboratory experiment of shear-induced natural ventilation', *Energy and Buildings*, 43(10), pp. 2631–2637. doi: 10.1016/j.enbuild.2011.06.014.

Chuang, H.-C., Jones, T. and BéruBé, K. (2012) 'Combustion particles emitted during church services: implications for human respiratory health', *Environment internationa*l, 40, pp. 137–142. doi: 10.1016/j.envint.2011.07.009.

Cockroft, J. P. and Robertson, P. (1976) 'Ventilation of an enclosure through a single opening', *Building and Environment*, 11(1), pp. 29–35. doi: 10.1016/0360-1323(76)90016-0.

Cook, M. J., Ji, Y. and Hunt, G. R. (2003) 'CFD modelling of natural ventilation: combined wind and buoyancy forces', *International Journal of Ventilation*, 1(3), pp. 169–179. doi: 10.1080/14733315.2003.11683632.

Cooper, E., Etheridge, D., Mattsson, M. and Wigö, H. (2011a) 'Measurement of the adventitious leakage of churches with a novel pulse technique', in *Roomvent 2011 : proceedings*. Trondheim: Tapir Academic Press, p. Paper no. 266.

Cooper, E., Etheridge, D., Mattsson, M. and Wigö, H. (2011b) 'Pressure Pulse Technique– A New Method for Measuring the Leakage of the Building Envelope of Churchesmms', in *Proceedings, Conference on Energy Efficiency in Historic Buildings, 9-11 February 2011, Visby, Sweden.*

Daish, N. C., da Graça, G. C., Linden, P. F. and Banks, D. (2016) 'Impact of aperture separation on wind-driven single-sided natural ventilation', *Building and Environment*, 108, pp. 122–134. doi: 10.1016/j.buildenv.2016.08.015.

Dick, J. B. (1950) 'The Fundamentals of Natural Ventilation of Houses', Journal of the Institution of *Heating and Ventilating Engineers*, 18(179), pp. 123–134.

Dols, W. S. and Polidoro, B. J. (2015) *CONTAM User Guide and Program Documentation Version 3.2.* Technical Note (NIST TN)-1887. Gaithersburg. doi: 10.6028/NIST.TN.1887.

Dorer, V., Haas, A., Weber, A., Feustel, H. E. and Smith, B. V (2001) 'COMIS 3.1 - User's Guide', *Swiss Federal Laboratories for Materials Testing and Research.*

Eftekhari, M. M. (1995) 'Single-sided natural ventilation measurements', *Building Services Engineering Research and Technology*, 16(4), pp. 221–225.

Eiraji, J. and Namdar, S. A. (2011) 'Sustainable systems in Iranian traditional architecture', *Procedia Engineering*. Elsevier, 21, pp. 553–559.

Etheridge, D. W. and Sandberg, M. (1996) 'Building ventilation: theory and measurement'. John Wiley & Sons.

Etheridge, D. (2012) 'Natural Ventilation of Building: Theory, measurement and design', 10(4), p. 4. doi: 10.1002/9781119951773.

Etheridge, D. W. (1977) 'Crack flow equations and scale effect', *Building and Environment*, 12(3), pp. 181–189. doi: 10.1016/0360-1323(77)90016-6.

European committee for standardization (2000) 'Thermal performance of buildings - Determination of air permeability of buildings - Fan pressurization method (ISO 9972:1996, modified) (EN13829)'. Brussels: European committee for standardization.

European Committee for Standardization (2012) 'ISO12569, Thermal performance of buildings and materials -- Determination of specific airflow rate in buildings -- Tracer gas dilution method. ISO Standard 12569:2012.'

Feustel, H. E. (1999) 'COMIS—an international multizone air-flow and contaminant transport model', *Energy and Buildings*, 30(1), pp. 3–18. doi: http://dx.doi.org/10.1016/S0378-7788(98)00043-7.

Francisco, P. W. and Palmiter, L. (1996) 'Modeled and measured infiltration in ten single family homes', in *Proceedings, ACEEE Summer Study on Energy Efficiency in Buildings: Vol. 1 Residential buildings: technologies, design, and performance analysis.* Washington: American Council for an Energy-Efficient Economy (AEEE), p. 1.103-1.115.

Fürbringer, J.-M. and Van Der Maas, J. (1995) 'Suitable algorithms for calculating air renewal rate by pulsating air flow through a single large opening', *Building and Environment*, 30(4), pp. 493–503. doi: 10.1016/0360-1323(95)00002-N.

Gerken, M., Kreienbrock, L., Wellmann, J., Kreuzer, M. and Wichmann, H. E. (2000) 'Models for retrospective quantification of indoor radon exposure in case-control studies', *Health physics*, 78(3), pp. 268–278.

De Gids, W. and Phaff, H. (1982) 'Ventilation rates and energy consumption due to open windows: a brief overview of research in the Netherlands', *Air Infiltration Review*, 4(1), pp. 4–5.

Haas, A., Weber, A., Dorer, V., Keilholz, W. and Pelletret, R. (2002) 'COMIS v3.1 simulation environment for multizone air flow and pollutant transport modelling', *Energy and Buildings*, 34(9), pp. 873–882. doi: 10.1016/S0378-7788(02)00062-2.

Haghighat, F., Brohus, H. and Rao, J. (2000) 'Modelling air infiltration due to wind fluctuations - a review', *Building and Environment*, 35(5), pp. 377–385. doi: 10.1016/S0360-1323(99)00028-1.

Haghighat, F., Rao, J. and Fazio, P. (1991) 'The influence of turbulent wind on air change rates - a modelling approach', *Building and Environment*, 26(2), pp. 95–109. doi: 10.1016/0360-1323(91)90017-6.

Harrysson, C. (1998) *Innemiljö- och energirevision av barnstugor och skolor : Registrering av energi- och vattenanvändning, enkätundersökning [Indoor environment and energy audit of children's homes and schools: Registration of energy and water use, questionnaire survey]*. Rapport 1998:3. Karlskrona: Boverket.

Hayati, A., Akander, J. and Mattsson, M. (2016) 'Development of a Numerical Air Infiltration Model Based On Pressurization Test Applied On a Church', in *Proceedings, ASHRAE and AIVC IAQ 2016 - Defining Indoor Air Quality: Policy, Standards and Best Practices, 12–14 September 2016, Alexandria, Virginia, USA*. Alexandria: ASHRAE, pp. 224–231.

Hayati, A., Mattsson, M. and Sandberg, M. (2014) 'Evaluation of the LBL and AIM-2 air infiltration models on large single zones: Three historical churches', *Building and Environment*. Elsevier, 81, pp. 365–379. doi: 10.1016/j.buildenv.2014.07.013.

Hayati, A., Mattsson, M. and Sandberg, M. (2016) 'A Study on Airing Through the Porches of a Historical Church–Measurements and IDA-ICE Modelling', in *Proceedings, ASHRAE and AIVC IAQ 2016—Defining Indoor Air Quality: Policy, Standards and Best Practices, 12–14 September 2016, Alexandria, Virginia, USA*. Alexandria: ASHRAE, pp. 216–223.

Hayati, A., Mattsson, M. and Sandberg, M. (2017) 'Single-sided ventilation through external doors: Measurements and model evaluation in five historical churches', *Energy and Buildings*, 141, pp. 114–124. doi: 10.1016/j.enbuild.2017.02.034.

Hayati, A., Mattsson, M. and Sandberg, M. n.d. (no date) 'A wind tunnel study of wind-driven airing through open doors', *Submitted for journal publication*.

Heiselberg, P. (ed.) (2002) *Principles of Hybrid Ventilation, IEA Energy Conservation in Buildings and Community systems Programme Annex 35: Hybrid ventilation in New and Retrofitted Office Buildings*. Aalborg: Hybrid Ventilation Centre, Aalborg University (IEA Energy Conservation in Buildings and Community Systems Programme Annex 35: Hybrid Ventilation in New and Retrofitted Office Buildin). Available at: http://www.hybvent.civil.aau.dk/puplications/report/Principles of H V.pdf.

Heiselberg, P., Svidt, K. and Nielsen, P. V (2001) 'Characteristics of airflow from open windows', *Building and Environment*, 36(7), pp. 859–869. doi: 10.1016/S0360-1323(01)00012-9.

Hilliaho, K., Lahdensivu, J. and Vinha, J. (2015) 'Glazed space thermal simulation with IDA-ICE 4.61 software - Suitability analysis with case study', *Energy and Buildings*. Elsevier, 89, pp. 132–141. doi: 10.1016/j.enbuild.2014.12.041.

Kalamees, T. (2004) 'IDA ICE: the simulation tool for making the whole building energy and HAM analysis', in *Proceedings, Annex 41 MOIST-ENG, Working meeting May 12-14, Zurich, Switzerland*. Zürich, pp. 12–14. Available at: https://www.kuleuven.be/bwf/projects/annex41/protected/data/TTU May 2004 Paper A41-T1-EE-04-1.pdf.

Karakatsanis, C., Bahadori, M. N. and Vickery, B. J. (1986) 'Evaluation of pressure coefficients and estimation of air flow rates in buildings employing wind towers', *Solar Energy*, 37(5), pp. 363–374. doi: 10.1016/0038-092X(86)90132-5.

Kato, S., Kono, R., Hasama, T., Ooka, R. and Takahashi, T. (2006) 'A wind tunnel experimental analysis of the ventilation characteristics of a room with single-sided opening in uniform flow', *International Journal of Ventilation*, 5(1), pp. 171–178. doi: 10.1080/14733315.2006.11683734.

Kiel, D. E. and Wilson, D. J. (1989) 'Combining door swing pumping with density driven flow', *ASHRAE Transactions*, 95(2), pp. 590–599.

Kropf, S. and Zweifel, G. (2001) Validation of the Building Simulation Program IDA-ICE According to CEN 13791 *'Thermal Performance of Buildings–Calculation of Internal Temperatures of a Room in Summer Without Mechanical Cooling - General Criteria and Validation Procedures'.* Horw: Fachhochschule Zentralschweiz. Available at: http://www.equaonline.com/iceuser/validation/ice_vs_pren 13791.pdf.

Lane-Serff, G. (1989) *Heat flow and air movement in buildings.* University of Cambridge.

Larsen, T. S. and Heiselberg, P. (2008) 'Single-sided natural ventilation driven by wind pressure and temperature difference', *Energy and Buildings*, 40(6), pp. 1031–1040. doi: 10.1016/j.enbuild.2006.07.012.

Li, Y. and Delsante, A. (2001) 'Natural ventilation induced by combined wind and thermal forces', *Building and Environment*, 36(1), pp. 59–71. doi: 10.1016/S0360-1323(99)00070-0.

Liddament, M. W. (1986) *Air Infiltration Calculation Techniques: An Application Guide.* Conventry: The Air Infiltration and Ventilation Centre. Available at: http://www.aivc.org/sites/default/files/members_area/medias/pdf/Guides/GU02 AIR INFILTRATION CALCULATION TECHNIQUES.PDF.

Liddament, M. W. (1987) 'Power law rules - OK?', *Air Infiltration Review*, 8(2), pp. 4–6.

Liddament, M. W. and Allen, C. (1983) *The validation and comparision of mathematical models of air infiltration*. Air Infiltration Centre.

Liese, W. and Usemann, K. W. (1980) 'untersuchung der CO2-konzentration in einem klassenraum', *Zeitschrift Gesundheits-Ingengieur - Gebäudetechnik in Wissenschaft und Praxis,* 101(8), pp. 225–256.

Limb, M. J. (1994) *TN: 42 Current ventilation and air conditioning systems and strategies.* AIVC Technical Note 42. AIVC.

Lundström, H., Blomqvist, C., Jonsson, P. and Pettersson, I. (1990) 'A microprocessor-based anemometer for low air velocities', *Proceedings of Roomvent, Oslo, Norway.*

Lundström, L. (2016) *Shiny Weather Data*. Available at: https://rokka.shinyapps.io/shinyweatherdata/ (Accessed: 1 January 2016).

van der Maas, J., Allard, F., Bienfait, D., Haghighat, F., Libbecq, G., Pelletret, R., Vandaele, L. and Walker, R. (1992) *Air flow through large openings in buildings*. LESO-PB [Laboratoire d'énergie solaire et de physique du bâtiment].

Malinowski, H. K. (1971) 'Wind effect on the air movement inside buildings', in *Proceedings, 3rd International Conference 'Wind effects on buildings and Structures' Tokyo Sept. 6-9 1971.* Tokyo: Saikon Shuppan Co. ltd., pp. 125–134.

Mattsson, M., Lindström, S., Linden, E. and Sandberg, M. (2011a) 'Methods to Identify Air Leakages in the Building Envelope of Churches', in Broström, T. and Nilsen, L. (eds) *Proceedings, EEHB 2011: Conference on Energy Efficiency in Historic Buildings.* Visby: EEHB.

Mattsson, M., Lindström, S., Linden, E. and Sandberg, M. (2011b) 'Tracer Gas Techniques For Quantifying The Air Change Rate In Churches–Field Investigation Experiences', in Mathisen, H. M. (ed.) *Proc. Roomvent 2011: 12th International conference on air distribution in rooms.* Trondheim, Norway, p. Paper No 235-Paper No 235.

Mattsson, M., Sandberg, M., Claesson, L., Lindström, S. and Hayati, A. (2013) 'Fan pressurization method for measuring air leakage in churches - wind and stack induced uncertainties', in *Proceedings, Cultural heritage preservation - 3rd European Workshop on Cultural Heritage Preservation.* Bozen/Bolzano, Italy, pp. 63–68. Available at: http://www.3encult.eu/en/deliverables/Documents/EWCHP2013_10.pdf.

van Moeseke, G., Bruy?re, I. and De Herde, A. (2007) 'Impact of control rules on the efficiency of shading devices and free cooling for office buildings', *Building and Environment*, 42(2), pp. 784–793. doi: 10.1016/j.buildenv.2005.09.015.

Montazeri, H. (2011) 'Experimental and numerical study on natural ventilation performance of various multi-opening wind catchers', *Building and Environment.* Elsevier, 46(2), pp. 370–378. doi: 10.1016/j.buildenv.2010.07.031.

Montazeri, H. and Azizian, R. (2009) 'Experimental study on natural ventilation performance of a two-sided wind catcher', *Journal of power and energy,* 223(4), pp. 387–400. doi: 10.1243/09576509JPE651.

Montazeri, H., Montazeri, F., Azizian, R. and Mostafavi, S. (2010) 'Two-sided wind catcher performance evaluation using experimental, numerical and analytical modeling', *Renewable Energy*. Elsevier, 35(7), pp. 1424–1435. doi: 10.1016/j.renene.2009.12.003.

Moosberger, S. (2007) *IDA ICE CIBSE-Validation: Test of IDA Indoor Climate and Energy version 4.0 according to CIBSE TM33,* issue 3. Horw: detechnik; Hochschule für technik+architektur Luzern. Available at: http://www.equaonline.com/iceuser/validation/ice-validation-cibse_tm33.pdf.

Nilsson, B.-G. (1996) 'Undersökning av inneklimat och skolor i Lunds kommun'. Lund: Miljöförvaltningen.

Nordquist, B. (2002) Ventilation and window opening in schools, Experiments and Analysis. Division of Building Services; Lund University.

Nordquist, B. (2007) Analys av skolor med fläktförstärkt självdrag. Division of Building Services; Lund University.

Nordquist, B. (2008) 'Air flows in a school with fan-assisted natural ventilation, with the focus on the opening of the exhaust windows', in Proceedings, 11th International Conference on Indoor Air Quality and Climate [Paper ID 541].

Orme, M., Liddament, M. W., Wilson, A. and Infiltration, A. (1994) *An analysis and data summary of the AIVC's numerical database.* AIVC Technical Note 44. AIVC.

Orme, M., Liddament, M. W. and Wilson, A. (1998) *Numerical Data for Air Infiltration & Natural Ventilation Calculation*, Air Infiltration and Ventilation Centre, Technical Note 44. Coventry, UK.

Palmiter, L. and Bond, T. (1994) *Modeled and measured infiltration: Phase II. A detailed case study of three homes; Final report.* Palo Alto: Electric Power Research Inst.

Palmiter, L. S., Brown, I. A. and Bond, T. C. (1991) 'Measured infiltration and ventilation in 472 all-electric homes', *ASHRAE Transactions*, 97(2), pp. 979–987.

Passivhuscentrum (2012) 'Kravspecifikation för nollenergihus, passivhus och minienergihus: Lokaler [Demand specification for zero-energy house, passive house, and minimal energy house: non-residential premises.]', *FEBY 12*. Sveriges centrum för nollenergihus. Available at: http://www.passivhuscentrum.se/sites/default/files/kravspecifikation_feby12_-_lokaler_sept.pdf.

Persily, A. K. and Linteris, G. T. (1983) 'A comparison of measured and predicted infiltration rates', *ASHRAE Transaction*s, 89(2B), pp. 183–200.

Reardon, J. T. (1989) 'Air infiltration modelling study', *Contract report No. CR5446.3, prepared for Energy Mines and Resources Canada*. Ottawa: Energy Mines and Resources Canada.

Riffat, S. B. (1991) 'Algorithms for airflows through large internal and external openings', *Applied Energy*, 40(3), pp. 171–188. doi: 10.1016/0306-2619(91)90056-4.

Roaf, S. (1989) 'BĀDGĪR', in *ENCYCLOPÆDIA IRANICA*. Winona Lake, IN: Eisenbrauns, Inc., pp. 368–370. Available at: http://www.iranicaonline.org/articles/badgir-traditional-structure-for-passive-air-conditioning.

Rydberg, J. (1945) ‘Modellförsök rörande fönstervädring m.m. [Model tests regarding window airing, etc.]’, *VVS : tidskrift för värme-, ventilations- och sanitetsteknik.*

Sahlin, P., Eriksson, L., Grozman, P., Johnsson, H., Shapovalov, A. and Vuolle, M. (2004) ‘Whole-building simulation with symbolic DAE equations and general purpose solvers’, *Building and Environment,* 39(8), pp. 949–958. doi: 10.1016/j.buildenv.2004.01.019.

Sandberg, M., Mattsson, M., Hayati, A. and Sattari, A. (2014) ‘Energibesparing i kyrkor: Luftläckage-, nedsmutsnings- och klimatmätningar. [Energy saving in churches: Air leakage, soiling and climate measurements]’. Available at: http://www.energimyndigheten.se/forskning-och-innovation/projektdatabas/sokresultat/GetDocument/?id=86234&documentName=34964-1 Slutrapport SoB 2011-2014 HiG%5B1%5D.pdf.

Sandberg, M., Mattsson, M., Wigö, H., Hayati, A., Claesson, L., Linden, E. and Khan, M. A. (2015) ‘Viewpoints on wind and air infiltration phenomena at buildings illustrated by field and model studies’, *Building and Environment,* 92, pp. 504–517. doi: http://dx.doi.org/10.1016/j.buildenv.2015.05.001.

Sekkei, N. (2017) *Stable natural ventilation in high-rise tenant office buildings.* Available at: http://www.nikken.co.jp/en/solutions/natural_ventilation.html.

Shaw, C. Y. (1985) *Methods for Estimating Air Change Rates and Sizing Mechanical Ventilation Systems for Houses, Building Research Note 237*. Building Research Note (BRN) 237. Ottawa: National Research Council Canada. Available at: http://nparc.cisti-icist.nrc-cnrc.gc.ca/eng/view/object/?id=61e3e988-2cdb-45b6-ab27-72fd84237b6c.

Sherman, M. H. (1992) ‘Superposition in Infiltration Modeling’, *Indoor Air,* 2(2), pp. 101–114. doi: 10.1111/j.1600-0668.1992.04-22.x.

Sherman, M. H. and Grimsrud, D. T. (1980a) *Infiltration-pressurization correlation: Simplified physical modeling.* Berkley: Lawrence berkeley laboratory; University of California. Available at: http://escholarship.org/uc/item/8wd4n2f7.

Sherman, M. H. and Grimsrud, D. T. (1980b) *Measurement of Infiltration using Fan Pressurization and Weather Data.* Berkley: Lawrence berkeley laboratory; University of California. Available at: https://simulationresearch.lbl.gov/dirpubs/10852_ShermanGrimsrud.pdf.

Sherman, M. H. and Modera, M. P. (1986) ‘Comparison of Measured and Predicted Infiltration using the LBL Infiltration Model’, in Trechsel, H. R. and Lagus, P. L. (eds) *Measured Air Leakage of Buildings, ASTMSTP904.* Philadelphia: American Society for Testing and Materials (ASTM), pp. 325–347.

Stabat, P., Caciolo, M. and Marchio, D. (2012) ‘Progress on single-sided ventilation techniques for buildings’, *Advances in Building Energy Research,* 6(2), pp. 212–241. doi: 10.1080/17512549.2012.740903.

Sundell, J. and Kjellman, M. (1994) *Luften vi andas inomhus : inomhusmiljöns betydelse för allergi och annan överkänslighet : vetenskaplig kunskapssammanställning [The air we breathe indoors: the importance of the indoor environment for allergy and other hypersensitivity: A scientific review]*. Stockholm: Folkhälsoinstitutet.

VDI (2000) ‘VDI 3783/12:2000: Environmental Meteorology -Physical Modelling of Flow and Dispersion Processes in the Atmospheric Boundary Layer - Applications of Wind Tunnels’. Düsseldorf: Verlag des Vereins Deutscher Ingenieure.

Walker, I. S. and Wilson, D. J. (1990) *The Alberta Air Infiltration Model (AIM-2), University of Alberta, Department of Mechanical Engineering Report 71.*

Walker, I. S. and Wilson, D. J. (1993) ‘Evaluating models for superposition of wind and stack effect in air infiltration’, *Building and Environment,* 28(2), pp. 201–210. doi: http://dx.doi.org/10.1016/0360-1323(93)90053-6.

Walker, I. S. and Wilson, D. J. (1998) ‘Field Validation of Algebraic Equations for Stack and Wind Driven Air Infiltration Calculations’, *HVAC&R Research*, 4(2), pp. 119–139. doi: 10.1080/10789669.1998.10391395.

Walker, I. S., Wilson, D. J. and Sherman, M. H. (1998) 'A comparison of the power law to quadratic formulations for air infiltration calculations', *Energy and Buildings,* 2(3), pp. 293–299. doi: 10.1016/S0378-7788(97)00047-9.

Wang, H. and Chen, Q. (2012) 'A new empirical model for predicting single-sided, wind-driven natural ventilation in buildings', *Energy and Buildings,* 54, pp. 386–394. doi: 10.1016/j.enbuild.2012.07.028.

Wang, W., Beausoleil-Morrison, I. and Reardon, J. (2009) 'Evaluation of the Alberta air infiltration model using measurements and inter-model comparisons', *Building and Environment,* 44(2), pp. 309–318. doi: 10.1016/j.buildenv.2008.03.005.

Wargocki, P., Sundell, J., Bischof, W., Brundrett, G., Fanger, P. O., Gyntelberg, F., Hanssen, S. O., Harrison, P., Pickering, A., Seppanen, O. and Wouters, P. (2002) 'Ventilation and health in non-industrial indoor environments: report from a European Multidisciplinary Scientific Consensus Meeting (EUROVEN)', *Indoor Air*, 12(2), pp. 113–128. doi: 10.1034/j.1600-0668.2002.01145.x.

Warren, P. R. (1977) *'Ventilation through openings on one wall only', in Proceedings, Unesco International Seminar, Heat Transfer in Buildings, Dubrovnik 1977.* Dubrovnik: Air Infiltration and Ventilation Centre (AIVC).

Warren, P. R. and Parkins, L. M. (1984) 'Single-sided ventilation through open windows', in *Proceedings, 'Windows in building design and maintenance', Gothenburg, Sweden, 13-15 June 1984.* Gothenburg: Air Infiltration and Ventilation Centre (AIVC), p. 487.

Warren, P. R. and Webb, B. C. (1980) 'The relationship between tracer gas and pressurization techniques in dwellings', in *Proc. First Air Infiltration Center Conference*, pp. 245–276.

White, F. M. (2011) *Fluid mechanics*. 7th edn. Singapore: McGraw-Hill.

World Health Organization (2007) *Infection prevention and control of epidemic- and pandemic-prone acute respiratory diseases in health care: WHO interim guidelines.* Geneva: World Health Organization. Available at: http://www.who.int/csr/resources/publications/WHO_CDS_EPR_2007_6c.pdf.

Wouters, P., De Gids, W. F., Warren, P. R. and Jackman, P. J. (1987) 'Ventilation rates and energy losses due to window opening behaviour', in *Proceedings, 8th AIVC Conference 'Ventilation technology research and application' Ueberlingen, West Germany*, 21-24 September 1987. Ueberlingen: Air Infiltration and Ventilation Centre (AIVC).

Yamanaka, T., Kotani, H., Iwamoto, K. and Kato, M. (2006) 'Natural, wind-forced ventilation caused by turbulence in a room with a single opening', *International Journal of Ventilation*, 5(1), pp. 179–187. doi: 10.1080/14733315.2006.11683735.

Papers

Associated papers have been removed in the electronic version of this thesis.

For more details about the papers see:
http://urn.kb.se/resolve?urn=urn:nbn:se:hig:diva-24612

Gävle University Press
ISBN 978-91-88145-17-8
ISBN 978-91-88145-18-5 (PDF)

University of Gävle
Faculty of Engineering
and Sustainable Development
SE-801 76 Gävle, Sweden
+46 26 64 85 00
www.hig.se

UNIVERSITY
OF GÄVLE

Natural Ventilation and Air Infiltration in Large Single Zone Buildings – Measurements and Modelling with Reference to Historical Churches

Natural ventilation is the dominating ventilation process in ancient buildings like churches, and also in most domestic buildings in Sweden and in the rest of the world. These buildings are naturally ventilated via *air infiltration* and *airing*. *Air infiltration* is the airflow through adventitious leakages in the building envelope, while *airing* is the intentional air exchange through large openings like windows and doors. Airing can in turn be performed either as *single-sided* (one or several openings located on the same wall) or as *cross flow* ventilation (two or more openings located on different walls). The total air exchange affects heating energy and indoor air quality. In churches, deposition of airborne particles causes gradual soiling of indoor surfaces, including paintings and other pieces of art. Significant amounts of particles are emitted from visitors and from candles, incense, etc. Temporary airing is likely to reduce this problem, and can also be used to adjust the indoor temperature. The present study investigates mechanisms and prediction models regarding wind- and buoyancy driven air infiltration and open-door airing by means of field measurements, experiments in wind tunnel and computer modelling. The results of the study can be applied also to other kinds of large single-zone buildings, like industry halls, atriums, and sports halls.

Abolfazl Hayati